

DEVELOPMENT OF MICROCARRIER SYSTEMS
FOR BONE TISSUE ENGINEERING

A THESIS SUBMITTED TO
THE GRADUATE SCHOOL OF NATURAL AND APPLIED SCIENCES
OF
MIDDLE EAST TECHNICAL UNIVERSITY

BY

HAZAL AYDOĞDU

IN PARTIAL FULFILLMENT OF THE REQUIREMENTS
FOR
THE DEGREE OF MASTER OF SCIENCE
IN
BIOMEDICAL ENGINEERING

FEBRUARY 2015

Approval of the thesis:

**DEVELOPMENT MICROCARRIER SYSTEMS FOR
BONE TISSUE ENGINEERING**

submitted by **HAZAL AYDOĞDU** in partial fulfillment of the requirements for the degree of **Master of Science in Biomedical Engineering Department, Middle East Technical University** by,

Prof. Dr. Gülbin Dural Ünver
Dean, Graduate School of **Natural and Applied Sciences**

Prof. Dr. Hakan Işık Tarman
Head of Department, **Biomedical Engineering**

Assoc. Prof. Dr. Ayşen Tezcaner
Supervisor, **Engineering Sciences Department, METU**

Assoc. Prof. Dr. Erkan Türker Baran
Co-supervisor, **BIOMATEN, METU**

Examining Committee Members:

Prof. Dr. Vasıf Hasırcı
Biology Department, METU

Assoc. Prof. Dr. Ayşen Tezcaner
Engineering Sciences Department, METU

Assoc. Prof. Dr. Erkan Türker Baran
BIOMATEN, METU

Assoc. Prof. Dr. Dilek Keskin
Engineering Sciences Department, METU

Assoc. Prof. Dr. Sreeparna Banerjee
Biology Department, METU

Date: 02.02.2015

I hereby declare that all information in this document has been obtained and presented in accordance with academic rules and ethical conduct. I also declare that, as required by these rules and conduct, I have fully cited and referenced all material and results that are not original to this work.

Name, Last name: Hazal, Aydođdu

Signature :

ABSTRACT

DEVELOPMENT OF MICROCARRIER SYSTEMS FOR BONE TISSUE ENGINEERING

Aydođdu, Hazal

M. S., Department of Biomedical Engineering

Supervisor: Assoc. Prof. Dr. Ayşen Tezcaner

Co-Supervisor: Assoc. Prof. Dr. Erkan Türker Baran

February 2015, 115 pages

Current strategies in bone tissue engineering have largely focused on development of carrier systems for repair and regeneration of bone tissue defects. The microcarrier systems offer an efficient method of delivery of cells with non-invasive injectable system. In this study, three-dimensional hydrogel microspheres were developed via water-in-oil emulsion method. In the first part of the thesis, porous pullulan (PULL) microspheres, with average size of $153\pm 46\ \mu\text{m}$, were prepared and the surface of the microspheres were modified with (a) silk fibroin (SF) by reductive amination via surface oxidation of PULL microspheres, and (b) biomimetic mineralization by incubating the PULL microspheres in order to enhance the cell attachment and proliferation. The degradation analyses revealed that PULL microspheres had a slow degradation rate with 8% degradation in a two weeks' period, which would support new bone tissue formation. Furthermore, the mechanical analysis showed that the microspheres had good mechanical properties that

were enhanced significantly with the biomimetic mineralization with SBF incubation. Cell culture studies were conducted with SaOs-2 cell line and revealed that the SF coating and mineralization on the surface of PULL microspheres significantly increased the initial cell attachment and proliferation. In the second part of the thesis, urine derived mesenchymal stem cells were encapsulated in microspheres composed of oxidized PULL (oxPULL), alginate (ALG) and gelatin (GEL). The oxPULL with a degree of oxidation of $68\pm 4\%$, and gelatin were crosslinked via borax catalyzed crosslinking while alginate was crosslinked with calcium and the average size for microspheres was found to be 530 ± 32 μm . The cell culture studies indicated that the cells were successfully encapsulated, retained their viability and proliferated. According to these results, it can be suggested that the PULL microcarriers are suitable for use as injectable systems and have potential in bone tissue engineering applications.

Keywords: Tissue engineering, bone tissue, pullulan, silk fibroin, gelatin

ÖZ

KEMİK DOKU MÜHENDİSLİĞİ İÇİN MİKROTAŞIYICI SİSTEMLERİN GELİŞTİRİLMESİ

Aydođdu, Hazal

Yüksek Lisans, Biyomedikal Mühendisliđi Bölümü

Tez Yöneticisi: Doç. Dr. Ayşen Tezcaner

Ortak Tez Yöneticisi: Doç. Dr. Erkan Türker Baran

Şubat 2015, 115 sayfa

Kemik doku mühendisliğinde güncel stratejiler, büyük ölçüde kemik doku defektlerinin onarım ve rejenerasyonu için taşıyıcı sistemlerinin geliştirilmesine odaklanmıştır. Mikrotaşıyıcı sistemleri, non-invaziv enjekte edilebilir sistemlerle hücre taşınması için etkili bir yöntem sunar. Bu çalışmada, üç-boyutlu hidrojel mikrotaşıyıcılar, su-içinde-yağ emülsiyonları ile geliştirilir. Tezin ilk bölümünde, 153 ± 46 μm arasında ortalama boyutu olan, gözenekli pullulan (PULL) mikroküreler üretilmiş ve hücre yapışması ve çoğalmasını arttırmak için mikroküre yüzeyleri (a) okside edilerek indirgeyici aminasyon ile ipek fibroin (SF) proteini ile kaplanarak ve (b) vücut sıvısı simülasyonu içinde inkübe edilerek biomimetik mineralizasyonu ile modifiye edilmiştir. Bozunma analizi, PULL mikrokürelerin iki haftalık sürede ortalama %8 bozulması ile yavaş bozulma oranına sahip olması ile daha uzun süre yeni kemik dokusu oluşumunu destekleyebileceğini ortaya koymuştur. Ayrıca, yapılan mekanik analizler mikrokürelerin iyi mekanik özelliklere

sahip olduğunu ve mikroküre yüzeyindeki mineralizasyonun bunu geliştirdiğini göstermiştir. SaOs-2 hücre hattı ile yapılan hücre kültürü çalışmaları ile, PULL mikroküreler yüzeyinde yapılan SF kaplama ve mineralizasyonun önemli ölçüde ilk hücre bağlanmasını ve çoğalmasını arttırdığını ortaya çıkarmıştır. İkinci bölümde ise, idrar kaynaklı mezenkimal kök hücreler okside PULL (oxPULL) ve jelatin (GEL) kompozitinin içine hapsedildi. Oksidasyon derecesi %68±4 olan oxPULL ve jelatinin boraks vasıtası ile çapraz bağlanmış mikrokürelerin ortalama büyüklüğünün 530±32 µm olduğu bulunmuştur. Bu sonuçlara göre, PULL ile geliştirilen mikrotasıyıcılar enjekte edilebilir sistemlere uygun olup, kemik doku mühendisliği uygulamaları için taşıdığı potansiyeller nedeniyle önerilebilirler

Anahtar Kelimeler: Doku mühendisliği, kemik dokusu, pullulan, ipek fibroin, jelatin

It only happens if it doesn't matter

ACKNOWLEDGMENTS

I would like to express my sincere gratitude to my supervisor Assoc. Prof. Dr. Ayşen Tezcaner for her guidance, advice, encouragements and insight throughout the study, co-supervisor Assoc. Prof. Dr. Erkan Türker Baran for his constant supportive attitude during my research, and Assoc. Prof. Dr. Dilek Keskin for her cooperative academic advisory all through my master study. Special thanks to other committee members of my thesis Prof. Dr. Vasıf Hasırcı and Assoc. Prof. Dr. Sreeparna Banerjee for their valuable contribution to finalize my thesis.

I wish to thank to BIOMATEN- Center of Excellence in Biomaterials and Tissue Engineering for allowing me to use their laboratory and I would like to thank BIOMATEN members Arda Büyüksungur, Senem Heper and Selcen Alagöz for their help to me on micro-CT and FTIR analyses. I also want to thank to Assoc. Prof. Dr. Zafer Evis for his sharing facilities and consumables in our laboratory.

I would like to add my special thanks to Sibel Ataoğlu for conducting the urine derived stem cell isolation. She always showed me the optimistic way of life since the day we met in our first year of undergraduate studies.

I thank to my lab mates for being the great teachers and fellows. In particular, thanks to my seniors and friends: Dr. Ayşegül Kavas, Dr. Bengi Yılmaz, Dr. Ömer Aktürk, Dr. Özge Erdemli, Ali Deniz Dalgıç, Alişan Kayabölen, Aydın Tahmasebifar, Deniz Atıla, Engin Pazarçeviren, Merve Güldiken, Nil Göl, Reza Moonesirad and Zeynep Barçın for their contributions to my studies and endless friendship.

I also have to thank to Graduate School of Natural and Applied Sciences personnel for moral support in the office environment, especially my roommate Derya Gökçay for her problem-solving attitude and precious friendship.

I would like to state my special thanks to Ozan Kayadelen for being my greatest support not only during my thesis study but also during my lifetime.

A special thanks to my family. I would like to express my grateful feelings for my mother Ayşe Aydoğdu and my father Hüseyin Aydoğdu and my brother Erman Aydoğdu for supporting me for all the time with their endless encouragement and love.

TABLE OF CONTENTS

ABSTRACT	v
ÖZ.....	vii
ACKNOWLEDGMENTS.....	x
TABLE OF CONTENTS	xii
LIST OF TABLES	xvi
LIST OF FIGURES.....	xvii
LIST OF ABBREVIATIONS	xxii
CHAPTERS	
1.INTRODUCTION.....	1
1.1. Tissue Engineering.....	1
1.2. Bone Tissue Engineering	3
1.2.1. Bone Tissue and Its Properties	3
1.2.2. Bone Tissue Regeneration and Bone Tissue Engineering Approaches	6
1.3. Microcarrier Production Methods.....	7
1.4. Surface Modifications.....	9
1.5. Biomaterials for Microcarriers.....	11
1.5.1. Pullulan.....	11
1.5.2.Silk Fibroin.....	14

1.5.3. Gelatin.....	15
1.6. Aim of the Study	16
2. MATERIALS & METHODS.....	17
2.1. Materials.....	17
2.2. Porous PULL Microsphere Preparation and Characterization.....	18
2.3. Calcium Content	21
2.3.1. Ash Content Assay.....	21
2.3.2. O-Cresolphthalein Complexone Method	21
2.4. Micro-Computed Tomography (Micro-CT)	22
2.5. Silk Fibroin (SF) Coating of Porous PULL Microspheres	22
2.5.1. Fluorescent Labelling of PULL and SF	25
2.6. SBF Incubation	26
2.6.1. Characterization of SBF Incubated Microspheres	27
2.7. Cell Culture Studies	28
2.7.1. Live/Dead Assay (Calcein AM, Propidium Iodide Staining)	28
2.7.2. Cell Viability Study (Alamar Blue)	28
2.7.3. ALP Assay	29
2.8. Degradation Study.....	30
2.9. Measurement of Stiffness.....	30
2.10. Periodate Oxidation of PULL	31
2.10.1. Fourier Transform Infrared Spectroscopy - Attenuated Total Reflectance (FTIR-ATR).....	31

2.10.2. Iodometric Titration	32
2.11. Isolation of Urine Derived Stem Cells	32
2.12. Cell Encapsulation.....	33
2.13. Cell Culture	35
2.13.1. Live/Dead Assay (Calcein AM, Propidium Iodide Staining)	35
2.13.2. Cell Viability Study (Alamar Blue)	36
2.14. Statistical Analysis	36
3. RESULTS AND DISCUSSION	37
3.1. Porous PULL Microsphere Preparation and Characterization	37
3.1.1. Residual Calcium Content Analysis.....	48
3.2. Silk Fibroin (SF) Coating of Porous PULL Microspheres.....	50
3.3. Simulated Body Fluid Incubation of PULL Microspheres	55
3.4. Size Analysis of Microspheres	62
3.5. Degradation Analysis	63
3.6. Measurement of Stiffness.....	65
3.7. <i>In vitro</i> Cell Culture Studies.....	66
3.7.1. ALP Assay.....	72
3.8. Periodate Oxidation of PULL and Crosslinking with GEL	75
3.9. Isolation of Urine Derived Stem Cells	77
4. CONCLUSIONS.....	81
REFERENCES	83

APPENDICES

A.CALCIUM ASSAY CALIBRATION CURVE.....	105
B.CELL NUMBER CALIBRATION CURVE FOR VIABILITY ASSAY (PART I) .	107
C.CALIBRATION CURVE FOR ALP ACTIVITY ASSAY	109
D.CALIBRATION CURVE FOR ALP ACTIVITY ASSAY	111
E.ETHICS COMMITTEE APPROVAL REPORT	113
F.CELL NUMBER CALIBRATION CURVE FOR VIABILITY ASSAY (PART II)	115

LIST OF TABLES

TABLES

Table 1. 1 Tissue engineering applications of different forms of PULL.	13
Table 3. 1 Gelation times of PULL prepared by using varying concentrations of PULL, STMP and NaOH.	38
Table 3. 2 Ca and P analysis results of Inductively Coupled Plasma Optical Emission Spectrometry (ICP).	61
Table 3. 3 Size analysis of microspheres.	63
Table 3.4 Stiffness measurement analysis of plain, fibroin coated and SBF coated microspheres (n=3).....	65

LIST OF FIGURES

FIGURES

Figure 1. 1 (a) The structure of bone. (b) The organization of osteons and lamellae in compact bone. (c) The orientation of collagen fibers in adjacent lamellae (Martini et al., 2012).	4
Figure 1. 2 Chemical structure of pullulan.....	11
Figure 2. 1 Set up used for PULL microsphere preparation.	19
Figure 2. 2. Proposed mechanism for the crosslinking reaction of PULL with STMP ...	20
Figure 2. 3 Reaction scheme for the PULL and SF conjugation.	24
Figure 2. 4. Reaction schemes for the labelling of SF with fuoresceine isothiocyanate (X) and PULL with rhodamine isothiocyanate (Y) (Lamprecht et al., 2000).	26
Figure 2. 5 Crosslinking mechanism of gelatin (GEL) and oxidized pullulan (oxPULL).	34
Figure 2. 6 Scheme for encapsulation method for PULL//ALG/GEL blend.	35
Figure 3. 1 Stereomicroscope images of crosslinked PULL microspheres produced by water-in-oil emulsion at 500 rpm rotation speed. (A) 1 X (B) 4X, (C) 6X (D) 11.5X scale bar: 200 μm	40

Figure 3. 2 Light microscopy images of pullulan microspheres with 5% (w/w) KCl as porogen. Magnification 40X Scale bar: 200 μm42

Figure 3. 3 Light microscopy images of pullulan microspheres with 5% (w/w) NaCl as porogen. Magnification 10X. Scale bar: 100 μm42

Figure 3. 4 Light reflection microscopy image of PULL microspheres with 10% (w/w) NaCl porogen (11.25 X magnification) after water leaching.....43

Figure 3. 5 CaCO_3 particles used as porogen had a size about 20 μm . Scale bar: 100 μm44

Figure 3. 6 Light microscopy images of 20% calcium carbonate containing (a) and 30% calcium carbonate containing (b) swollen microspheres. Magnification 40X. Scale bars: 100 μm45

Figure 3. 7 SEM images of (A) 20% calcium carbonate containing and (B) 30% calcium carbonate containing dry PULL microspheres. Magnification 200 X. Scale bars: 100 μm45

Figure 3. 8. Light microscopy images of HCl treated PULL microspheres with 30% CaCO_3 . Magnification 100X. Scale bar: 100 μm46

Figure 3. 9 Micro-CT images of (A) upper, (B) frontal section of incorporating pullulan microspheres. (C) Close view of a single microsphere showing its cross-section and internal CaCO_3 particles.47

Figure 3. 10 Residual calcium amount within the microspheres obtained by o-cresolphthalein complexone method (n=3).49

Figure 3. 11 SEM images of 30% calcium carbonate containing dry microspheres coated with silk fibroin.51

Figure 3. 12 Fluorescence microscopy images of FITC-fibroin coated pullulan microspheres. Magnification 40X (A), 100X (B) and 200X (C).52

Figure 3. 13 Visible light (A, E) and fluorescence (B, F) microscopy images of surface oxidized microspheres respectively. Visible light (C, G), and fluorescence (D, H) microscope images of non-oxidized pullulan microsphere surfaces are shown after FITC-SF treatment and washing.	53
Figure 3. 14 (A) Light transmission (B-C) and fluorescence light microscope images of FITC-labelled SF coated RBITC-labelled PULL microspheres Magnification 40X. Scale bars: 200µm.....	54
Figure 3. 15 Light transmission (A), fluorescence light microscope of RBITC labelled pullulan microspheres (B) and FITC labelled silk fibroin coating (C) after microtome sectioning.	55
Figure 3. 16 Calcium amount of the plain PULL microspheres and 4, 7 and 14 days SBF incubated microspheres obtained by o-cresolphthalein complexone method (n=3).....	56
Figure 3. 17 Fluorescence microscope images of calcein stained pullulan microspheres before SBF (A, B) and 14 days of SBF incubation (C, D).	57
Figure 3. 18 Scanning electron microscopy images of pullulan microspheres that were incubated in SBF for 0 (A), 4 (B), 7 (C) and 14 (D) days at 37°C.	59
Figure 3. 19 X-ray diffraction pattern of pullulan microsphere samples (a) without porogen CaCO ₃ , (b) with porogen CaCO ₃ , (c) after HCl treatment, (d) after 7 days SBF incubation and (e) after 14 days SBF incubation.	60
Figure 3. 20 Cumulative wet weight losses of the plain, surface oxidized, SF coated and SBF incubated PULL microspheres in PBS at 37°C in water bath in two weeks (n=3). 64	
Figure 3. 21 Transmission light microscopy images of 1% SF coated microspheres on the 3 rd day of incubation (A) magnification 4X (Scale bar: 200 µm) and (B) magnification 10X (Scale bar 100 µm).....	67

Figure 3. 22 Live/dead staining images of attached cell on microspheres that were incubated in SBF for 0 (A), 4 (B), 7 (C) and 14 (D) days. Upper images show the calcein stainings (green, live) and the bottom images show PI (red, dead) stainings. Magnification 100X.67

Figure 3. 23 Phase contrast and fluorescence microscope images of SaOs-2 cells seeded on native (A, B) and SBF incubated pullulan microspheres (B, C), respectively. Green illuminance shows Nile red stained cells. Magnification 100X. Scale bar: 100 μm 69

Figure 3. 24 SaOs-2 cell proliferation on plain, SF coated and 7 days SBF incubated PULL microspheres with their standard deviations under static and dynamic conditions, TCPS was used as control group. (n=5).71

Figure 3. 25 FTIR spectra of (a) PULL and (b) bulk oxPULL76

Figure 3. 26. Light microscopy images of cells in culture (A) First appearance of cells at day 5 (B) first colony formation at day 7 (C) interacted colonies at day 9.77

Figure 3. 27 (A) and (B) PULL/ALG/GEL microspheres without cells before PLL coating. Magnification 100X Scale bar: 100 μm78

Figure 3. 28 Live/dead staining images of urine derived mesenchymal cell encapsulated in microspheres (A) day 1 (B) day 3. Magnification 100X. Scale bar: 200 μm79

Figure 3. 29 Proliferation of urine derived mesenchymal stem cells encapsulated in PULL/ALG/GEL microspheres on 1st and 3rd day of incubation (n=3).80

Figure A. Calibration curve for o-cresolphthalein complexone method for calcium content.105

Figure B. Calibration curve for SaOs-2 cells for Alamar Blue viability assay.107

Figure C. The calibration curve constructed with p-nitrophenol for ALP activity assay	109
Figure D. The calibration curve of BCA assay constructed with bovine serum albumin as standard for protein amount determination.	111
Figure F. Calibration curve for urine derived stem cells for Alamar Blue viability assay.	115

LIST OF ABBREVIATIONS

ALG	Alginate
ALP	Alkaline Phosphatase
ANOVA	Analysis of Variance
ATCC	American Type Culture Collection
ATR	Attenuated Total Reflectance
BCA	Bicinchoninic Acid
BSA	Bovine Serum Albumin
DMEM	Dulbecco's Modified Eagle Medium
DMSO	Dimethyl Sulfoxide
DNPH	2,4-Dinitrophenylhydrazine
ELISA	Enzyme-Linked Immunosorbent Assay
FBS	Fetal Bovine Serum
FITC	Fluorescein Isothiocyanate
FT-IR	Fourier Transform Infrared
GEL	Gelatin
hMSC	Human mesenchymal stem cells
HA/Hap	Hydroxyapatite

ICP-MS	Inductively coupled plasma mass spectroscopy
KSFM	Keratinocyte serum free medium
USC	Urine derived stem cells
UV	Ultraviolet
PBS	Phosphate Buffered Saline
PI	Propidium Iodide
pNPP	p-Nitrophenyl Phosphate
PULL	Pullulan
SaOs-2	Human Osteogenic Sarcoma Cell Line
SBF	Simulated Body Fluid
SEM	Scanning Electron Microscopy
SF	Silk Fibroin
STMP	Trisodium Trimetaphosphate
TCPS	Cells seeded on polystyrene tissue culture wells
W	Weight of the sample (g)
XRD	X-Ray Diffraction

CHAPTER 1

INTRODUCTION

1.1. Tissue Engineering

Tissue engineering was initially defined as ‘an interdisciplinary field that applies the principles of engineering and life sciences toward the development of biological substitutes that restore, maintain, or improve tissue function or a whole organ’ by Lanza, Langer and Vacanti (1993). This definition was modified in time with the developing technology and techniques in this field. The definition has been expanded by incorporating cells and cell substitutes, growth factors, delivery vehicles, and scaffolds that are used as general strategies for tissue engineering.

Three fundamental components of tissue engineering are scaffold, cells and bioactive agents. The tissue engineered constructs that are intended to replace a certain target tissue, must comply with the properties of the target tissue. Besides mimicking biological properties of the target tissue in the constructs, other properties like chemical, physical and mechanical properties should also be considered (Hollister et al., 2005). For example, for skin tissue engineering a construct should have adequate water retention capability whereas for bone tissue engineering, the construct essentially requires high mechanical performance except for the non-load bearing bones in the body (Yannas, 2001).

The required properties are mainly obtained with a proper scaffold design. Hutmacher et al. (2012) suggested that a proper scaffold should ensure:

- three dimensional and highly porous structure to support cell/tissue growth within an interconnected pore network for delivery of nutrients and metabolic waste;
- biodegradability with a suitable degradation rate for *in vitro* and/or *in vivo* applications;
- appropriate surface chemistry for cell adherence, proliferation, and differentiation;
- mechanical properties to match those of the tissues at the site of implantation; and
- processibility to form a variety of shapes and sizes.

In order to design a scaffold carrying these characteristics, an appropriate material should be selected. Required scaffold material and its properties may change with the type of tissue of interest and the specific application (Drury and Mooney, 2003). The materials can be natural or synthetic materials, composites or biologically modified materials. In material selection, the material-tissue interaction is a major determinant. The material affects the tissue and the tissue affects the material, these material-tissue interactions indicate the biocompatibility of the materials for each specific case (Enderle and Bronzino, 2012).

In well accepted tissue engineering approach, cells are obtained from the same individual and they are reimplanted to the defect area with the scaffold. Although autologous cells have the least problems with rejection and pathogen transmission, in some cases it is not possible to obtain these cells. In recent years, stem cells have been widely studied and applied in tissue engineering. Stem cells are defined as undifferentiated cells that have high proliferation rate and self-renewal capacity with a multi-lineage differentiation

potential (Blau et al., 2001). These properties of stem cells and limitation in the use of patients' mature cells make the stem cells as the ideal cell source for tissue engineering approach. Stem cells have capacities for differentiation into various cell types or proliferation depending on their origin.

1.2. Bone Tissue Engineering

1.2.1. Bone Tissue and Its Properties

The composition of bone consists of different cell types, organic matrix and calcium minerals that are associated with the matrix for strength of the bone. Ninety-five percent of the organic matrix is composed of collagen and the remaining is non-collagenous proteins and proteoglycans. There are different types of collagen and non-collagenous proteins and they are found in a variety of combinations in cortical bone, cancellous bone and cartilage tissue. In a cortical bone the concentric lamellae in a form of tightly packed collagen fibrils is surrounded by an adjacent lamellae from which the fibrils are distributed in a perpendicular plane (Figure 1.1). The blood vessels pass through osteons and penetrate to the cortical part of the bone. (Fisher et al., 2007)

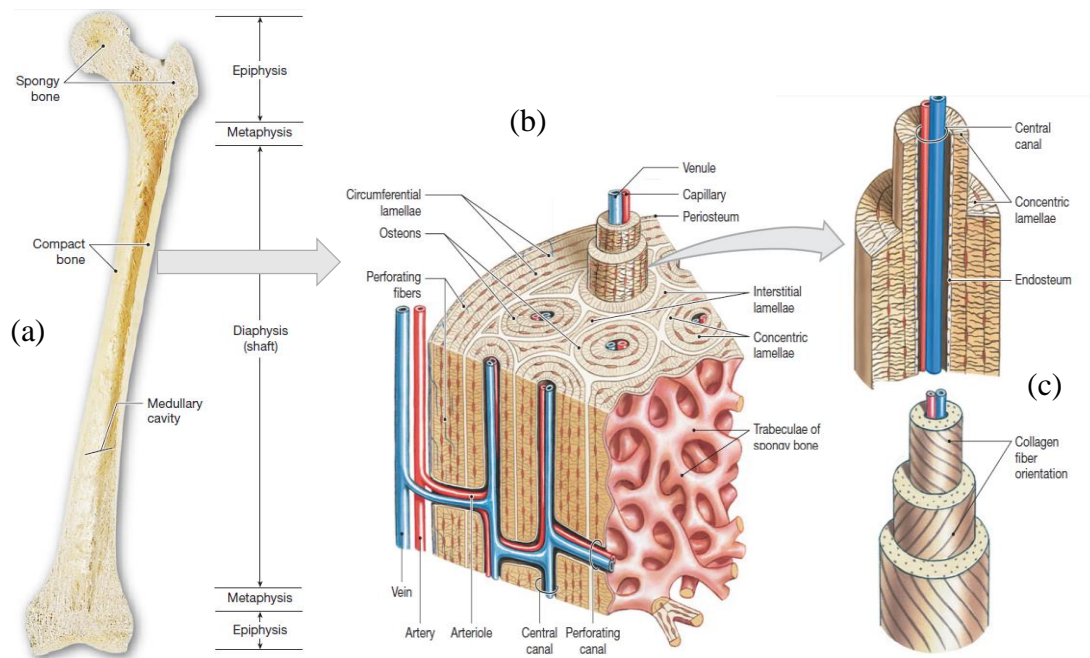


Figure 1. 1 (a) The structure of bone. (b) The organization of osteons and lamellae in compact bone. (c) The orientation of collagen fibers in adjacent lamellae (Martini et al., 2012).

The main cell composition of cortical bone is osteocytes. Osteocytes are differentiated osteoblasts that are surrounded by mineralized matrix. Cancellous bone is a porous structure with trabecular systems. Cell component of this system are osteoblasts and bone lining cells. The most important function of the trabecular system and the cells is load perception. Load perception allows the cancellous bone to be shaped according to amount and direction of the load on the bone (Warner et al., 2006).

Matrix mineralization has an important role in bone repair and regeneration. When the tissue is mineralized, the bone becomes mechanically competent (Zhang et al., 2002). As the matrix of bone is very rich in collagen, it allows apatite nucleation in the microenvironment for mineralization. Knowing the process of mineralization in bone matrix helps us to generate natural-like tissue constructs ex-vivo by mimicking the chemical features of the biomaterial used as scaffold or carrier. In this sense, increased mechanical properties of tissue engineering scaffolds by stimulated mineralization would enhance the repair mechanism in bone tissue (Salinas et al., 2013).

For mineralization, the content of extracellular matrix is very crucial. Depending on the location of the bone and cartilage tissues and stages of bone and cartilage regeneration, various collagen and non-collagenous proteins are expressed. Such as collagen type I is found in mature bone while collagen type II constitutes main matrix composition in mineralizing cartilage and epiphyseal growth plate, which is located on the growing ends of the long bone. Collagen type III has role in callus formation and development together with collagen type II and type V. Type II and III are secreted by osteoblasts and chondrocytes during the callus formation - a repair mechanism of bone after an injury forming fibrous structure serving as a cell migration center. Also in the early stages of bone formation in fetal development, studies showed that collagen types I, II, IX and X influence the endochondral ossification. (Yamasaki et al., 2001; Xian et al., 2004; Meyer et al., 2006)

Collagen and other matrix proteins together have effect on mineralization along with other mechanisms of repair and regeneration. In this regeneration, main groups of proteins are proteoglycans, glycoproteins and gamma-carboxyglutamic acid containing molecules. Three of these molecules (osteocalcin, osteonectin and bone sialoprotein) have special importance for bone and cartilage as they are all connected to hydroxyapatite mineralization (Butler and Ritchie, 1995). They are effective in early remodeling of bone by binding to hydroxyapatite and taking part in nucleation and crystallization.

1.2.2. Bone Tissue Regeneration and Bone Tissue Engineering Approaches

When a bone is injured, bone regeneration starts with formation of a repair tissue. This repair tissue is mostly composed of periosteum secreting signals as morphogens for inner cells to proliferate and differentiate. For repair tissue, not only adjacent cancellous and cortical bone cells but also surrounding muscle tissue contribute in this structure. Mesenchymal stem cell source is also assumed to be coming from these muscle tissues. During regeneration, the cells continuously synthesize matrix proteins mainly collagen types I and II (Meyer et al., 2006).

The defect size is critical for regeneration, as the signals for osteogenic cells change. Small size injuries in bone is being repaired spontaneously, however when a defect size is too large than repair tissue and the regeneration may not be completed. In addition, very complex signal systems from periosteum and bone marrow arise and release the content into the matrix. Firstly, the action of inflammatory system starts with cytokines, morphogens, proteases and angiogenic factors in order to direct repair response (Barnes et al., 1999).

Most therapies for bone defects are still based on the use of autografts or allografts. Autografts are tissues originated from the same individual and do not induce immunogenic reactions. Allografts, which are the transplantation of tissue between genetically nonidentical individuals of the same species, are an attractive alternative to autografts when it is not possible to use autologous sources even though it may induce immune reactions. In the use of autografts or allografts surgery time, post-operative pain, hematoma formation, blood loss, nerve injury, infection and cosmetic defects are considered to be some of the important drawbacks. Bone tissue engineering offers a new treatment for reducing these drawbacks. However, bone tissue engineering is not an established procedure as it must create a substitute with the proper mechanical properties, promote biomineralization and induce the differentiation of the seeded cells (Woodruff et

al. 2012). With this approach, bone tissue graft should also be osteoconductive, and osteoinductive and structurally similar to natural bone tissue (Reynolds et al., 2010). There are large number of commercially available bone-grafts alternatives, consisting of scaffolds made of natural or synthetic biomaterials that promote the migration, proliferation and differentiation of cells for bone regeneration. The reason of using biomaterials such as collagen, ceramics made from calcium phosphate (hydroxyapatite (HA) and β -tricalcium phosphate (β -TCP) etc.) and glass ceramics is due to the enhancement of biomineralization by these materials and mimicking organic or inorganic composition of bone.

1.3. Microcarrier Production Methods

Microcarrier systems have been an attractive form of scaffold that finds application in delivery of cells for tissue engineering. Many different materials like bioactive ceramics, degradable polymers, and their composites, have been utilized in the form of microspheres (Jamal et al., 2012; Bao et al., 2012; Miyazaki et al., 2013) The microcarrier systems enhance the capacity of cell delivery due to their high surface area to volume ratio. Microcarriers may be in the form of microsphere or in a thin shell to deliver cells on the surface or within the core space, respectively. Microcarriers carry not only cells but also, bioactive molecules that have therapeutic effects in regulating cell behaviors can be encapsulated (Mouriño et al., 2013).

The surface properties of the microspherical carriers are important as the cells first encounter the surface of spheres. The surface can be activated by modifying chemistry and microtopography to enhance cell attachment (Perez et al., 2011). Besides, the design of the carriers should be done to improve the cell delivery capacity by for example porosity. Porous microspherical carriers are preferred to effectively encapsulate host cells

and carry them for tissue engineering. Moreover, *in situ* encapsulation of cells within the hollow inner space is one other option for cell carrier and reservoir (Park et al., 2013).

For bone regeneration bioactive ceramics and degradable polymers and their composites have been used widely as scaffold materials (Lin et al., 2005; Umeki et al., 2010; Perez et al., 2014). Hydroxyapatite (HA) and tricalcium phosphate (TCP), and glass ceramics with bioactive compositions have also been a preferred material in preparation of spherical particulates at the size range of 20-400 μm (Victor et al., 2008; Emoto et al., 2010). Bioceramic microcarriers can be produced by emulsification or spray-drying, followed by a high-temperature heat treatment to consolidate. However, bioceramics generally require high temperature to consolidate their structure. Comparatively, the polymers utilized in microcarrier preparation frequently. Polymer spheres are generally formed by oil-in-water or water-in-oil emulsions with mechanical stirring (Shi et al., 2009; Zhang et al., 2010). Surfactants such as Tween 80, Span 80 and poly (vinyl alcohol) support and stabilize the spherical droplet during their transition into solid microspheres (Francis et al., 2007). The size of the spheres depends on the polymer solution viscosity, surfactant type and surfactant concentration, solvent and stirring speed (Wei et al., 2011; Yasuda et al., 2011).

Porous microspheres

The pore structure is another important criterion for enhancement of cell attachment and proliferation. Besides increasing the surface area of microcarrier, pores enable cells to move to inner parts and increase the proliferation of cells by cell-cell contact. Porous structure can be obtained by porogen leaching or gas foaming methods. Kim et al. (2006) used carbonate salt NH_4HCO_3 as a gas-foaming material to produce PLGA microspheres with the pore size of about 20 μm in which cells proliferated.

Microcapsules

Microcapsule type carriers have been developed to deliver cells within a core that is isolated, but is semipermeable to the outside environment. The encapsulating material should be permeable to nutrients and gas molecules, such as ions, growth factors, and oxygen, allowing cell interactions with the environment and removal of cell metabolites (Park et al., 2013). In case of allogenic cell encapsulation it is preferred that, the capsule wall should not allow immunoglobulins to avoid immunogenic reactions.

Microcapsules can be considered as a reservoir providing cells a microenvironment that supports proliferation and promote differentiation into specific tissues. Moreover, during culture, several biological molecules are secreted from the encapsulated cells, and the molecules can be accumulated and released to the surroundings.

The most preferred material for encapsulating cells has been hydrogels of alginate, collagen and gelatin. These polymers are known with their hydrophilic-nature and being permeable to nutrient diffusion. Besides that, they have flexible structure, which does not cause significant frictional force or mechanical irritation to surrounding tissues. (Sakai et al., 2005; Thakur et al., 2010)

1.4. Surface Modifications

Surface topography and hydrophobicity of scaffolds play a critical role in regulating initial cell behaviors, such as cell adhesion and proliferation. Surface modifications are widely used for cell carriers to enhance bioactive molecule immobilization, cell adhesion and proliferation. The synthetic polymers are generally hydrophobic and devoid functional chemical groups to conjugate adhesive ligands for favorable cell adhesion. Therefore, the surface often has to be engineered to be hydrophilic or to be cytocompatible by

modification with adhesive proteins, such as fibronectin or collagen (Hong et al., 2005; Tran et al., 2011). For example, coating of poly (DL-lactic-co-glycolic acid) (PLGA) with natural biomaterial solutions of collagen, chitosan, or N-succinyl-chitosan was used to increase the cell attachment on PLGA surface (Wu et al., 2006). *In vitro* studies revealed that chitosan and collagen treatment significantly improved the surface hydrophilic characteristics than N-succinyl chitosan and unmodified collagen, and this property in turn improved the cell attachment, proliferation and differentiation significantly in comparison to the unmodified samples. In another and recent study, Gishto et al. (2014) showed that coating of PCL nanofibers with proteins enhanced the myocyte cell attachment and cell viability on them.

Besides the surface modifications with organic molecules, inorganic coating methods such as hydroxyapatite (HA) nucleation on the biomaterial surfaces are potential strategies used in bone tissue engineering. For example, Rajzer et al. (2014) modified electrospun gelatin/poly (ϵ -caprolactone) fibrous scaffold with calcium phosphate to increase the biocompatibility and bioactivity. Upon incubation of these scaffolds in simulated body fluid (SBF), they observed that the bioactivity of composite scaffold increased in comparison to pure chitosan. They have also stated higher biocompatibility of these scaffolds by confirming with cell attachment and proliferation (Rajzer et al., 2014).

In addition to the biological improvements, the mechanical properties were also enhanced by *in vitro* mineralization approaches in bone tissue engineering. Lu et al. (2012) characterized the porous composite of polylactide-co-glycolide (PLGA) and 45S5 bioactive glass (BG) composite under compression. They observed that the mechanical properties of the composite were enhanced as the mineralization was improved.

1.5. Biomaterials for Microcarriers

1.5.1. Pullulan

Pullulan (PULL) is a linear glucosic polysaccharide produced by the fungus *Aureobasidium pullulans* (Mishra et al., 2011). Pullulan is solubilized in water easily, has high adhesion and film forming abilities. These properties of pullulan bring the unique linking process with structural flexibility (Leather, 2003). Biodegradable, non-toxic, non-immunogenic, non-mutagenic and noncarcinogenic characteristics allowed PULL to be used in tissue engineering field as a biomaterial.

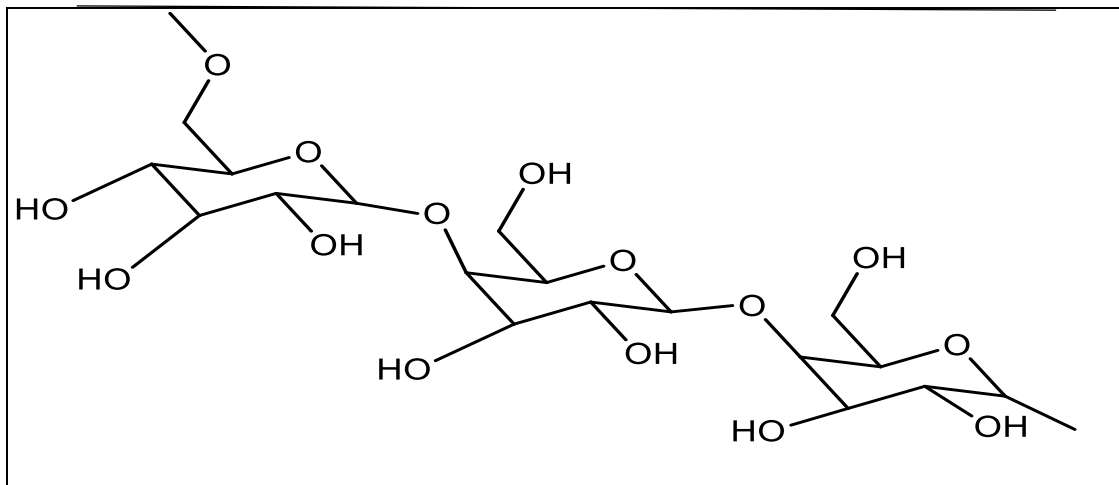


Figure 1. 2 Chemical structure of pullulan.

Previously, PULL was used in various forms for different applications. Such as, it is used as antibacterial film for food preservation (Kandemir et al., 2005). Modified PULL was also used in various applications. Carbonated PULL, for example, was used for drug delivery (Bruneel and Schacht, 1993), and carboxymethyl PULL gel found an application as a wound dressing material (Li et al., 2011). Table 1.1 shows some examples of PULL used in tissue engineering applications in the last decade.

Table 1. 1 Tissue engineering applications of different forms of PULL.

Form	Author	Year	Purpose
Pullulan with nano-crystalline hydroxyapatite and poly(3-hydroxybutyrate) micro-fibers	Amrita et al.	2015	Bone tissue engineering
Pullulan/tannic acid/chitosan composite nanofibers	Xu et al.	2014	Wound dressing
Gel–fiber composite scaffold formed by interfacial polyelectrolyte complexation fibers and pullulan–dextran hydrogel	Francene and Cutiongco	2014	Improved bioactivity
Pullulan nanoparticles	Punna Rao Ravi	2014	Drug delivery
Folate–low-molecular-weight polyethyleneimine–modified pullulan	Wang et al.	2013	DNA/short interfering RNA (siRNA) delivery
A nano-hydroxyapatite – pullulan/dextran polysaccharide composite macroporous material	Fricain et al.	2013	Bone tissue engineering
Pullulan nanogel	Fujioka-Kobayashi et al.	2012	Growth factor delivery
Multi-responsive pullulan hydrogels	Mocanu et al.	2011	Drug delivery
Hemocompatible pullulan–polyethyleneimine conjugates	Rekha et al.	2010	Gene delivery
Pullulan-collagen hydrogel scaffold	Galvez et al.	2009	Skin tissue engineering
Pullulan acetate nanoparticles	Zhang et al.	2008	Drug delivery

Recently, Cutiongco et al. has reported the use of pullulan and dextran composite (PD) due to the non-immunogenic and non-antigenic properties of both biopolymers. The PD composite fibers obtained by interfacial polyelectrolyte complexation (IPC) has showed improved cell adhesion and proliferation compared to the plain polysaccharide scaffold (2014).

In addition, for bone tissue engineering, PULL based scaffolds have received attention for last few years. For instance, osteogenic differentiation of human adipose derived stem cells on PULL based scaffold has been reported *in vitro* (Lalande et al., 2011). Furthermore, nano hydroxyapatite loaded PULL scaffolds were shown to induce bone formation *in vivo* (Fricain et al., 2013; Lalande et al., 2011).

1.5.2. Silk Fibroin

Fibroin is a protein that is produced by spiders, silkworms and scorpions (Phillips et al., 2004; Omenetto and Kaplan, 2010; Kaplan et al., 1997). Cocoons of domesticated silkworm, *Bombyx mori* are the most widely used silk protein source. Cocoons consist of water-soluble small globular protein sericin and fibrous fibroin protein. Cocoons mostly consist of fibroin protein. Silk fibroin (SF) gives structural and mechanical stability to cocoon. The major advantage of silk fibroin compared to other natural biopolymers is its excellent mechanical property with advantages of good biocompatibility, water based processing, biodegradability and the presence of easy accessible chemical groups for functional modifications (Kundu et al., 2013).

SF was used in tissue engineering applications of many different tissues, such as cartilage (Baek et al. 2008), vascular (Causin et al., 2011), cardiac (Yang et al., 2009), ocular (Kundu et al, 2012). In addition to these, SF has been widely used in bone tissue engineering. In a recent study by Chen et al. (2014), collagen-silk fibroin/hydroxyapatite

nanocomposites were evaluated and they revealed that involvement of SF improved the composite with higher elastic modulus compared to collagen-hydroxyapatite nanocomposites. They also showed a good biocompatibility with culture of MG63 cells. In another study, Kim et al. studied electrospun poly (ϵ -caprolactone) PCL nano/microfibrous composite scaffolds and they showed that SF addition to the scaffold provided a suitable environment for hMSC proliferation, adhesion, and differentiation into osteoblasts *in vitro*. These studies also verify the potential of SF for use in bone regeneration.

1.5.3. Gelatin

Gelatin (GEL) is a natural polymer that is derived from collagen, and is commonly used for pharmaceutical and medical applications because of its biodegradability and biocompatibility in physiological environments (Angele et al., 1999). GEL is a low cost material and is obtained from bones and skins generated as waste during animal slaughtering and processing (Nur Hanani et al., 2012). Thus, it is a well-known polymer as a biomaterial for tissue engineering applications as it has been studied for long time.

Gel formation of GEL is mainly associated with structure, molecular size and temperature. The solutions of GEL are colloidal solutions (sols) as the structure of GEL is composed of polymer chains of different lengths. When GEL solution is cooled the mobile molecules aggregate and these sols convert to gels. This process is thermo-reversible; GEL gels melt by raising the temperature (Schrieber and Gareis, 2007; Gómez-Guillén et al., 2011).

GEL has been extensively used in many areas such as food, pharmaceutical, medical and cosmetic industries. It found its main application in the food industry. GEL has been also used in pharmaceutical and medicine industries successfully in the forms of capsules or coatings (Schrieber and Gareis, 2007). GEL has been used in various applications in a

variety of forms for tissue engineering. Moreover, in the review of Park et al. (2012) it is stated that gelatin is one of the mostly used material in microencapsulation method. In the study of Binulal et al. nanofibrous (PCL)/gelatin scaffolds showed good wettability, bioactivity, and controlled degradability for bone tissue engineering applications.

1.6. Aim of the Study

By their small size and spherical shape, it is possible to prepare an injectable cell carrier system to repair bone defects conveniently with small incisions. In this study, we aimed to develop PULL based cell carriers for bone tissue engineering applications. In the first part of the study, silk fibroin coating and surface mineralization of the porous microspheres were used as different approaches to increase cell adhesion properties and cytocompatibility. Porous pullulan microspheres were seeded with SaOs-2 cells and proliferation and osteogenic differentiation of the seeded cells were investigated. In the second part of the study, PULL/GEL/ALG microspheres were fabricated for microencapsulation of human urine derived stem cells. The cell viabilities of microspheres were determined.

CHAPTER 2

MATERIALS & METHODS

2.1 Materials

Pullulan (PULL, Mw, 200 kDa) was provided by Kale Kimya Group, the distributor of Hayashibara Inc. (Okayama, Japan) in Turkey. Mineral oil was used as oil phase in microsphere preparation. Sodium carbonate, sodium periodate and sodium borohydrate were from Riedel-de Haen (Germany). Keratinocyte serum free medium (KSFM Invitrogen, USA), Dulbecco's Modified Eagle's Medium (DMEM) low glucose (1 g/L) with L-glutamine, DMEM high glucose (4.5 g/L) with L-glutamine, heat inactivated fetal bovine serum (FBS), trypsin EDTA and penicillin/streptomycin were purchased from Biochrom (Germany). Dimethyl sulfoxide (DMSO) and Triton X-100 were supplied by AppliChem GmbH (Germany). Non-essential amino acid solution was purchased from Sigma-Aldrich (Germany). Alamar Blue was obtained from Invitrogen (USA). Bovine serum albumin (BSA), biconchonic acid (BCA) reagent were the products of Sigma (Germany). Trisodium trimetaphosphate (STMP), sodium hydroxide and calcium carbonate were purchased from Sigma Aldrich, (USA). Gelatin (Type-A from porcine skin), sodium alginate, o-cresolphthalein complexone and 2-amino, 2-methyl, 1-propanol (AMP) were the products of Sigma (USA). Fluorescein isothiocyanite (FITC) and rhodamine B isothiocyanite (RBITC) were obtained from Aldrich (USA). All other chemicals were purchased from Sigma and Merck (New Jersey, U.S.A.).

PART I:

POROUS MICROSPHERE PREPARATION

2.2.Porous PULL Microsphere Preparation and Characterization

Water-in-oil emulsion method was used for the preparation of microspheres. PULL (15 w/v %) and STMP (7.1 w/v %) were dissolved in 2 mL distilled water at RT and a homogenous solution was obtained by stirring. Calcium carbonate powder (90 mg, mean size of 20 μm) was then suspended in the mixture and NaOH powder (8 % final concentration) was added to start crosslinking reaction. The mixture was added dropwise into mineral oil (50 mL) in a round bottom flask under continuous stirring at 500 rpm with an overhead stirrer (Heidolph RZR 2051, Germany) (Figure 2.1). Prior to addition of water phase Span 80 and Tween 80 (each 50 mg) were added as surfactant. After stirring for 4 h at room temperature, the emulsion was filtered through a 70 μm cell strainer to collect the microspheres. The microspheres were then washed on the strainer with acetone several times until oil was removed. These microspheres were dried at room temperature and stored in a desiccator for further use. For generating porous structure, microspheres were treated with excess amount of hydrochloric acid (10 mM), in which the calcium carbonate was dissolved leaving pores behind.

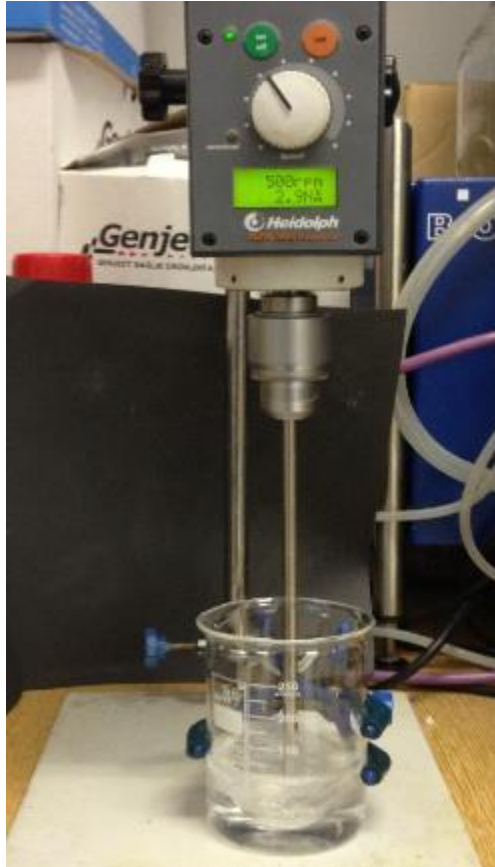


Figure 2. 1 Set up used for PULL microsphere preparation.

In order to obtain stable microspheres, PULL was crosslinked with STMP; NaOH was used as initiator in this reaction. Crosslinking scheme is shown in Figure 2.2; the crosslinking reaction was accompanied by the production of pyrophosphate links (Dulong et al., 2011).

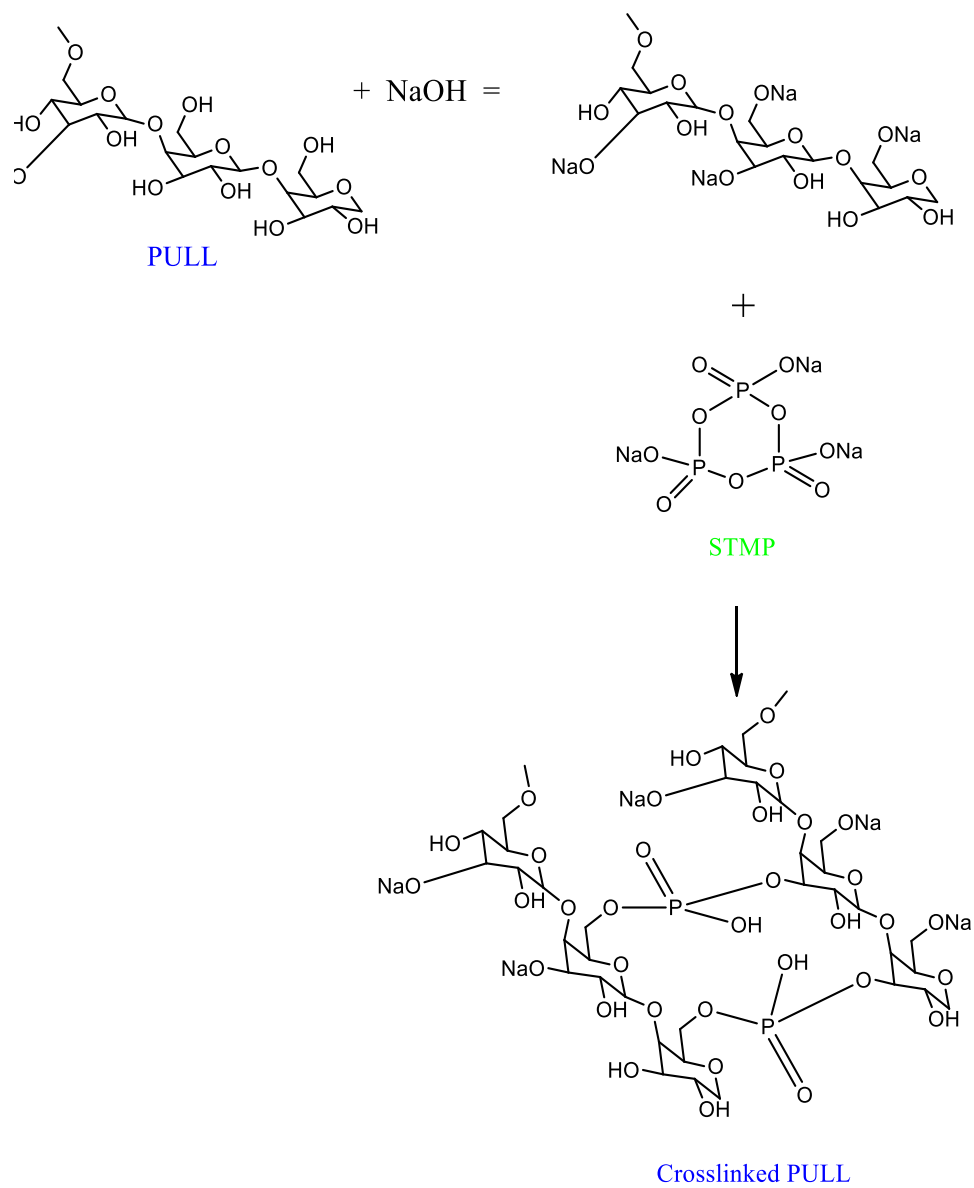


Figure 2. 2. Proposed mechanism for the crosslinking reaction of PULL with STMP

Microscopy images were used to determine the average microsphere size by measuring at least one hundred microspheres from microscopy images using ImageJ software.

2.3. Calcium Content

Calcium content of microspheres was determined to assess the amount of remaining calcium in the microspheres after HCl treatment.

2.3.1. Ash Content Assay

The technique is based on the combustion of all organic materials at high temperatures and leaving the inorganic material behind. The amount of burned organic material can be determined by simply subtracting the ash weight from unburned weight of the material. Ash contents of untreated and HCl treated samples were used to obtain the remaining calcium amounts in microspheres. Firstly, untreated and HCl treated microsphere samples were weighed in ceramic crucibles and they were then burned at 550°C for 6 h (Siddhanta, 2002). The remained or unleached mineral weight was found gravimetrically by subtracting the burned material amount from the initial weight of the dry microspheres.

2.3.2. O-Cresolphthalein Complexone Method

Previously HCl treated and untreated microspheres were dissolved in 6 N HCl overnight. A color reagent was prepared by dissolving o-cresolphthalein complexone (0.01% w/v) in distilled water to which 10% of concentric HCl was added. 25% v/v 2-amino, 2-methyl, 1-propanol (AMP) reagent was mixed with distilled water to make the buffer solution and

pH was adjusted to 10.7 with 6 N HCl. 100 μ L of each sample was added to 1 mL of color reagent and 1 mL of buffer solution. After mixing their optical densities were obtained at 540 nm by using μ Quant TM microplate spectrophotometer (Biotek Instruments Inc., USA). Calcium amounts of the microspheres were determined using the calibration curve prepared with a calcium carbonate in 0-125 mg/L range (Appendix A).

2.4. Micro-Computed Tomography (Micro-CT)

Micro-CT was used to determine the three dimensional porous architecture of PULL microspheres with the side and cross sectional images. Micro-CT was performed on SkyScan micro CT scanner (SkyScan 1172 X-ray microtomograph, Antwerp, Belgium) in Center of Excellence in Biomaterials and Tissue Engineering (BIOMATEN) at METU (Ankara, Turkey).

2.5. Silk Fibroin (SF) Coating of Porous PULL Microspheres

The SF isolation from *Bombyx mori* was done as described in procedure of Rockwood et al. (2011). Briefly, cocoons were cut into small pieces, boiled with 0.02 M Na_2CO_3 for 30 min, and washed with distilled water several times for 60 min to remove sericin proteins from the silk fibers. The degummed silk fibers were then dried overnight at 37°C. Dried fibers were dissolved in 9.3 M lithium bromide at 60°C for 4 h. The dissolved solution was centrifuged at 9000 rpm for 20 min in order to remove undissolved fibers or debris. The regenerated SF solution was dialyzed against deionized water for 48 h with several changes of water to remove the lithium bromide. The final concentration of the SF solution was determined gravimetrically after drying at 60°C. The final concentration was found to be about 8% (w/v).

SF coating was done after hydroxyl groups of PULL on microsphere surface was activated by periodate oxidation according to the procedure by Balmayor et al. (2012). 125 μ L sodium iodate was added to wet PULL microspheres (10 mg/mL of wet microspheres) in a light protected glass vessel. After mixing the suspension for 30 min at room temperature, glycerin (0.1 mL/mL) was added for stopping the reaction. Then, the suspension was stirred slowly for additional 10 min by a magnetic stirrer. The solution was transferred into a dialysis tube and dialyzed against distilled water for two days with several daily changes. The surface oxidized PULL microspheres were stored at 4°C in a light protected glass vessel until conjugation with SF.

SF was added on oxidized wet microspheres and pH was adjusted to 5.5 by using 0.5 M sodium hydroxide. After incubating for 2.5 h at room temperature under slow magnetic stirring, the microspheres were washed and transferred to sodium carbonate buffer (0.5 M, pH 8.5). The microspheres were incubated for 3 h to allow the conjugation between reactive aldehyde groups of PULL and primary amino groups of SF. After washing microspheres repeatedly with distilled water, reduction treatment was done by incubating in sodium borohydride solution (0.05%, w/v) for 1 h to reduce excess reactive aldehyde groups and stabilize imide bonds.

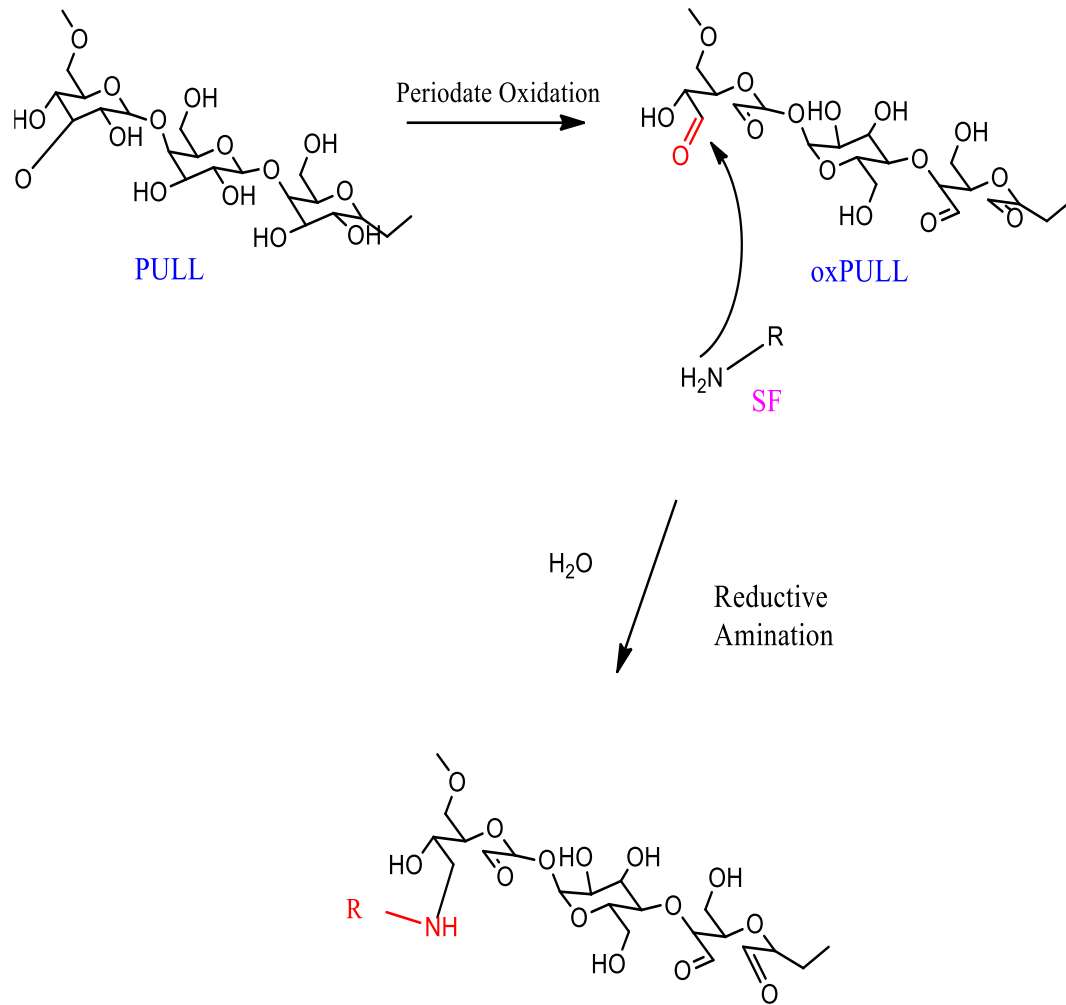


Figure 2. 3 Reaction scheme for the PULL and SF conjugation.

2.5.1. Fluorescent Labelling of PULL and SF

Fluorescence labelling procedure was modified from Lamprecht et al. (2000) (Figure 2.4). In order to label PULL, 10 mL of PULL solution (7.5%) was brought to pH 11 by 1 N NaOH. The fluorescent dye RBITC was dissolved in DMSO at 1 mg/mL of concentration. 100 μ L of dye solution was then added to the PULL solution and stirred at 40°C for 1 h. Then, the reaction was stopped with 50 μ L ethanolamine. For labeling SF, the pH of SF solution (10 mL, 2.5 w/v %) was adjusted to 8.5 and 100 μ L FITC (In DMSO, 1 mg/mL) was added and same procedure was then followed that was used in PULL labeling. FITC labeled SF coated RBITC labelled PULL microspheres were embedded in agarose and 100 μ m sections were taken by cryo-microtome (Leica CM1950, Leica Microsystems, Germany) and these slices were examined under fluorescent microscope (Leica, TCS SPE, Germany).

Labelling of protein (SF)



Labelling of polysaccharide (PULL)

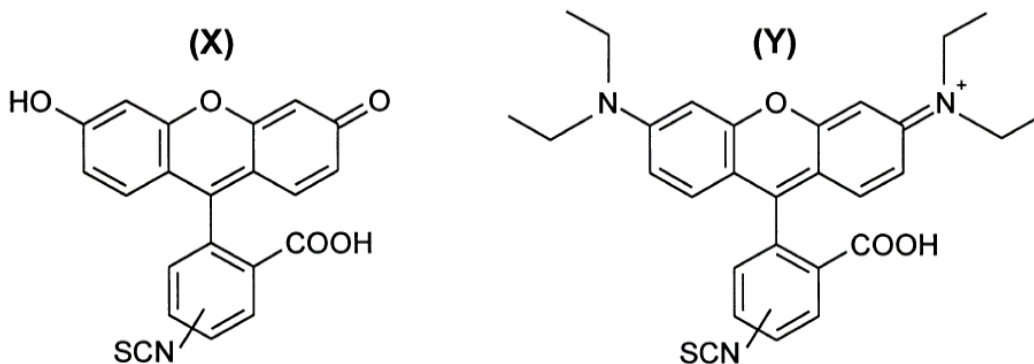
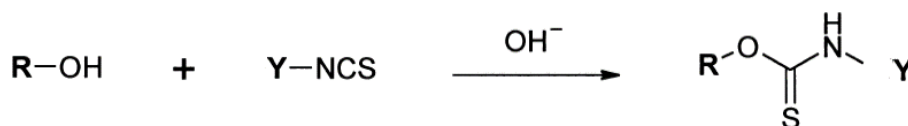


Figure 2. 4. Reaction schemes for the labelling of SF with fluorescein isothiocyanate (X) and PULL with rhodamine isothiocyanate (Y) (Lamprecht et al., 2000).

2.6. SBF Incubation

Biomimetic mineralization of PULL microspheres was done by incubating them in a simulated body fluid (SBF). SBF was prepared according to the method used by Kokubo et al. at pH 7.2 at 37.0°C (2006). The samples were incubated in SBF for 4, 7, and 14

days. Surfaces of naive PULL microspheres and 4, 7 and 14 days SBF incubated PULL microspheres were analyzed by scanning electron microscopy of JXA-8230 SuperProbe Electron Probe microanalyzer (JEOL Inc., USA).

2.6.1. Characterization of SBF Incubated Microspheres

Surface morphology of microspheres was analyzed by scanning electron microscopy. Samples were prepared for analysis by coating with gold using a sputter coating device (Hummler VII, Anatech, Istanbul, Turkey). Mineralization on microspheres was examined by micro and nano SEM devices (Stereoscan S4-10, Cambridge, UK and JSM-6400 Electron Microscope, Jeol Ltd., UK), equipped with NORAN System 6 X-ray Microanalysis System & Semafore Digitizer (Thermo Fisher Scientific Inc., USA) in the Department of Metallurgical and Materials Engineering at METU (Ankara, Turkey) and Quanta 400F Field Emission SEM device (FEI, USA) in Central Laboratory at METU (Ankara, Turkey).

The chemical composition of calcium carbonate sources in microspheres was analyzed with Inductively Coupled Plasma – Mass Spectrometer (ICP-MS, Perkin Elmer DRC II model) analysis. X-Ray diffraction (XRD) analyses were performed to study the calcium content and to verify hydroxyapatite precipitation occurs on the microspheres by using Rigaku X-ray diffractometer (Ultima D/MAX 2200/PC). $\text{CuK}\alpha$ radiation was used at 40 kV voltage and 40 mA current with a scanning angle range $20\text{-}40^\circ$ in 2θ with a scan speed of $2.0^\circ/\text{min}$.

2.7. Cell Culture Studies

Plain, silk fibroin coated and SBF incubated PULL microspheres were sterilized in wet state by UV exposure for 45 min. Firstly, after autoclaving agar solution (1.5 mg/100 mL), and cooling down to 40°C 200 µL agar was put into each well on forty eight well plate and solidified to obtain cell non-adherent plates. Microsphere suspension (300 µL) was added to each well (n=4 for each group). SaOs-2 cells were seeded at a density of 1.5×10^4 cells/cm² onto microspheres in each well and incubated for 1 h for cells to attach. Finally, 300 µL of high glucose DMEM with 10% FBS and 1% penicillin medium was added to wells and incubated at 37°C in 5% CO₂ atmosphere in carbon dioxide incubator (5215 Shel Lab., Cornelius, OR, USA).

2.7.1. Live/Dead Assay (Calcein AM, Propidium Iodide Staining)

The microspheres were gently washed with phosphate-buffered saline (PBS) twice to remove phenol red containing DMEM and detached cells. Then the cells were stained using the live/dead reagent 2 µM propidium iodide (1 mg/mL) solution and 10 µM calcein (1 mg/mL) solution in 5 mL of PBS. After 20 min of incubation the microspheres were washed with PBS again and observed under fluorescent microscope (Leica, TCS SPE, Germany).

2.7.2. Cell Viability Study (Alamar Blue)

Alamar Blue assay was performed after a culture period of 1, 3 and 7 days. At each interval, the culture medium in the 48-well plate was replaced by 200 µL medium, with 15% (v/v) serum and 10% (v/v) Alamar Blue (Invitrogen, USA). The cells were incubated under standard cell culture conditions for 1 to 4 h. Later the optical absorbance of the

medium was read at 600 and 570 nm against a medium of negative control set with Alamar Blue. Blank was normalized by the values of untreated microspheres and the results were presented as cell number according to standard curve constructed using known number of cells (Appendix B).

2.7.3. ALP Assay

After 7 and 14 days of culture, the osteoblastic differentiation of SaOs-2 cells on microspheres was determined by measuring alkaline phosphatase (ALP) activity of cells. The media were removed from the wells and the microspheres with attached cells were washed twice with PBS. Then the 200 μ L/well of 0.1% Triton X-100 with 0.1% w/v sodium azide and 1% protease inhibitor in phosphate buffer was used to lyse the cells on ice. After 30 min of freezing followed by thawing 25 μ L of lysate was added on 200 μ L chromogenic substrate for ALP 10 mM 4-nitrophenyl phosphate dissolved in water with 0.5 M Tris-base and incubated for 30 min at 37°C. The ALP activity of cells was determined by kinetic measurement of the absorbance at 405 nm using enzyme standards of the kit (Sabokbar et al., 1994) (Appendix C). Further, calibration curve constructed with p-nitrophenol in a concentration interval of 25-250 μ M and the enzyme activity for each lysate was normalized by its protein content. . Specific ALP activity was indicated by in nmol/mg protein/min. The protein content of the lysates was determined by bicinchoninic acid assay (bicinchoninic acid assay - B) using the calibration constructed with bovine serum albumin (BSA) (0 to 12 mg /mL) (Appendix D).

2.8.Degradation Study

For degradation studies, 50 mg dry microspheres (n=3) were put into 4 mL phosphate buffered saline (PBS, 0.1 M, pH 7.2) solution at 37°C in water bath (Nüve Bath NB 5, Turkey). Wet weights of the samples and pH values of PBS were determined at the end of each time period. Weight loss was calculated according to the equation below.

$$\text{Weight Loss (\%)} = \frac{W_0 - W_1}{W_0} * 100$$

W₀: Initial weight of the sample (g)

W₁: Weight of the sample at a time point (g)

2.9. Measurement of Stiffness

For mechanical testing, microsphere suspensions of each group (n=3) were centrifuged at various centrifugal forces between 100 and 3500. A set of 100 microspheres was examined under the microscope and the number of deformed microspheres was counted.

PART II:

MICROENCAPSULATION

2.10. Periodate Oxidation of PULL

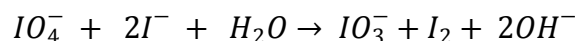
Sodium periodate oxidation of PULL was carried out to form aldehyde groups on PULL chains which eventually can be crosslinked with gelatin by using, borax as crosslinker. PULL (1 g) was dissolved in 8 mL distilled water (total volume). The solution was placed in a light protected glass vessel and 0.125 mL of sodium iodate (100 mg/mL) was added per mL of PULL solution. After incubating at room temperature for 30 min under slow magnetic stirring, glycerin (0.1 mL/mL) solution was added and stirred for additional 10 min. The solution was transferred into a dialysis tube and dialyzed against distilled water for 2 days with several daily changes. The oxidized PULL (oxPULL) solution was stored at 4°C in a light protected glass vessel until being freeze-dried for further use (Hermanson, 1997; Balmayor et al, 2012).

2.10.1. Fourier Transform Infrared Spectroscopy - Attenuated Total Reflectance (FTIR-ATR)

FTIR- ATR analyses were conducted to determine periodate oxidation of PULL via a spectrometer of PerkinElmer L1050002 series (Perkin Elmer, Inc., UK) using spectrum 100/100N software program in transmission mode. The analysis was performed within the wavelength range 400-4000 cm^{-1} , with a resolution of 4 cm^{-1} . The spectra of all samples were corrected for background and atmosphere inside the FTIR.

2.10.2. Iodometric Titration

The degree of oxidation was determined by measuring the unconsumed periodate by iodometric titration (Balakrishnan et al., 2005). Three 5 mL aliquot samples of the oxidation reaction mixture were neutralized with 10 mL of 10% sodium bicarbonate solution. Iodine was liberated by the addition 2 mL of 20% potassium iodide solution. This was kept under dark for 15 min and liberated iodine was then titrated with standardized sodium thiosulphate solution using starch as the indicator. The amount of excess periodate was found according to the chemical reaction formula below.



2.11. Isolation of Urine Derived Stem Cells

With the consent of Middle East Technical University Human Subjects Ethic Committee (Appendix E), urine derived stem cells were isolated from spontaneously voided healthy human urine. The procedure for the isolation of urine derived cells was obtained from previously used studies (Zhang et al., 2008; Bharadvaj et al., 2010; Liu et al., 2014). The procedure is follows; sterile mid-stream urine samples were centrifuged at 2000 rpm for 5 min, then cells were rinsed with PBS and they were cultivated in 6 well plates in a mixture of 1:1 ratio of Keratinocyte serum free medium (KSFM) and Embryonic fibroblast medium (EFM). EFM consists of Dulbecco's modified Eagle's medium (DMEM), heat inactivated fetal bovine serum (HI-FBS, 10% v/v), and 1% non-essential amino acids and was supplemented with penicillin/streptomycin (100 units/mL), 5 ng/mL epidermal growth factor (EGF) and 50 ng/mL bovine pituitary extract (BPE). Urine derived stem cells were cultured at 37°C in 5% CO₂ incubator (5215, Shel Lab, USA).

Every day, the cultured cells were controlled and after the appearance of the first cells medium was changed regularly every third day. When cells reached to 80% confluency, they were passaged at a ratio of 3:1 using 0.1% trypsin EDTA.

2.12. Cell Encapsulation

Cell entrapped microspheres were prepared by single emulsion by manual shaking of oxPULL (10%) / gelatin (GEL) (15%) / alginate (ALG) (1%) solution containing 0.125 M borax and cells. Firstly, 0.28 M borax and 2% ALG were dissolved in 20% oxPULL and in another container 30% GEL was dissolved in distilled water at 40°C. These solutions were autoclaved after preparation. Prior to cell encapsulation, the solutions were put in 37°C water bath. Each solution (200 µL) and 50 µL of cell suspension (10^6 cells/mL) were mixed and added on sterile mineral oil. 50 µL Tween 80 was used as surfactant in the oil phase. As the crosslinking is fast, hand shaking started immediately after the addition of mixture onto the mineral oil. The crosslinking mechanism for oxPULL and GEL is given in Figure 2.4.

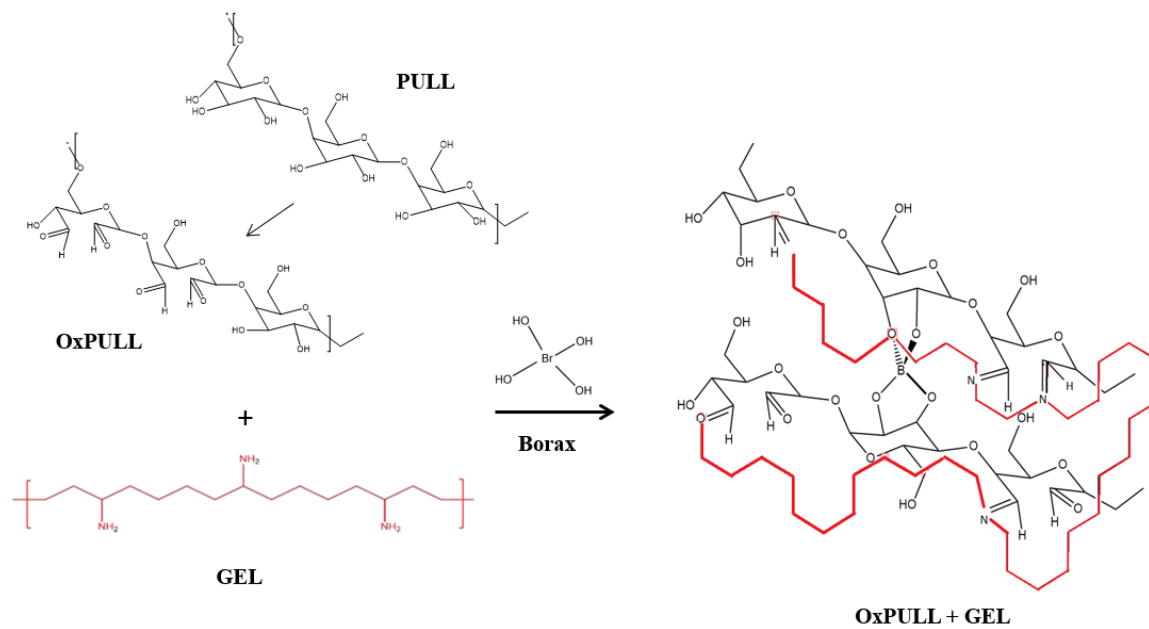


Figure 2. 5 Crosslinking mechanism of gelatin (GEL) and oxidized pullulan (oxPULL).

This was followed by removal of oil and addition of CaCl_2 solution with shaking at 300 rpm by using orbital shaker under (BOECO OS-20, UK) ice for 10 min. Later, microspheres were washed with buffer (0.9% NaCl, 0.1M CaCl_2 0.1M Tris) and coated with poly (L) lysine for stabilization of the microspheres (Figure 5).

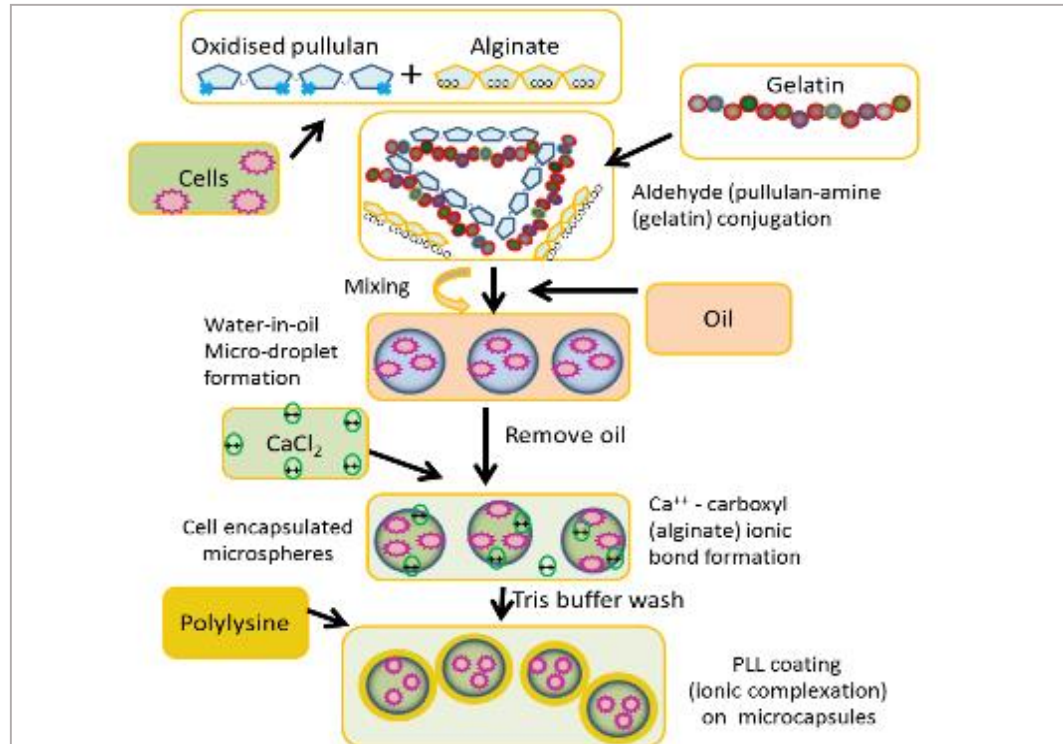


Figure 2. 6 Scheme for encapsulation method for PULL/ALG/GEL blend.

2.13. Cell Culture

2.13.1. Live/Dead Assay (Calcein AM, Propidium Iodide Staining)

The microspheres were gently washed with phosphate-buffered saline (PBS) twice to remove phenol red containing DMEM and detached cells. Then the same procedure in Section 2.7.1. was followed.

2.13.2. Cell Viability Study (Alamar Blue)

Alamar Blue assay was performed after a culture period of 1 and 3 days. At each interval, the culture medium in the 6-well plate was replaced by 2 mL medium, with 15% (v/v) serum and 10% (v/v) Alamar Blue (Invitrogen, USA). The cells were incubated under standard cell culture conditions for 1 to 4 h. Later the optical absorbance of the medium was read at 600 and 570 nm against a medium of negative control set with Alamar Blue. Blank was normalized by the values of untreated microspheres and the results were presented as cell number according to standard curve constructed using known number of cells (Appendix F).

2.14. Statistical Analysis

All data were expressed as mean \pm standard deviation. SPSS-20 (SPSS Inc.) software is used for the one-way analysis of variance (ANOVA), with Tukey's multiple comparison test. Differences were considered as significant for $p \leq 0.05$.

CHAPTER 3

RESULTS AND DISCUSSION

PART I:

POROUS MICROSPHERE PREPARATION

3.1 Porous PULL Microsphere Preparation and Characterization

The primary factors that determine the kinetics of crosslinking reaction are the concentrations of polymer, crosslinking agent and initiator together with the environmental factors such as temperature. In this study, PULL was crosslinked by STMP with alkaline (NaOH) catalysis. The gelling time of PULL was adjusted by mixing different concentrations of the agents of crosslinking and the polymer. As previously recorded by Lack et al. (2004) increasing amount of PULL, STMP and NaOH decreases the gelling time. We intended to keep the gelling time around 10 minutes in order to be able to add the solution into oil phase drop by drop to form an emulsion. Fast gelling of PULL disabled dropping the solution into oil phase. Thus, PULL, STMP and NaOH concentrations were chosen to a final concentration to 15%, 7.1% and 0.8% (w/v), respectively to obtain the gelling time in desired range (Table 3.1.).

Table 3. 1 Gelation times of PULL prepared by using varying concentrations of PULL, STMP and NaOH.

Weight %			Gelling Time (min.)
PULL	STMP	NaOH	
15	7.1	0.4	35-45
15	7.1	0.8	10-12
15	3.5	0.4	>240
15	3.5	0.8	>150
7.5	7.1	0.8	35-45
7.5	3.5	0.8	>150

Later, different rotation speeds were applied to polymer in oil through head propeller and the effects of rotation speed on size and shape of the resulting microspheres were observed. The rotation speeds between 400-700 rpm were surveyed. Between the values 400-500 rpm, the spherical shape was not achieved, microstructures with deformed spherical geometries were produced. Beyond 500 rpm, as also previously reported by Jain et al. (2004), diameter of the microsphere decreased with increasing rotation speed. Therefore, we used 500 rpm for microsphere production for the rest of studies.

In the review of Sahil et al. (2011), it is reported that average size of spherical cell microcarrier systems varies between 200- 350 μm depending on the method used. Natesan et al. (2010) used water-in-oil emulsion to produce chitosan microspheres for cell delivery and showed that the size of the microspheres was mostly (>90%) in the range of 175–250 μm . We also used water-in-oil emulsion and, aimed to obtain microspheres with sizes around 200 μm , which was achieved at 500 rpm rotation speed.

Tween 80 and Span 80 were used as surfactants in the oil and water phases of the emulsion, respectively. The effect of different amounts of both surfactants were analysed to conserve the best shape, size and stability of pullulan microspheres. As stated by Pachua et al. (2009), microsphere diameter decreases by increasing surfactant amount. However, absence of either Tween 80 or Span 80 created problems in preserving stability and spherical shape of the resulting microspheres. Also lower concentrations than 1 mg/mL of both surfactants did not provide required stability in the resultant microspheres. To produce larger sized microspheres without compromising the high stability 1 mg/mL of each surfactant was used in the preparation of the PULL microspheres.

Apart from the rotation time crosslinking time of the droplets in oil phase is another parameter for microsphere preparation. The spherical shape was obtained by optimizing the rotation time, which should be at least 4 h. Less than 4 h of rotation, fragile or irregular shaped microspheres were obtained due to incomplete crosslinking and agglomeration. As also reported in literature, the timing is crucial as the mechanical properties may change by the crosslinking process of the polymer in the emulsion (Shu&Zhu, 2002).

After all these parameters were optimized, the average size for PULL microspheres was determined to be about 150 μm in wet state. It is clearly visible in Figure 3.1 that produced microspheres had spherical shape and homogenous size distribution.

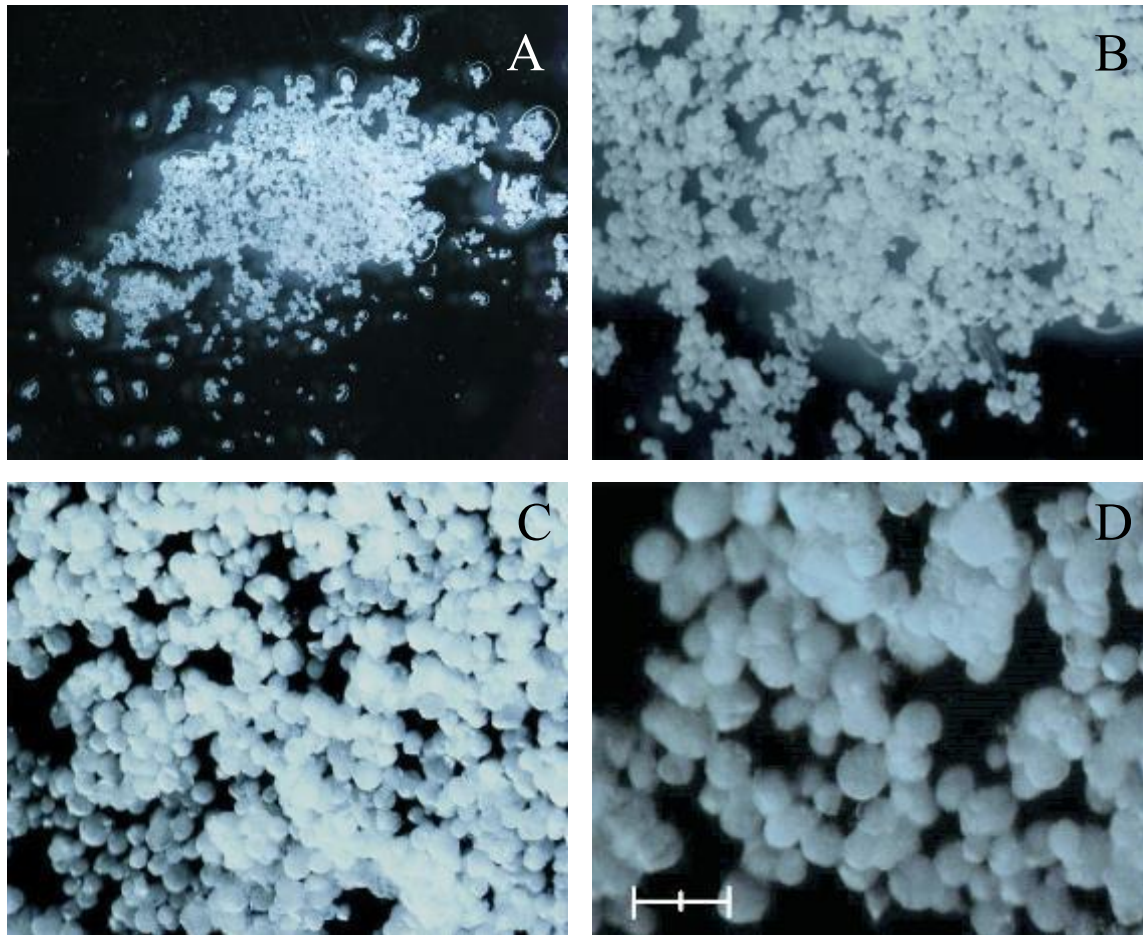


Figure 3. 1 Stereomicroscope images of crosslinked PULL microspheres produced by water-in-oil emulsion at 500 rpm rotation speed. (A) 1 X (B) 4X, (C) 6X (D) 11.5X scale bar: 200 μm .

Designing a cell carrier system is a complex and challenging task as it includes architecture, porosity, mechanical properties, surface properties and degradation properties of the carrier (Hutmacher et al., 2004). Being an essential part of cell carrier design, porosity plays an important role for the optimal interaction of adhered cells with

the carrier. Specifically, porosity in terms of pore magnitude, the pore size distribution, and its interconnectivity is an important parameter. Size of the pores determines the cells seeding efficiency to the scaffold; small pores prevent the cells from penetrating into the scaffold, while too large pores prevent cell attachment due to reduced available ligand density around the cell (Freyman et al., 2001). In our study, for maximizing the cell attachment and growth of cells, porous structures with adequate pore size are aimed in microcarrier systems. Here, enhancement porosity in the microspheres was achieved by using the porogen leaching method.

NaCl, KCl and CaCO₃ minerals were tested as porogen in PULL microspheres. In literature, these salts are frequently used porogens for tissue engineering purposes. To illustrate, in a recent study NaCl was used by Fang et al. (2015) in order to form a porous structure on poly(γ -benzyl-L-glutamate) microspheres for cartilage tissue engineering, KCl was leached from poly(D,L-lactic acid) scaffolds to increase the bone cell ingrowth in the scaffold by introducing pores (Yu & Fan, 2008) and Du et al. (2010) used CaCO₃ in agarose to form a superporous structure in the microbeads.

We started by investigating the porogens, NaCl and KCl salts for preparing the porous microspheres. They were added at a concentration of 5% and 10% of PULL (w/w). Although the average diameters of microsphere samples containing 5% of NaCl and KCl were around 140 μ m, which was a close value to our optimum reached size (Figures 3.2 and 3.3), porous structures could not be observed. Thus, the concentration was increased to 10% to observe the difference.

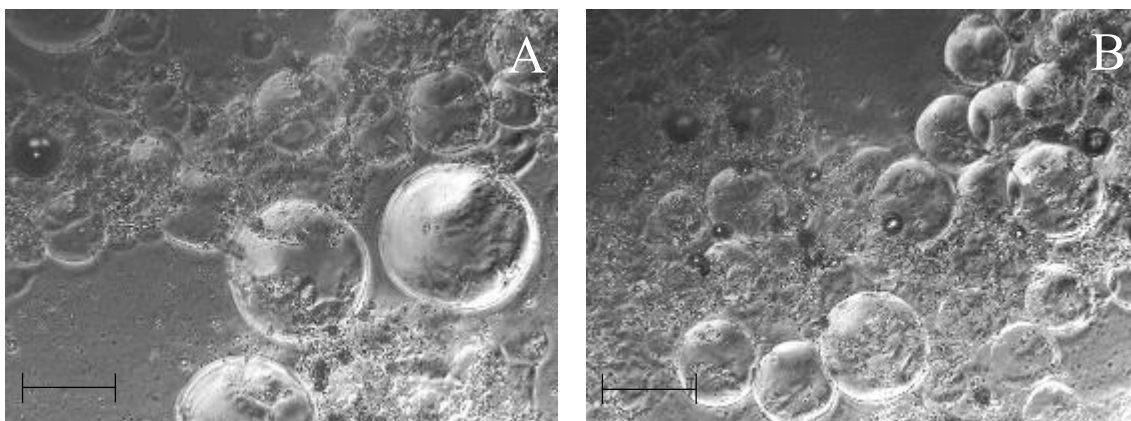


Figure 3. 2 Light microscopy images of pullulan microspheres with 5% (w/w) KCl as porogen. Magnification 40X Scale bar: 200 μm .

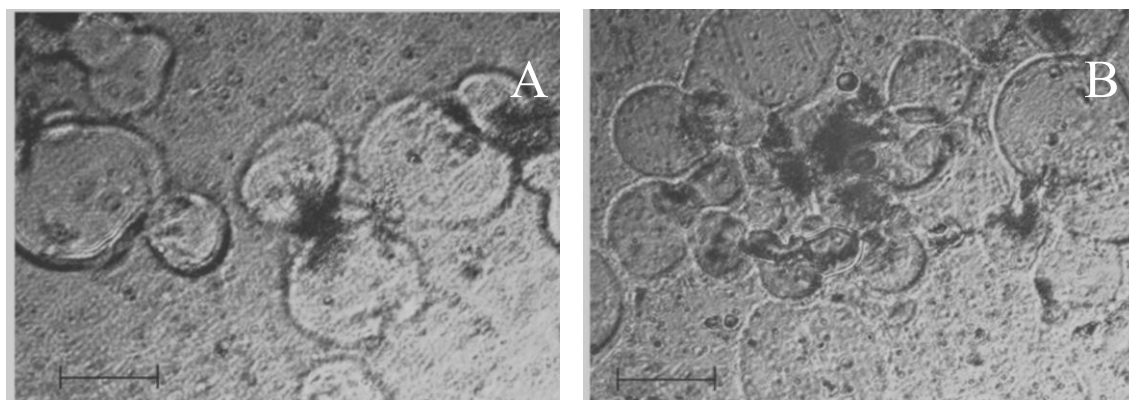


Figure 3. 3 Light microscopy images of pullulan microspheres with 5% (w/w) NaCl as porogen. Magnification 10X. Scale bar: 100 μm

NaCl and KCl are ionic salts and they could dissolve fast in viscous polymer solution. When water was added for porogen leaching, large salt crystals disintegrated the microspheres while dissolving them from inner parts. As seen on Figure 3.4. the microspheres were disintegrated into small pieces. The crystal sizes may be too large or PULL microsphere structure may be fragile for this process.



Figure 3. 4 Light reflection microscopy image of PULL microspheres with 10% (w/w) NaCl porogen (11.25 X magnification) after water leaching.

CaCO₃ mineral was another alternative porogen as its solubility in water is low compared with the previous salts used as porogens. CaCO₃ particles had an average size of 20 μm (Figure 3.5) and it can be used for obtaining porous structure in gels. Pore size can be an important factor for the cell attachment depending on the cell size. It was decided that

CaCO₃ porogen with about 20 μm particle size would be suitable for creating pores on and in the microspheres of about 150 μm and large enough for bone cells to infiltrate.

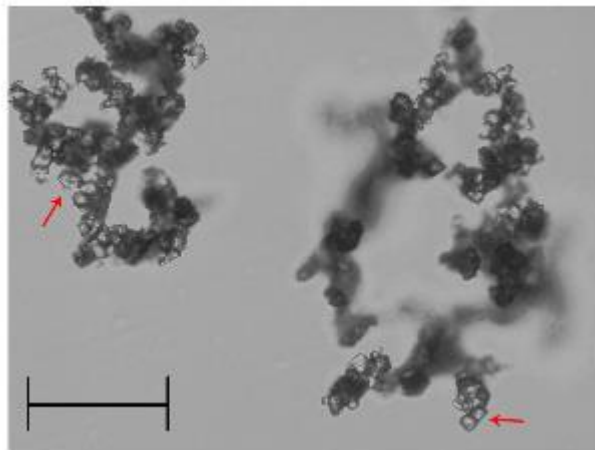


Figure 3. 5 CaCO₃ particles used as porogen had a size about 20 μm. Scale bar: 100 μm.

Leaching CaCO₃ out from the microspheres was done by incubating them in 10 mM HCl for 2 h at room temperature as done before by Du et al. (2010). Later, the microspheres were washed several times with distilled water to remove unreacted HCl and ions. Unlike NaCl and KCl, removal of CaCO₃ particles did not disintegrate the microspheres. Different concentrations of CaCO₃ (10, 20 and 30% w/w) were then used during the preparation of microspheres to find the maximum amount of porogen without disintegrating gel structure. Size, shape and porogen distribution of microspheres were analyzed from light microscopy and SEM images (Figures 3.6 and 3.7).

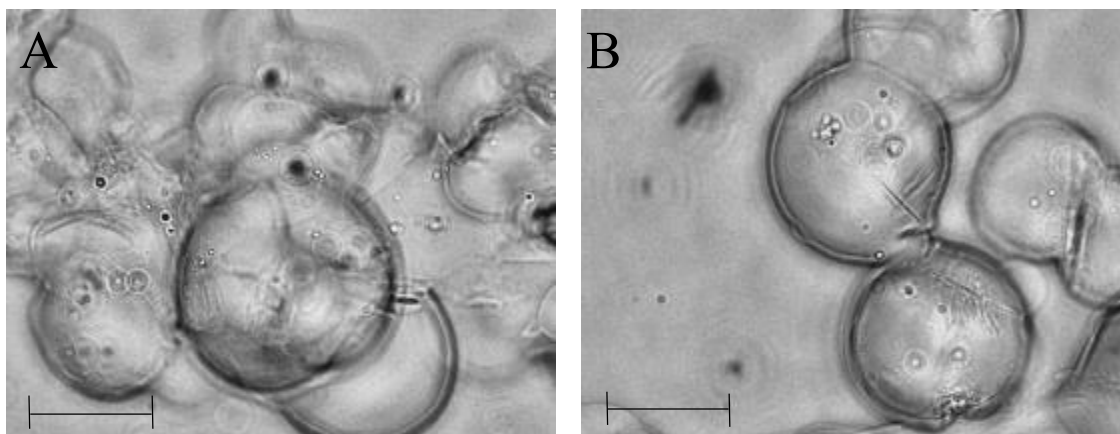


Figure 3. 6 Light microscopy images of 20% calcium carbonate containing (a) and 30% calcium carbonate containing (b) swollen microspheres. Magnification 40X. Scale bars: 100 μm .

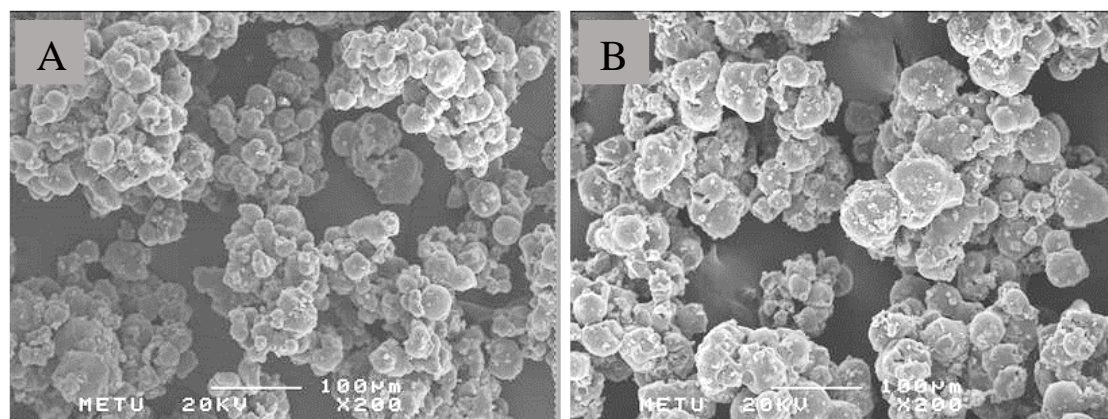


Figure 3. 7 SEM images of (A) 20% calcium carbonate containing and (B) 30% calcium carbonate containing dry PULL microspheres. Magnification 200 X. Scale bars: 100 μm .

The light microscope views of the microspheres in swollen state are shown in Figure 3.6, 20% porogen containing spheres had an average diameter of around 120 μm whereas 30% porogen containing ones were 140 μm in diameter. In Figure 3.7 SEM images of the dry microspheres can be seen. 20% porogen containing spheres had an average diameter of around 43 μm whereas 30% porogen containing ones had an average diameter of around 65 μm . When the amount of calcium carbonate was increased, it directly affected the size of microspheres. The reason for this might be the effect of removal of higher rate of CaCO_3 caused a higher porosity and, consequently higher swelling capacity.

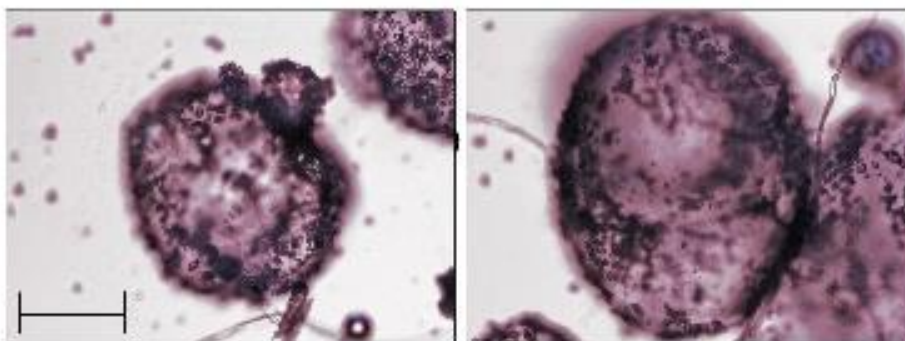


Figure 3. 8. Light microscopy images of HCl treated PULL microspheres with 30% CaCO_3 . Magnification 100X. Scale bar: 100 μm .

In the final optimized formulation, pullulan microspheres had a spherical shape and porous structure with an average diameter of 153 ± 46 (SD) μm after leaching out 30% porogen CaCO_3 . Various characterization tests were conducted on these PULL microspheres and these results will be discussed.

In the last decade, for characterization and evaluation of microstructure of scaffolds, micro-computed tomography (Micro-CT) has been widely used. Furthermore, the clinical potential of the scaffolds was demonstrated in various case studies (i.e., designed scaffolds as well as clinically applied scaffolds) with computed tomography (CT) data because it allows a non-destructive scanning of the samples *in vivo*. The technique was commonly used for hard tissue engineering studies (Tuan et al., 2005; Williams et al., 2005; Kerckhofs et al., 2011). In a similar study, Kim et al. (2009) studied three-dimensional porous poly (ϵ -caprolactone fumarate) (PCLF) scaffolds with porogen sodium chloride and showed that when salt particles were leached out, pore distribution in the scaffold were observed with Micro-CT scanning.

In the current study, porogen containing dry microspheres were analyzed by Micro-CT for determining the CaCO_3 particle distribution in microspheres. Micro-CT images of upper and frontal sections of PULL microspheres showed the particle size distribution of the microspheres (Figure 3.9). The porogen distribution within microspheres was found to be homogenous in the cross-sections of the microspheres.

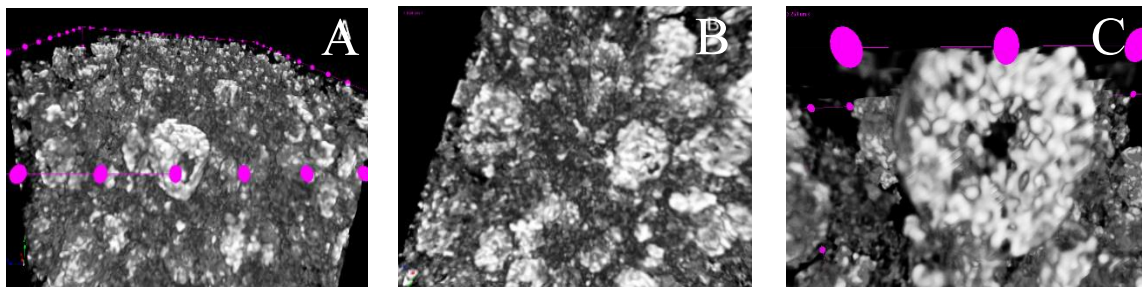


Figure 3. 9 Micro-CT images of (A) upper, (B) frontal section of incorporating pullulan microspheres. (C) Close view of a single microsphere showing its cross-section and internal CaCO_3 particles.

3.1.1. Residual Calcium Content Analysis

The porogen leaching step removes significantly high amount of the CaCO_3 . However, there remains a residual porogen in the deeper parts of the microspheres. Ash content assay was conducted to check the residual calcium content after leaching out the porogen. For this, both untreated and 10 mM HCl treated samples were burned at 550°C for 6 h.

When porogen containing and porogen leached microspheres were burned and remaining residual weights were evaluated, less than 40% of the porogen remained in the microspheres. The samples were weighed out within the ceramic container. Since the weight of residual ash left was significantly smaller compared to the weight of the container, it was not possible to measure accurate values sensitively within the confidence. Thus, the residual porogen amount was quantified with *o*-cresolphthalein complexone method.

According to the *o*-cresolphthalein complexone method the porogen leaching attempt with 10 mM HCl solution resulted with about 25% residual calcium carbonate (CaCO_3) inside the microspheres (Figure 3.10). Similarly, Kim et al. (2009) showed that some salt particles remained in the PCLF scaffolds after leaching out NaCl salt crystals, especially in the core section and the pore morphology of the resulting PCLF scaffolds was mostly cubical.

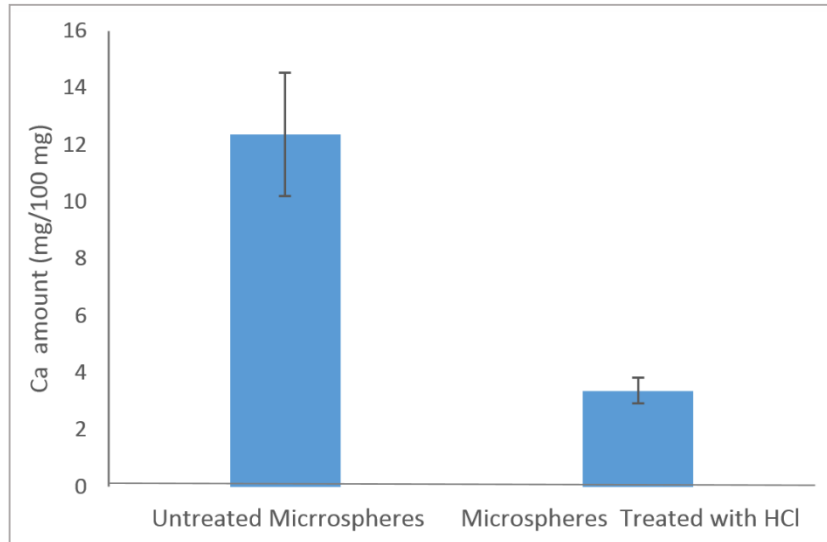


Figure 3. 10 Residual calcium amount within the microspheres obtained by o-cresolphthalein complexone method (n=3).

The remaining calcium carbonate can be useful in further cell attachment, proliferation and differentiation (Kim et al., 2006). Calcium ion can be an important parameter for bone regeneration as the calcium sensing receptors induce the differentiation and mineralization of osteoblast cells (Takaoka et al., 2010; Jung et al., 2010). Moreover, the remaining calcium also would support apatite nucleation on and in the microspheres upon incubation in SBF improving the osteoconductive character. Accordingly, Zhu et al. (2004) showed that the biomaterial surface triggered initial hydroxy apatite nucleation in the presence of calcium ions.

A typical nucleation is explained in five stages; firstly formation of ion clusters and amorphous calcium phosphate (ACP); secondly, stabilization of ACP occurs; then, ACP transforms into HAP via dissolution and crystallization; continues with classical crystal growth of hydroxyapatite (HAP); finally in the 5th stage, HAP aging under a near equilibrium state (Ding et al. 2014). In the first stage of the HAP nucleation, the findings

of Jiang et al. (2013) showed that the residual calcium ion in the native solution is the key to trigger ACP phase transformation in biomineralization that accelerates HAP formation.

3.2. Silk Fibroin (SF) Coating of Porous PULL Microspheres

It has been shown that, silk fibroin enhances the growth of anchorage dependent mammalian cells (Inouye et al., 1998). Similarly, in the present study, we aimed to benefit SF's biological performance to enhance cytocompatibility of pullulan microspheres.

Our first attempt was SF coating PULL microspheres with sonication method. For this, wet PULL microspheres were sonicated in 0.1% SF solution and the samples were examined with scanning electron microscopy after drying.

From the SEM images (Figure 3.11) it was seen that, there were some irregularities on the spheres and the pore-like structures were closed by the fibroin coating, although the average diameter of microspheres did not change significantly compared to uncoated ones. The procedure involved shaking and sonication steps that increase the deposition of silk fibroin on microspheres. Additionally, such coating increases the strength of the coating by silk crystalline β -sheet structure formation. In order not to close the pore-like structures we decided to remove sonication step.

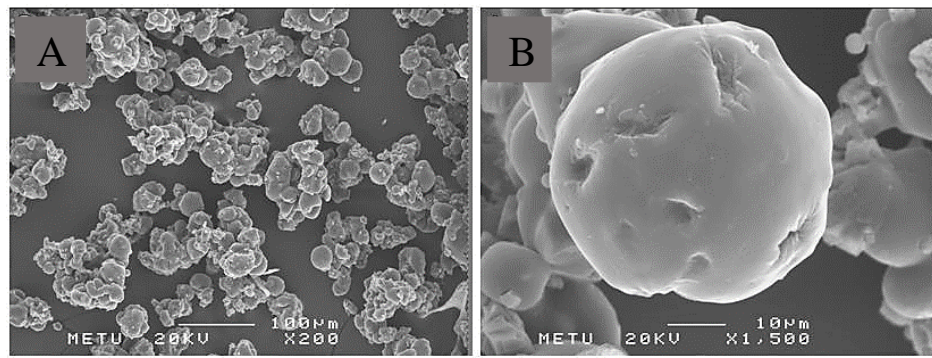


Figure 3. 11 SEM images of 30% calcium carbonate containing dry microspheres coated with silk fibroin.

The periodate oxidation coupled with reductive amination is widely used in biochemistry field as it allows the conjugation of aldehyde and amine groups with amide bonds (Cosenza et al., 2011). The oxidized molecules couple with a primary amine to give an imine with a Schiff's base reaction. This reaction proceeds in high yields at acidic pH and the imine is reduced to give a secondary amine. The reduction reaction is usually carried out using sodium borohydride.

For tissue engineering purposes, polysaccharides are generally modified as in the study of Rinaudo (2011) where methylcellulose was oxidized with periodate and aldehyde functional group rich structure was obtained. The oxidation process improved the flexibility in the backbone of methylcellulose; however, the opening of ring structure of polysaccharide caused a decrease in molecular weight.

Another example for widely used polysaccharide with this procedure is alginate (ALG) (Balakrishnan et al., 2005; Jeon et al., 2011; Kim et al., 2012). In the study by Balakrishnan et al. (2005) low concentrations of oxidized alginate (ADA) were used to crosslink and stabilize gelatin. The study of Balakrishnan et al. reported preparation of an

injectable polymer scaffold with ADA and gelatin polymers. They evaluated the crosslinking procedure and biocompatibility of the final product. A rapid crosslinking of ADA and gelatin scaffold was observed with a 60% weight loss in 5 weeks period. The group suggested that this crosslinking scheme was suitable for in situ gel formation (2005).

In our study, SF was conjugated onto periodate oxidized pullulan microspheres to form a very thin layer of silk fibroin on the microspheres without blocking the pores. The neighboring hydroxyl groups of glucose in pullulan can be oxidized by sodium periodate to dialdehyde groups and the amino residues in silk fibroin can conjugate with these aldehydes via reductive amination and form a hydrogel structure (Pan et al., 2014).

Silk fibroin coating was analyzed by using FITC-labelled fibroin and fluorescent microscopy imaging to check the efficiency of conjugation (Figure 3.12). As seen from the microscopy images the silk fibroin coated homogenously the surface of microspheres that indicated that surface oxidation of pullulan and conjugation procedure were successfully applied.

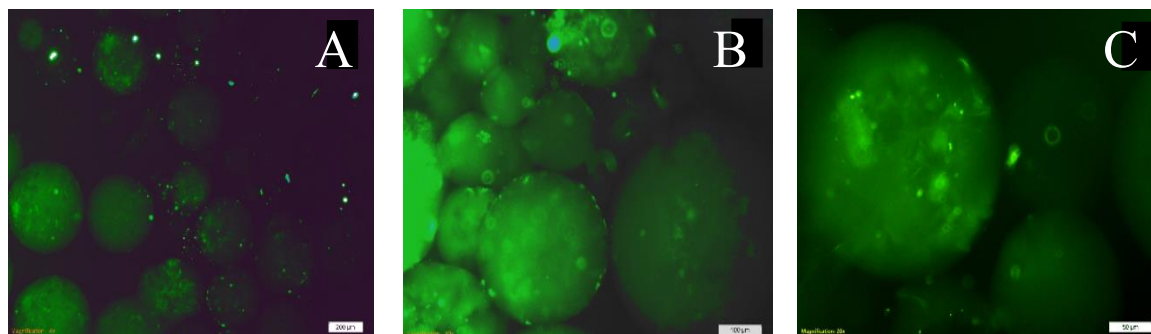


Figure 3. 12 Fluorescence microscopy images of FITC-fibroin coated pullulan microspheres. Magnification 40X (A), 100X (B) and 200X (C).

We checked whether SF coating occurred on non-oxidized surface of PULL microspheres. When the surface of the microspheres was not activated via periodate oxidation, SF could not be adsorbed and achieve coating of the surface of PULL microspheres (Figure 3.14).

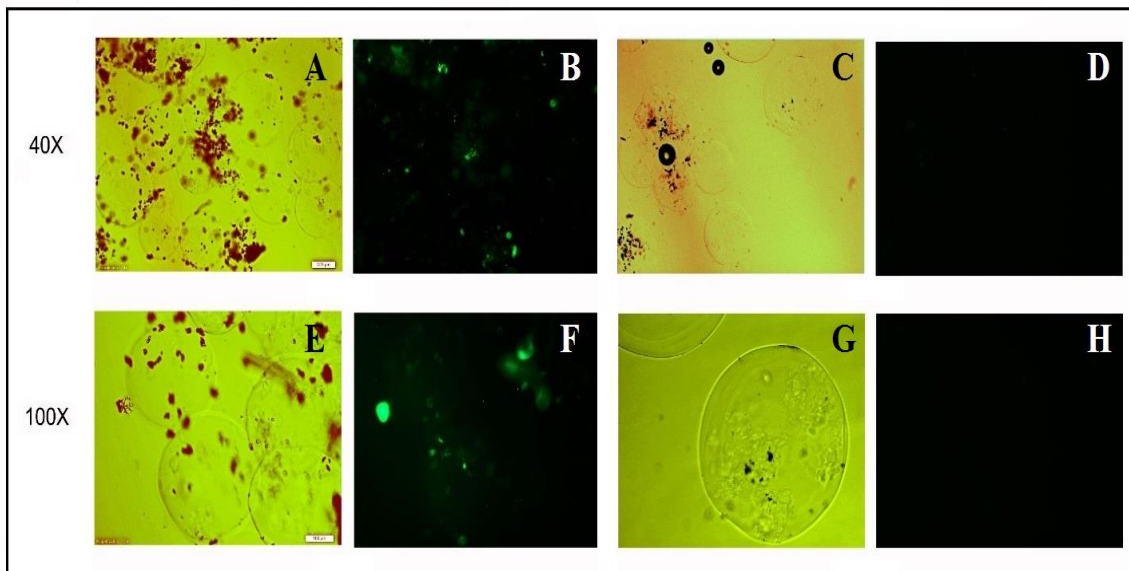


Figure 3. 13 Visible light (A, E) and fluorescence (B, F) microscopy images of surface oxidized microspheres respectively. Visible light (C, G), and fluorescence (D, H) microscope images of non-oxidized pullulan microsphere surfaces are shown after FITC-SF treatment and washing.

FITC and RBITC fluorescent dyes can be simultaneously detected in different fluorescence channels. Thus, PULL microspheres were labelled with RBITC while SF was labelled with FITC before used for coating polymer. Then, after coating the

microsphere with FITC-fibroin fluorescent microscope images were acquired (Figure 3.14).

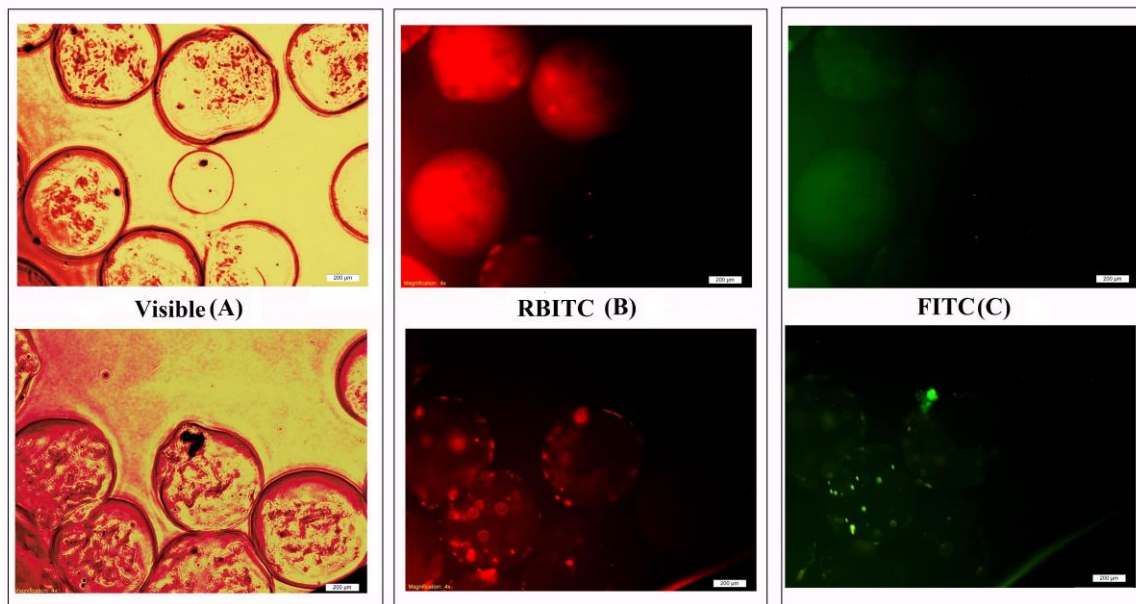


Figure 3. 14 (A) Light transmission (B-C) and fluorescence light microscope images of FITC-labelled SF coated RBITC-labelled PULL microspheres Magnification 40X. Scale bars: 200μm.

Further microscopy analysis was done with cryo-microtome sections of RBITC-labelled pullulan microspheres and FITC-fibroin coating microsphere images to detect both polymers simultaneously (Figure3.15). This technique was used by Lamprecht et al. (1999) to characterize the deposition of fluorescent-labelled gelatin and Arabic gum on microcapsule surface. As shown from cross-sections of the microspheres pullulan was successfully labeled with RBITC (Figure 3.15B) and the FITC-fibroin layer was detected around the microspheres (Figure 3.15C).

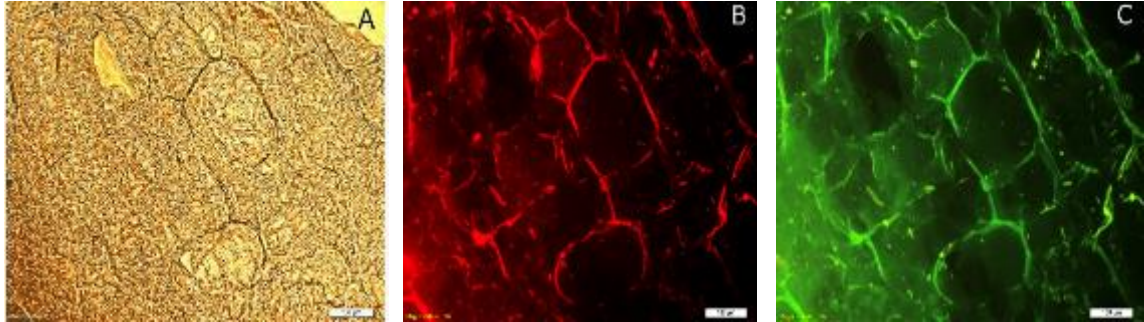


Figure 3. 15 Light transmission (A), fluorescence light microscope of RBITC labelled pullulan microspheres (B) and FITC labelled silk fibroin coating (C) after microtome sectioning.

3.3. Simulated Body Fluid Incubation of PULL Microspheres

The bioactivity of PULL microspheres was studied by incubating in simulated body fluid (SBF) for different incubation periods at 37°C (0, 4, 7 and 14 days). It was previously reported that mineralization of PLGA microspheres in SBF forms similar to the mineralization process of natural bone tissue environment (Kang et al., 2008). The bioactivities were characterized using calcium assay, scanning electron microscopy (SEM), X-ray diffraction (XRD) and Inductively Coupled Plasma Optical Emission Spectrometry (ICP).

Calcium amounts that were determined with o-cresolphthalein complexone method revealed that calcium significantly increased in SBF (Figure 3.16). However, these amounts unexpectedly did not vary significantly for different incubation periods.

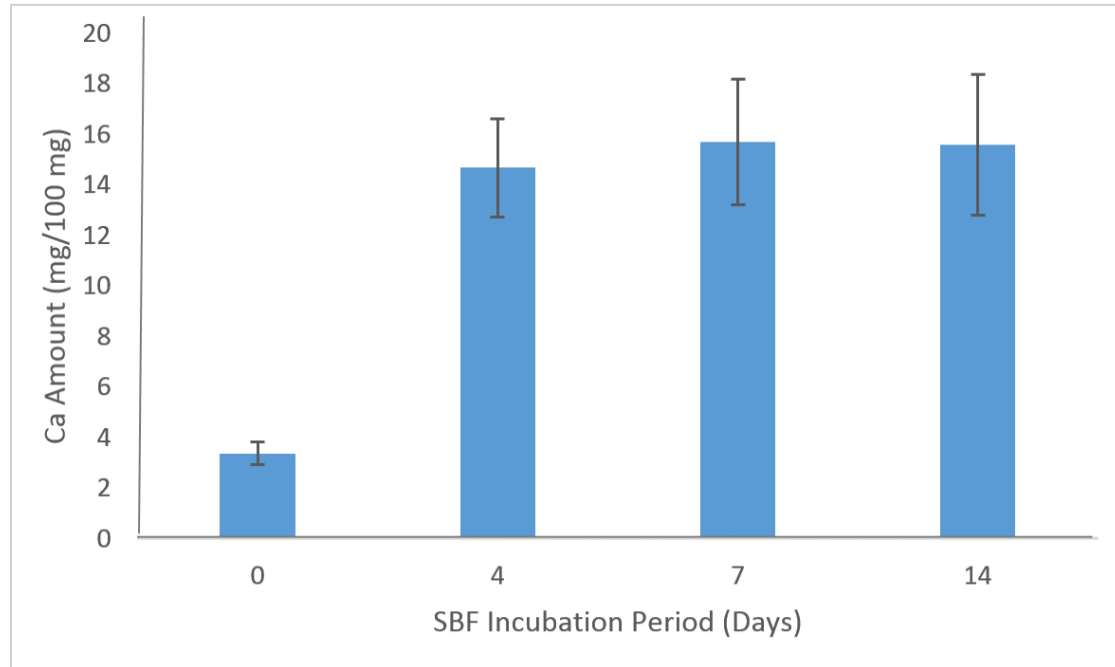


Figure 3. 16 Calcium amount of the plain PULL microspheres and 4, 7 and 14 days SBF incubated microspheres obtained by o-cresolphthalein complexone method (n=3)

Although we did not see a significant increase in the calcium amount, images of calcein stained microspheres revealed that there was a visible increase of mineralization on the surface with the increase of incubation time in SBF as expected. The reason behind this can be the continuous changes in the dissolution and precipitation kinetics of calcium carbonate in the SBF solutions (Liu & Dreybrodt, 1997).

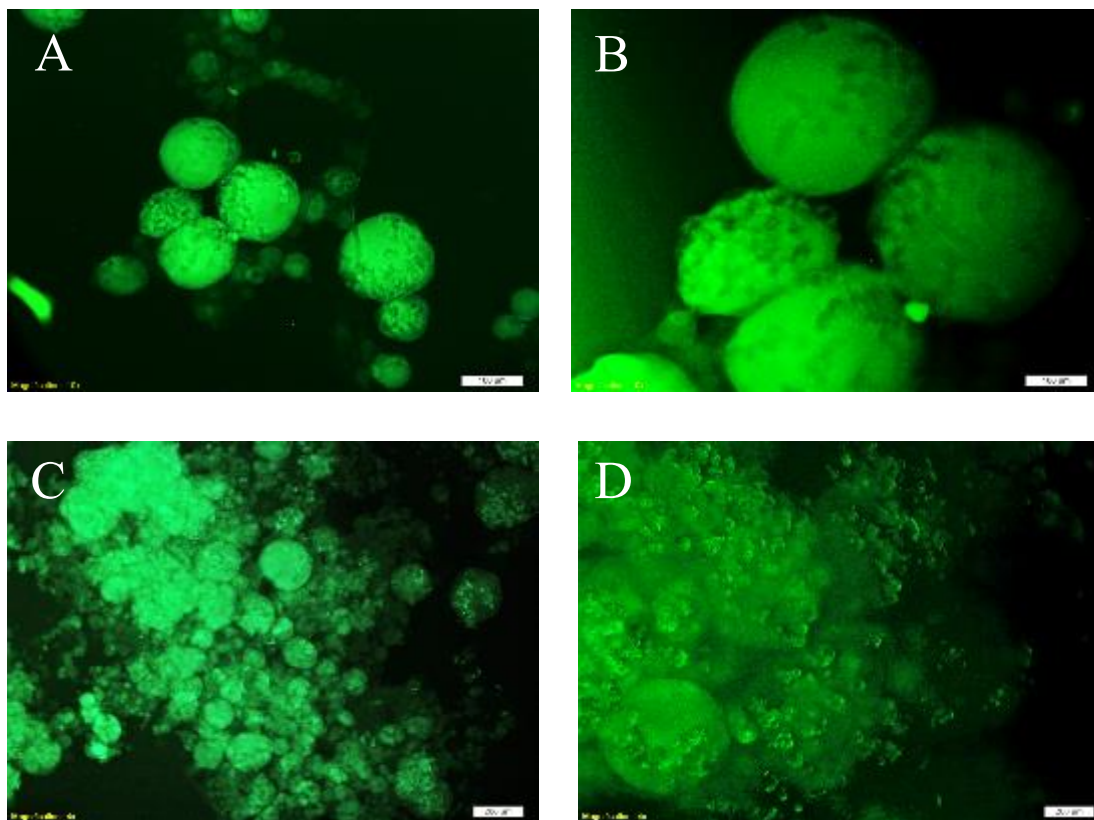


Figure 3. 17 Fluorescence microscope images of calcein stained pullulan microspheres before SBF (A, B) and 14 days of SBF incubation (C, D).

Based on fluorescent microscopy and SEM images (Figures 3.17 and 3.18), it is evident that after incubation in SBF, an apatite layer was formed on the surface of microspheres. Figures 3.17 A, B and 3.18 A showed no apatite formation on microspheres that were not incubated in SBF. Apatite formation occurred extensively in all samples that were incubated in SBF for 14 days (Figure 3.16C and D) and the increase in the apatite like structures on the surface increased with time (4, 7, and 14 days of incubation in SBF) as seen in Figure 3.18 B, C and D, respectively. Besides, there was an increase of apatite like

formations on the surfaces with increasing incubation time in SBF. However, for the sample that was incubated for 14 days in SBF (Figure 3.17 D and Figure 3.18 D), the mineralization process was more accelerated and it was observed that the apatite structures started to make bulks resulting in merging of microspheres. This result supports the findings of Du et al. that; the apatite formation on the surface accelerates after 7 days of incubation in SBF with the increase of nucleation sites (2013). One of the most advantageous properties of microspheres is their injectability and high surface area to volume ratio (Andersen et al., 2012). When the microspheres merge, we lose these properties. Therefore, we used SBF incubation in shaking water bath, but agglomeration was not resolved completely. Hence, we chose 7 days of SBF incubation under static conditions for further tests.

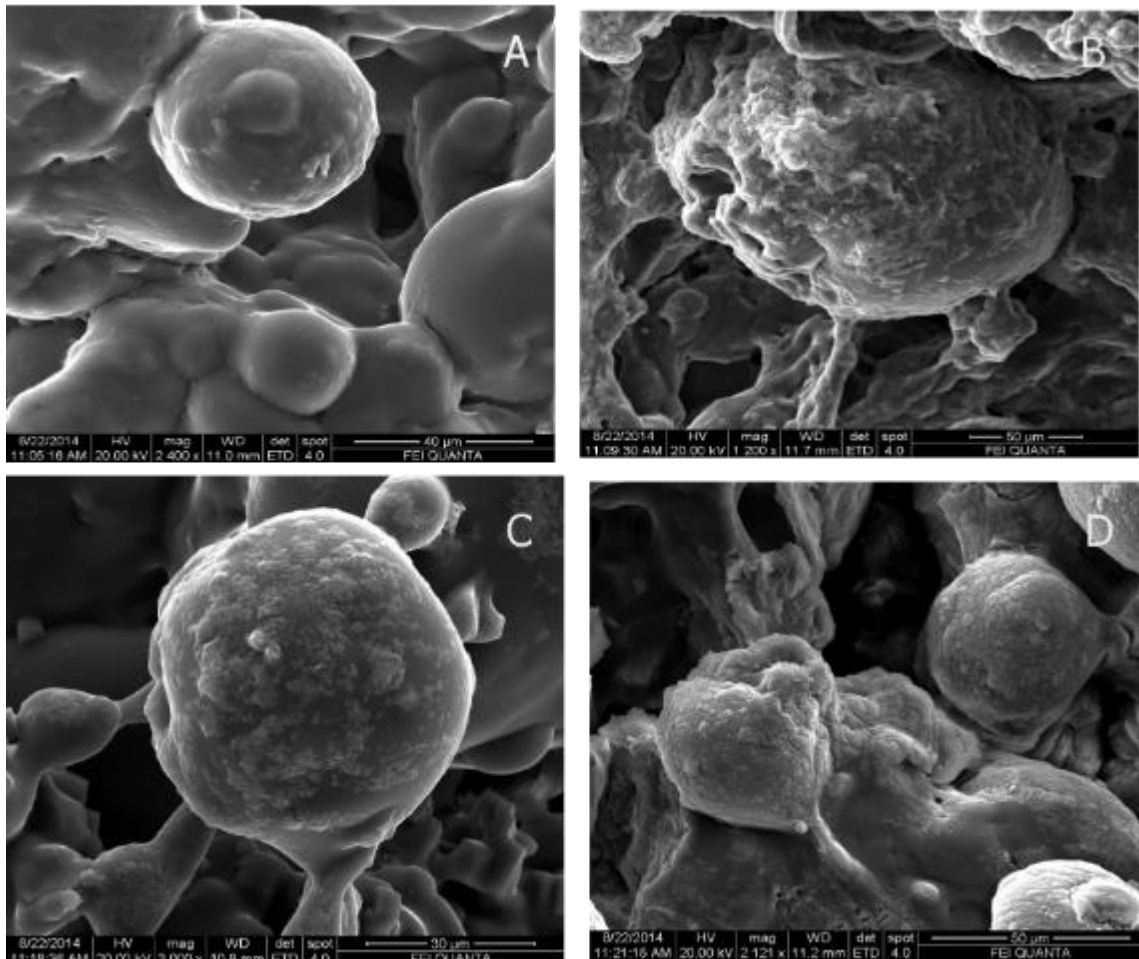


Figure 3. 18 Scanning electron microscopy images of pullulan microspheres that were incubated in SBF for 0 (A), 4 (B), 7 (C) and 14 (D) days at 37°C.

XRD was used to evaluate the phase compositions of microspheres (Figure 3.19). As control group, calcium carbonate free pullulan microspheres were used. The other sample groups were calcium carbonate (as porogen) containing pullulan microspheres with or without, HCl treatment and native pullulan microspheres that were incubated in SBF for 7 days. The result obtained with 7 day SBF incubation of microspheres was comparable

with those in literature, which showed high intensity calcium carbonate and relatively lower apatite peak (Kontoyannis & Vagenas, 2000; Ikawa et al., 2009; Nakai et al., 2012). Although the XRD analysis of 14 day SBF incubated microsphere showed an apatite-like structure peak, the intensity was almost the same when compared to the result from 7 day SBF incubated microspheres. This was an unexpected result as we expected an increase in HAP formation with the increasing incubation time in SBF.

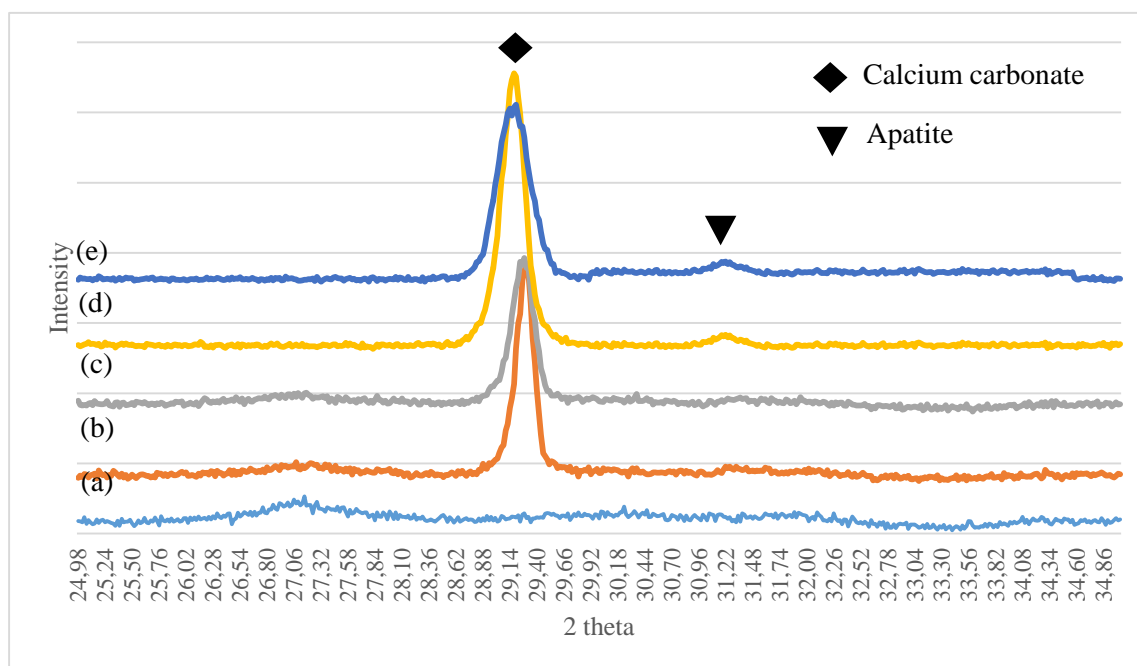


Figure 3. 19 X-ray diffraction pattern of pullulan microsphere samples (a) without porogen CaCO_3 , (b) with porogen CaCO_3 , (c) after HCl treatment, (d) after 7 days SBF incubation and (e) after 14 days SBF incubation.

ICP analyses of the ionic concentrations of SBF for calcium (Ca), phosphorus (P) after immersing PULL microspheres in the SBF are shown in Table 3.2. According to Hart et al. (2005), the Ca concentration of the SBF incubated with silica-calcium phosphate nanocomposite (SCPC) discs drops drastically after the first days of immersion. Then the Ca concentration reached an equilibrium between the dissolution and precipitation reactions at the material-solution interface. After accumulation of Ca on the scaffold surface, the concentration P started to increase and eventually reach a plateau with the equilibrium. However, in our case, the Ca amount of the microspheres dropped and with increase of P on these microspheres, the Ca/P ratio diverged from the expected result of stoichiometric hydroxyapatite Ca/P ratio, which is around 1.67. This unexpected drop of Ca level on the microspheres may be due to rapid dissolution of Ca, which is readily found inner parts of the microspheres as residual porogen CaCO_3 . While some portion of the residual Ca act as nucleation centers for apatite formation by increasing P amount on the microspheres, some of the remaining porogen dissolved in SBF solution.

Table 3. 2 Ca and P analysis results of Inductively Coupled Plasma Optical Emission Spectrometry (ICP).

	<i>PULL Microspheres</i>		<i>SBF</i>	
(mg/L)	Plain Microspheres	Incubated in SBF for 7 Days	Original SBF	After 7 Days Incubation
Ca	136±1.00	56±1.00	108±1	112±1
P	-	62±1.00	31.5±2.3	35.4±1.0

3.4. Size Analysis of Microspheres

Table 3.4 shows the size analysis of four microsphere groups. Similarly, native PULL and 7 days SBF incubated microspheres had average diameter of $153\pm 46\ \mu\text{m}$ and $150\pm 50\ \mu\text{m}$, respectively. However, for the SF coated microspheres there was a significant increase with average diameter of $170\pm 45\ \mu\text{m}$. As a thin layer of mineral coating on the microspheres must have happened, we did not expect a significant difference between plain PULL microspheres and SF coated microspheres. Hence, we also measured the size of surface oxidized PULL microspheres that had average diameter of $171\pm 39\ \mu\text{m}$. The oxidation procedure, which open glucose ring of pullulan during formation of aldehyde groups on the surface of the microspheres, must be the reason of higher diameter of SF coated microspheres.

Similarly, Wang et al. (2005) oxidized the surface of multiwalled carbon nanotubes (MWNT) to generate carboxylic acid, carbonyl and hydroxyl functional groups on the surface. Thus, the surface of MWNT possessed hydrophobic and hydrophilic acidic regions. Likewise, the surface oxidized PULL microspheres, with the carbonyl groups, which is negatively charged because of the oxygen, also had hydrophilic regions. The reason of higher diameter of the surface oxidized and SF coated PULL microspheres can be due to the higher water absorption capacities of these regions.

Table 3. 3 Size analysis of microspheres.

	<i>Size (μm)</i>
Pullulan microspheres	152.83±47.69
Surface oxidized pullulan microspheres	171.34±38.88
Fibroin coated microspheres	169.94±45.44
7 days SBF incubated microspheres	150.14±50.12

3.5. Degradation Analysis

Degradation analysis was done with plain PULL, surface oxidized, SF coated microspheres and 7 days SBF incubated microspheres.

PULL and SBF incubated microspheres showed 7% and 5.5% weight losses, respectively at 14th day. Degradation studies showed that SF coated microspheres lost approximately 12% of their weights at 14th day, which indicated that surface oxidation of PULL microspheres probably caused a faster weight loss (Figure 3.21). Hence, the surface oxidized pullulan microspheres were also observed in degradation studies and the results revealed that oxidized PULL microspheres lost 63% of their weight at the first day and on the 3rd day remaining microspheres also degraded. We previously reported that, surface oxidized PULL microspheres showed relatively higher diameter in the wet state as the functional carbonyl groups around the microsphere tend to increase the water absorption capacity (Wang et al., 2005). Wu et al. reported that high water absorption into surface-modified PLGA scaffolds led to faster degradation (2006). Gpferich (2011) explains this

state as follows; the intrusion of the water into the polymer bulk triggers the chemical polymer degradation, leading to the fragmentation of polymer into oligomers and monomers, which are later released, leading to the weight loss of polymer particles. A study of Wong et al., suggested that PULL plays a major role in hydrogel stability of engineered PULL-collagen composite for the degradation over 3 weeks. The degradation profile showed 59% weight loss in first week and the following week only 11% of weight was retained, which eventually degraded in the third week. In our study, the degradation of all three groups plain, SF coated and 7 days SBF incubated PULL microspheres showed slower degradation rate for the same time intervals, which is a desirable property for bone tissue engineering application.

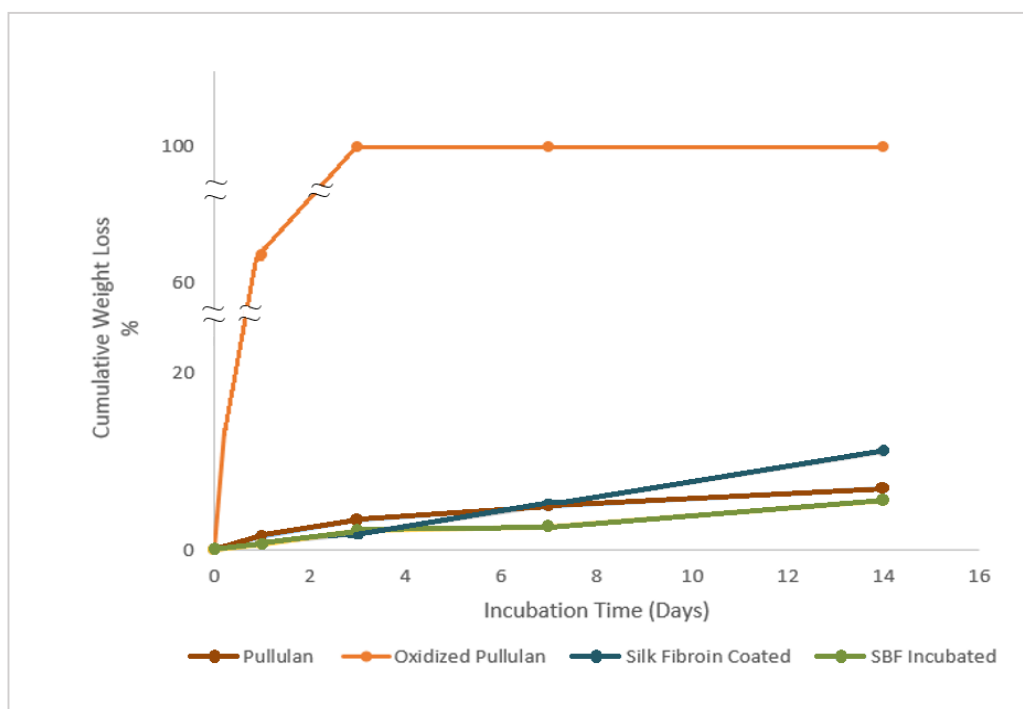


Figure 3. 20 Cumulative wet weight losses of the plain, surface oxidized, SF coated and SBF incubated PULL microspheres in PBS at 37°C in water bath in two weeks (n=3).

3.6. Measurement of Stiffness

The stiffness and flexibility of the microspheres were studied to investigate the influence of surface modifications on the microspheres. The percentages of deformed microspheres after exposing the microspheres to different centrifugal forces by centrifugation are given in Table 3.5. It is clearly seen that SF coating did not improve the flexibility of pullulan microspheres since percent deformed particles obtained (9.33%) at the highest centrifugal forces were similar to the percentage obtained for plain PULL microspheres. On the other hand, SBF incubated and mineralized microsphere samples showed enhanced stiffness and flexibility with less microsphere deformation (5.67 %) in comparison to fibroin coated and plain microspheres. Similarly, there are studies in literature that reported the improved mechanical properties of biomaterials for bone tissue engineering by using SBF coating method (Mi et al., 2013).

Table 3.4 Stiffness measurement analysis of plain, fibroin coated and SBF coated microspheres (n=3).

	<i>Centrifugal force (G)</i>	200	400	1000	2000	4000	6000
<i>% Deformed microspheres</i>	Plain PULL	1.0±1.0	1.7±0.6	3.7±0.6	3.7±1.5	7.3±1.5	9.7±1.5
	SF Coated	1.0±1.0	2.0±1.0	2.0±1.0	4.3±0.6	7.0±1.0	9.3±0.6
	SBF Incubated	0.3±0.6	0.7±0.6	1.7±0.6	1.7±0.6	2.7±0.6	5.7±1.2

As Bohner and Lemaitre (2009) reported, calcium ions released from the material that was soaked in SBF results in the acceleration of apatite nucleation. Our microspheres retained calcium carbonate partially in the deeper parts after porogen leaching. The remaining calcium carbonate from which calcium ions might have released slowly and might have initiated apatite nucleation on the surface, even inside of the microspheres. We observed that the apatite layer coated microspheres improved mechanical properties such as stiffness and flexibility. The results were consistent with findings of previous study by Renke-Gluszko and El Fray (2004), in which poly (aliphatic/aromatic-ester) (PED) copolymers were incubated in SBF. Biomimetically mineralized PED copolymers exhibited improved mechanical properties compared to the untreated material. This difference was explained with the deposition of SBF crystals forming an apatite layer on the polymers surface resulting in the phenomena of crystal formation on the polymer surface provides improved static and dynamic mechanical properties.

3.7. *In vitro* Cell Culture Studies

For cell culture studies the microspheres were sterilized by UV irradiation (Umeki et al., 2010), however we prolonged the exposure time to 45 minutes. Sarcoma osteoblast cells (SaOs-2) were used to test the biocompatibility of the microspheres.

Surface modified microspheres were tested for their surface cytocompatibility. SF coated microspheres were incubated with SaOs-2 cells and as Figure 3.20 revealed on the third day of incubation, cells were attached on SF coated PULL microspheres.

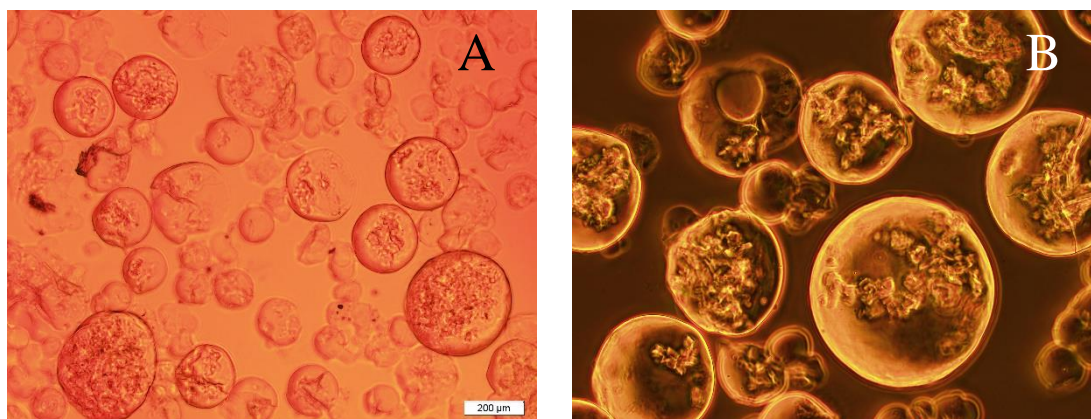


Figure 3. 21 Transmission light microscopy images of 1% SF coated microspheres on the 3rd day of incubation (A) magnification 4X (Scale bar: 200 μm) and (B) magnification 10X (Scale bar 100 μm)

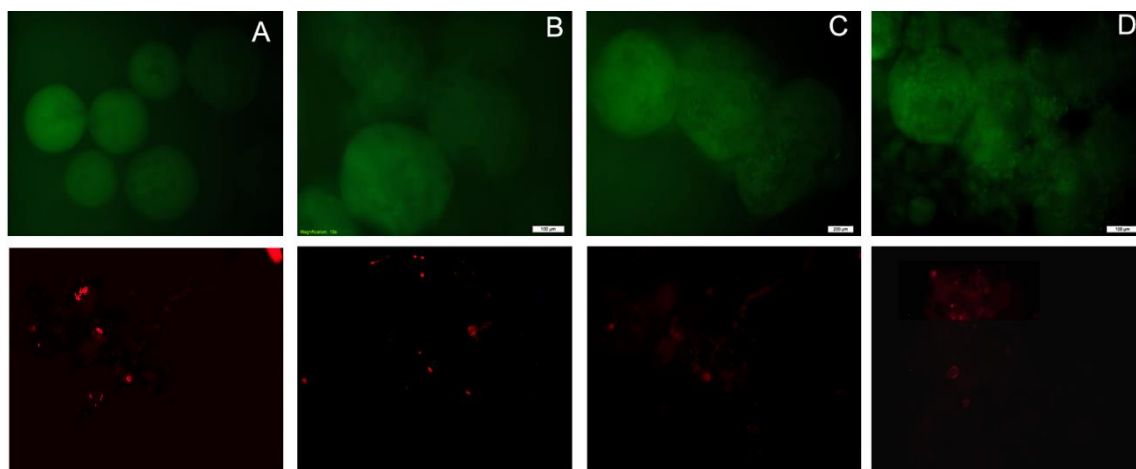


Figure 3. 22 Live/dead staining images of attached cell on microspheres that were incubated in SBF for 0 (A), 4 (B), 7 (C) and 14 (D) days. Upper images show the calcein stainings (green, live) and the bottom images show PI (red, dead) stainings. Magnification 100X.

In Figure 3.21, live/dead staining method was applied to cells on the plain PULL and mineralized PULL microspheres after 3 days of incubation. On the PULL microspheres non-specific binding of calcein was also observed, hence the living cells attached on the microspheres could not be observed clearly. However, the PI staining showed the dead cell distribution on the microcarriers. According to PI staining, the observed dead cell distribution decreased with the increasing incubation time in SBF, which indicated the biocompatibility of mineral formation. The roughness formed by formation of crystals and the ionic groups presented by minerals on the surface added a favorable environment for cell attachment (Cipitria et al., 2011).

The higher cell attachment on SBF incubated microspheres was supported with the Nile red staining of the cells on the microspheres (Figure 3.23). On the micrographs, the intensity and the distribution of the cells on SBF incubated microspheres was significantly higher.

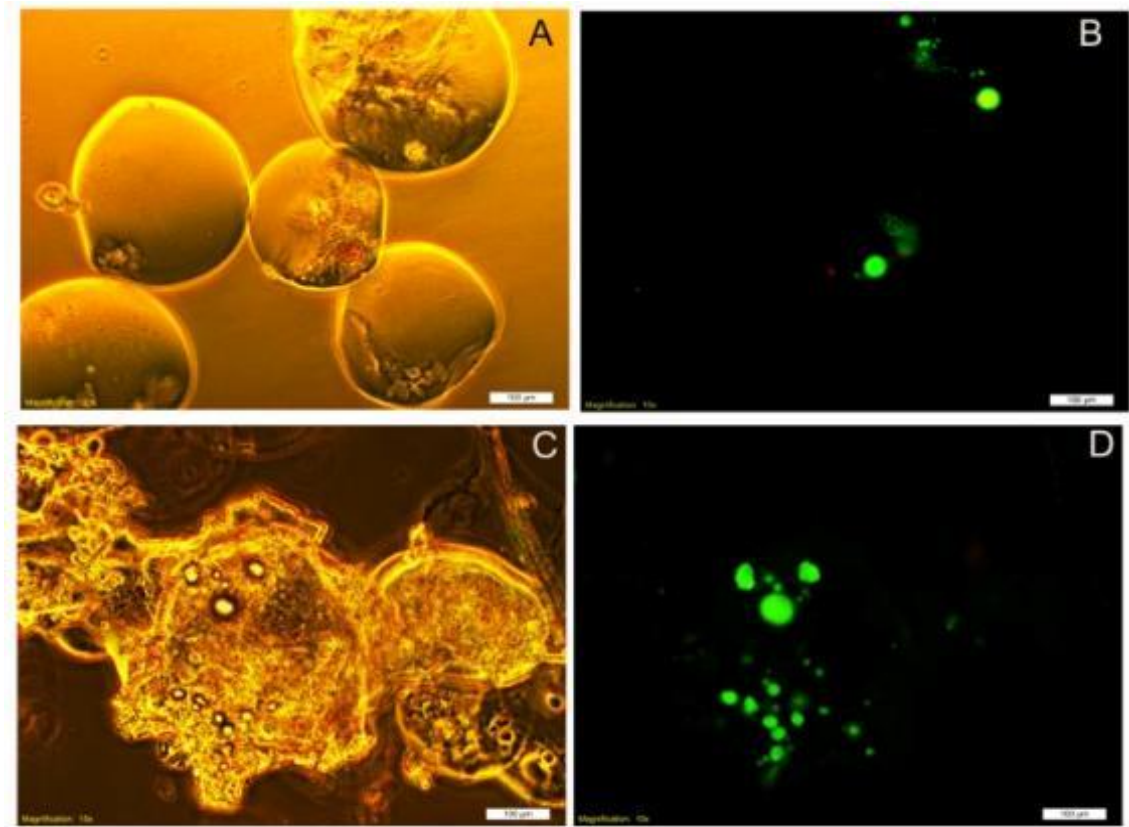


Figure 3. 23 Phase contrast and fluorescence microscope images of SaOs-2 cells seeded on native (A, B) and SBF incubated pullulan microspheres (B, C), respectively. Green illuminance shows Nile red stained cells. Magnification 100X. Scale bar: 100 µm

In order to compare the biological response to plain, SF coated and mineralized PULL microspheres, viability assay was conducted for all three groups Alamar Blue cell viability assay was conducted to study the attachment and proliferation of the cells on three groups of microspheres; plain, SF coated and 7 days SBF incubated PULL microspheres. A calibration curve was constructed for cell number of SaOs-2 cells using known number of cells as standards (Appendix A). Cells plated on polystyrene culture wells (TCPS) and three microsphere groups without cells were used as control groups. At day 1, plain PULL,

SF coated and SBF incubated microspheres showed 25%, 24% and 16% cell adhesion, respectively for static culture and 13%, 32% and 19% cell adhesion, respectively for dynamic culture (Figure 3.24). On day 1, the control TCPS showed relatively high number of attached cells. It was seen that cell attachment on TCPS was two folds higher than observed on microsphere groups. The reason might be the high cell seeding density for wells (15.000 cells/cm²). The studies of Rodan et al. (1997) revealed that, the doubling time of SaOs-2 cell line was about 37 h. Thus on the 3rd day, a high cell number was reached on TCPS and this showed the confluency of cells. At day 7, the cell number on TCPS declined dramatically. Probably, a decrease in cell viability was observed which could be due to lack of surface area and contact inhibition or aging after reaching confluency. For dynamic culture conditions, on day 1, the cells adapted more on the fibroin coated surface and this groups showed highest initial cell attachment among all tested groups. Whereas, SBF incubated microsphere group showed significantly lower cell attachment for dynamic culture conditions.

At day 3, there were significant increases in cell number for all microsphere groups. . However, relatively higher proliferation was seen on fibroin modified and mineralized microsphere groups than the plain PULL microspheres. For all three groups of microspheres 7th day showed higher cell numbers than 3rd day for static and dynamic conditions. However, the modified groups showed different results for static and dynamic cell culture. The fibroin coated microspheres showed a sharp increase at day 7 for static cell culture, while the microsphere group incubated in SBF showed significantly higher increase under dynamic cell culture conditions.

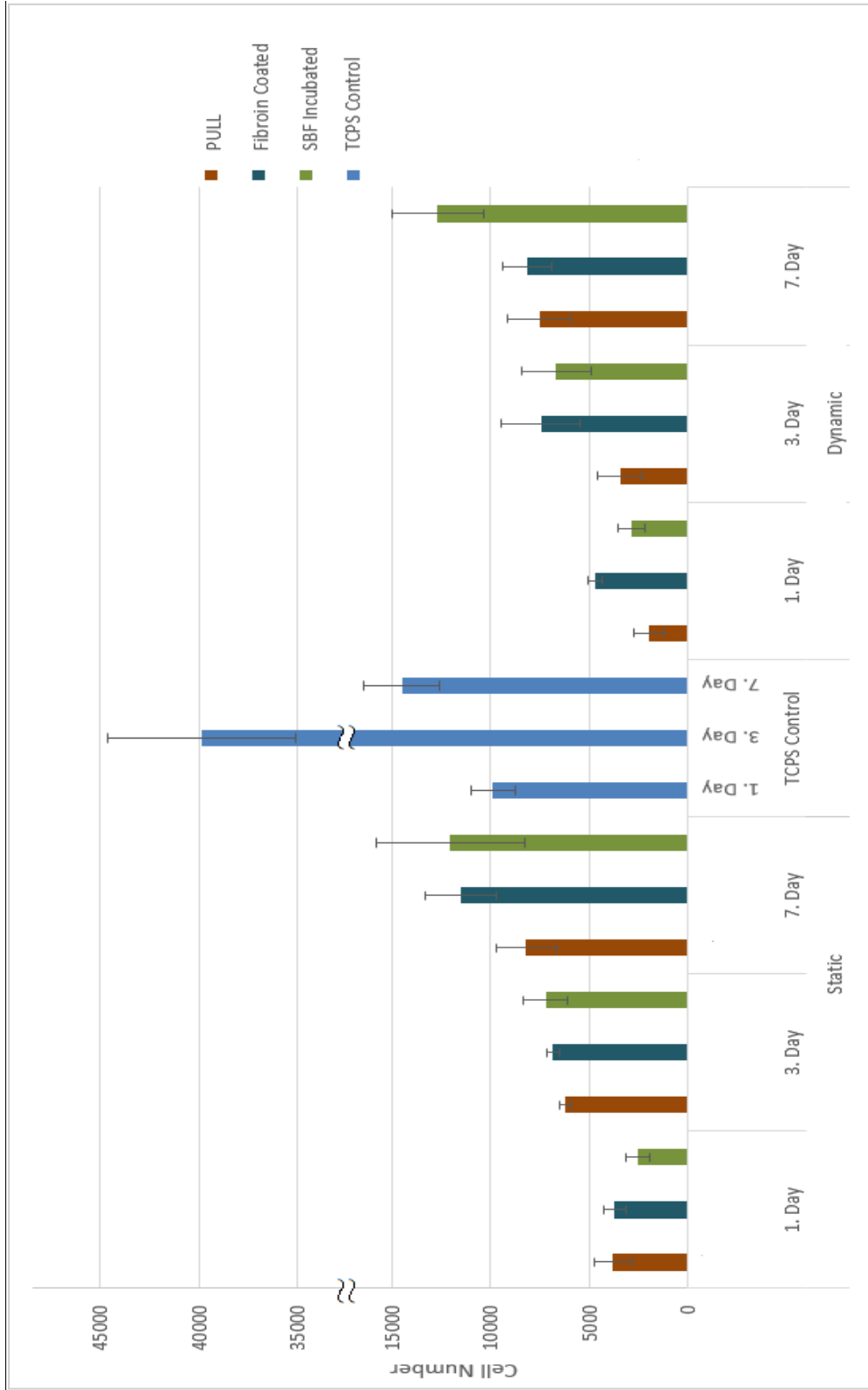


Figure 3. 24 SaOs-2 cell proliferation on plain, SF coated and 7 days SBF incubated PULL microspheres with their standard deviations under static and dynamic conditions, TCPS was used as control group. (n=5).

Cai et al. (2002) studied SF effect on cell adhesion and proliferation. They stated that silk fibroin modification on poly (d,l-lactic acid) (PDLLA) surface improved the cell attachment and proliferation on the surface. On the 4th day of viability test SF modified PDLLA showed almost 60% higher cell proliferation than plain PDLLA scaffolds. Similarly, in our study, SF coating resulted with higher cell attachment and proliferation compared to plain PULL microspheres.

As stated by Kumbar and coworkers (2010), mineralization on polymeric scaffolds makes them mechanically competent to the bone tissue and forms a better cell attachment surface for osteoblasts. Similarly, 7 days SBF incubated PULL microspheres also showed higher attachment and proliferation of cells. Kokkinos et al. (2011) reported a relatively higher cell attachment and proliferation on rougher surface of HAP. They suggested that enhanced cell adhesion on HAP could be the result of the selective adsorption of serum proteins. Cellular interactions are modulated by adsorbed proteins and another theory suggested by El-Ghannam et al. (1999) that adsorption of serum fibronectin to the surface of calcium phosphate may enhance the osteoblast adhesion.

3.7.1. ALP Assay

Osteogenic differentiation of SaOs-2 cells on PULL based microspheres was conducted in osteogenic differentiation medium for 7 and 14 days. Alkaline phosphatase (ALP) enzyme activity was studied in order to characterize the osteogenic differentiation on plain, SF coated and SBF incubated PULL microspheres for both static and dynamic conditions.

For 7th day, the ALP assay results are given on Figure 3.25. Specific ALP enzyme activity was given in nmol/min/mg protein unit. Among all groups studied, in SF coated PULL microsphere group, cell had relatively higher ALP activity for static and dynamic

conditions. However, related with the high cell attachment and proliferation on TCPS, TCPS control group showed significantly higher ALP activity than the sample groups.

According to the study of Rath et al. (2012), in dynamic cell culture, the osteoinductive conditions not only favoured osteogenic cell survival but also supported their differentiation in biphasic calcium phosphate (BCP) scaffolds. For our study, an unexpected result was observed for the dynamic culture SBF incubated group ALP activity. This group showed significantly lower values for ALP enzyme activity.

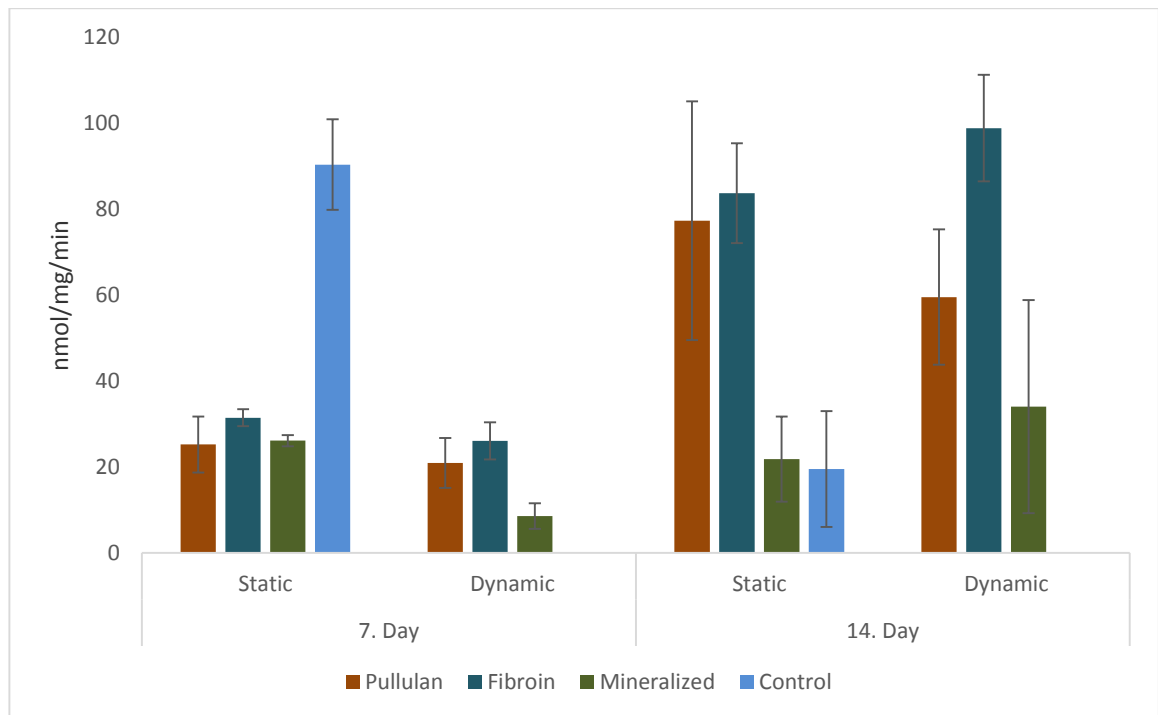


Figure 3. 25. ALP activity of SaOs-2 cells at day 7 and day 14 on plain, SF coated and 7 days SBF incubated PULL microspheres with their standard deviations cultivated under static and dynamic conditions, TCPS was used as control group. (n=5).

On day 14, cells seeded on TCPS showed significantly lower ALP enzyme activity than observed at 7th day. However, ALP enzyme activity SF coated and SBF incubated microspheres groups peaked at day 14. The reason for earlier peak for TCPS might be the earlier confluency of the cells on TCPS control group. Sudo et al. (1983) stated that cells in the growing state has very low potential for ALP activity, however, the enzyme activity peaks after reaching a confluent state. Our TCPS control reached confluent state at day 3, whereas the sample groups reached confluency at about day 7. Related with the delayed confluency state of the cells on microsphere samples, the ALP activity level increased at day 14 rather than on day 7 observed for TCPS.

Plain PULL microspheres showed a similar pattern on both time points for static and dynamic culture conditions. ALP activity for SaOs-2 cells on plain PULL microspheres reduced on dynamic culture. However, SF coated microsphere group showed increase on ALP activity on 14th day on dynamic conditions as expected. These two groups of plain and SF coated PULL microspheres showed significantly higher ALP activity on 14th day. For SBF incubated PULL microsphere culture, ALP activity of SaOs-2 cells increased only for dynamic culture, whereas the enzyme activity level was sustained on the static culture conditions on 14th day. Furthermore, significantly lower enzyme activity was observed for all SBF incubated PULL microsphere groups, it could be stated that, the cell confluency might still not be reached at 14th day.

PART II:

MICROENCAPSULATION

3.8. Periodate Oxidation of PULL and Crosslinking with GEL

Periodate oxidation was conducted on bulk PULL to increased solubility and chain flexibility suitable for potential use in crosslinking with other polymers (Vold et al., 2004). In our study, periodate oxidation formed carbonyl groups on PULL and with the help of borax as crosslinker, oxPULL and GEL are crosslinked, in which urine derived stem cells were entrapped.

FTIR spectra of oxPULL showed absorption band at 1642 cm^{-1} (Figure 3.25). Gupta and coworkers (2013) studied periodate oxidation of carbohydrates and their demonstrations showed that formed carbonyl group had characteristic band at 1734 cm^{-1} in the FTIR spectra. They further revealed that partial ionization of $-\text{COOH}$ groups led to an absorption band at 1614 cm^{-1} . For our oxPULL, $-\text{COOH}$ groups probably showed partial ionization and FTIR results that, oxidation was successfully applied on PULL structure.

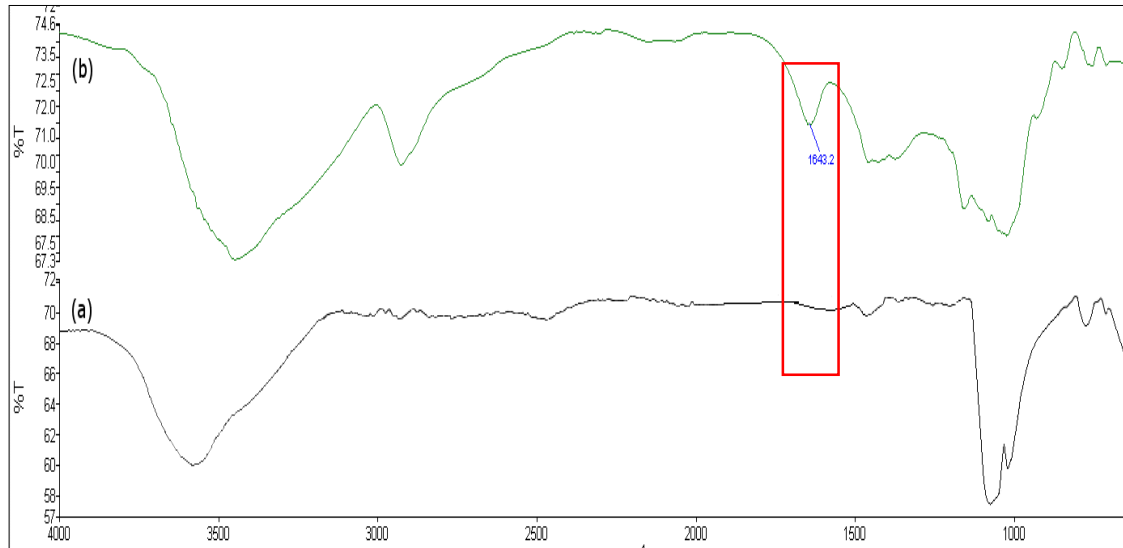


Figure 3. 25 FTIR spectra of (a) PULL and (b) bulk oxPULL

Degree of oxidation of PULL was found investigated by iodometric titration (Balakrishnan et al., 2005). Degree of oxidation is tightly related with the degree and the time of crosslinking with GEL. The degree of crosslinking and gelling time of oxidized alginate and GEL increased by increased degree of periodate oxidation (Balakrishnan et al., 2014).

Degree of oxidation was found to be 68 ± 4 percentage by titration and the resultant oxPULL and GEL were conjugated within seconds in the presence of borax. The fast gelling is essential for decreasing the encapsulating process time of the cells in order not to cause the cell death.

3.9. Isolation of Urine Derived Stem Cells

Urine derived stem cells were isolated from spontaneously voided healthy human urine (male, 24 years). On Figure 3.26 first appearance of cells, first colony formation and interacted colonies are seen respectively at 5th, 7th and 9th days of culture.

Isolated cells were shown to have mesenchymal stem cell markers in immunophenotyping of cells done by flow cytometric analysis; CD 73, CD105, and CD 44 were used as mesenchymal positive markers with CD 34 and CD 45 as negative markers (Ataol et al., 2015). Recently, researchers have achieved committed differentiation of MSCs into well-defined lineages (Liu et al., 2012). In a study by Zhang et al. (2009), they showed enhanced proliferative and osteogenic capacity of allogenic MSC, and they applied MSC seeded scaffold in dynamic bioreactor culture comparing with standard static culture environment. The results showed high osteogenic differentiation of MSCs in a dynamic culture.

In particular, urine derived mesenchymal stem cells were also studied frequently in recent years. Mostly characterization studies were conducted about urine derived MSCs (Bharadvaj et al., 2011; Guan et al., 2014).



Figure 3. 26. Light microscopy images of cells in culture (A) First appearance of cells at day 5 (B) first colony formation at day 7 (C) interacted colonies at day 9.

PULL/ALG/GEL microspheres were produced by water in oil emulsion. The microspheres had spherical shape with an average diameter $530 \pm 32 \mu\text{m}$. The microsphere size was found to be homogeneously distributed (Figure 3.27).

The microspheres then coated with poly (L-lysine) (PLL) in order to enhance stability of the surface and cell attachment on it with polycationic amino acid. Nojehdehiana et al. (2009) coated negative charged PLGA with cationic PLL; by creating a network on the microspheres, they provided improved cell attachment on three-dimensional environment. They stated that precoating the material with ECM molecules can significantly improve their cell affinity.

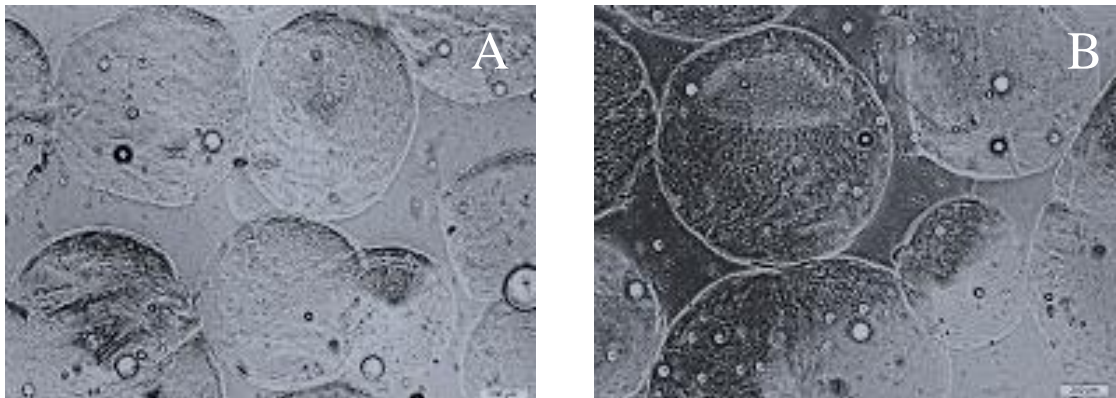


Figure 3.27 (A) and (B) PULL/ALG/GEL microspheres without cells before PLL coating. Magnification 100X Scale bar: 100 μm .

Viability of the encapsulated cells was studied by dead/live staining and cell proliferation in microspheres was determined by Alamar Blue assay. On Figure 3.28, the entrapped cells were shown after 1 and 3 days of incubation, the green dots seen on the second

column indicated the living cells that are labelled with calcein and the last column images shows the dead cells in red with staining with propidium iodide.

As seen on Figure 3.28, after one day of cell encapsulation the cells were successfully entrapped in microspheres and retained their viability. On the 3rd day the cell density on the surface of the microspheres decreased according to live/dead cell assay (Figure 3. 28 B), the cells might have moved to inner parts of microspheres and their visibility may decrease on the surface.

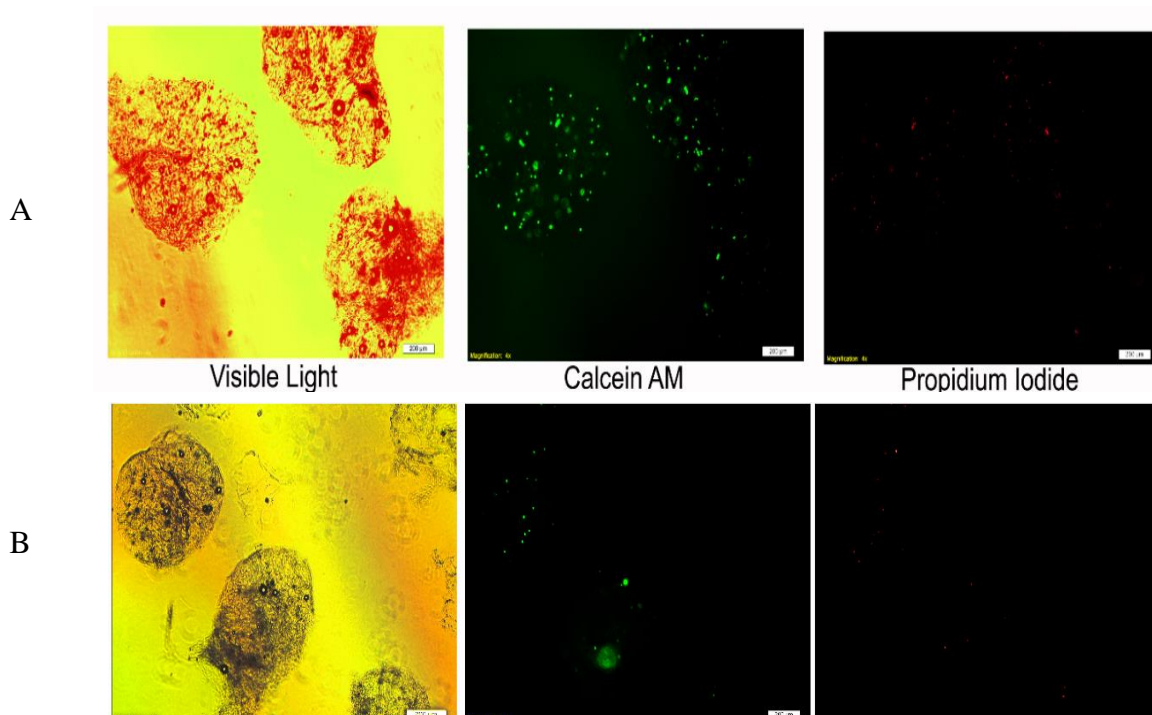


Figure 3. 28 Live/dead staining images of urine derived mesenchymal cell encapsulated in microspheres (A) day 1 (B) day 3. Magnification 100X. Scale bar: 200 μ m.

The Alamar Blue viability assay results showed that, on the third day there was an insignificant increase in the cell number (Figure 3.29). This result reveals that, the attached cells retained their viability; however, their proliferation was inhibited.

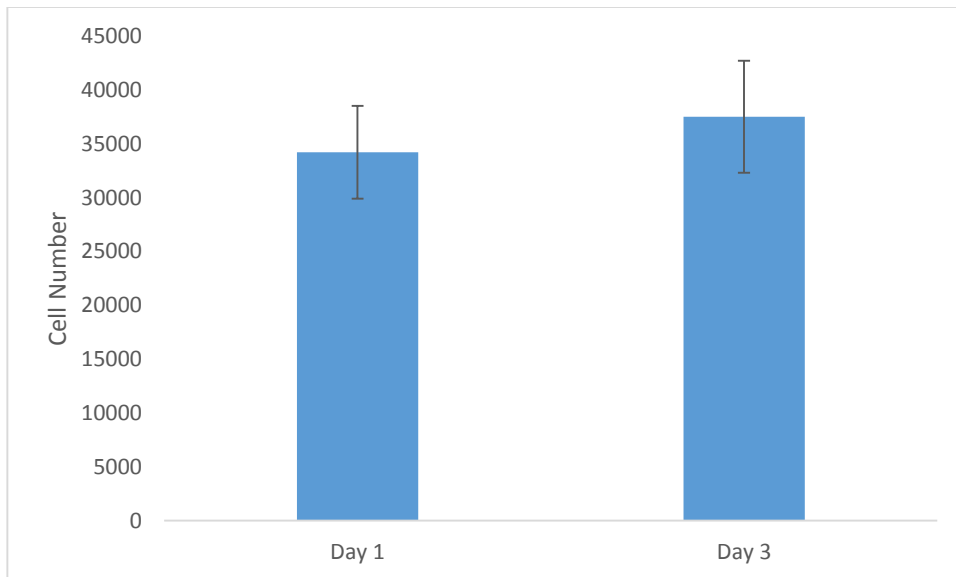


Figure 3. 29 Proliferation of urine derived mesenchymal stem cells encapsulated in PULL/ALG/GEL microspheres on 1st and 3rd day of incubation (n=3).

As previously stated, GEL is commonly used in microencapsulation method. Hoshikawa et al. (2006) produced microspheres of GEL for encapsulation of osteoblasts and chondrocytes and revealed promising results with respect to cell proliferation, osteogenic and chondrogenic differentiation. In our study, these effects of GEL was attempted to enhance by the high water absorption ability and biocompatibility of carbohydrate polymer PULL.

CHAPTER 4

CONCLUSION

In order to produce injectable microcarrier systems for bone tissue engineering, PULL based microcarriers were prepared by water-in-oil emulsion. In the first part of thesis, PULL microspheres, with average size of 153 ± 46 μm , were produced and two surface modification techniques were applied separately in order to enhance cell interaction of PULL microspheres. SF was coated through periodate oxidation of PULL microsphere surfaces and conjugation of SF by reductive amination. SF coated PULL microspheres showed significantly higher cell attachment and proliferation, while the mechanical properties were not significantly different from plain PULL microspheres. When degradation rates were compared, SF coated microspheres showed almost two-fold faster degradation than PULL microspheres, which can be due to the chain scission of PULL by oxidation prior to coating. For the second surface modification method, PULL microspheres were incubated in SBF for 4, 7 and 14 day. It has been shown that when incubation time increases, mineralization rate on the microspheres increases with it. However, we observed aggregation of microspheres due to the start of accumulation of minerals between the microspheres after 7 days of incubation. Thus, for further studies 7 day SBF incubated microspheres were used. XRD data showed that there were HA precursor formation on the microspheres, which has increased the cell attachment and viability when compared to plain PULL microspheres. Furthermore, the mechanical

properties has increased with the mineralized surface and degradation was slower than the plain microspheres. In the second part of thesis, oxPULL/GEL blend was used to encapsulate urine derived stem cells. Two polymers were crosslinked with the catalysis of borax. The microspheres, with average size of 530 ± 32 μm , showed high cell carrying capacity and microspheres' viability according to the conducted cell culture and viability studies.

In this group of studies, we observed that PULL can be used as base material for microspheres or microspheres. However, for increased cytocompatibility and viability of cells surface modification methods are necessary for higher performance of these microcarriers. Fibroin coated and mineralized PULL microcarriers can be used safely for bone tissue engineering as proved by viability tests. Besides using PULL based microcarriers as injectable systems for bone tissue engineering purpose, there carriers are suitable candidates to expand cells in bioreactor systems and use them in *in vivo* experiments.

REFERENCES

- [1] Anderson, J. M. and Shive, M. S. (2012). "Biodegradation and biocompatibility of PLA and PLGA microspheres." *Advanced drug delivery reviews* 64: 72-82.
- [2] Angele, P., Kujat, R., M. Nerlich, J. Yoo, V. Goldberg and Johnstone B. (1999). "Engineering of osteochondral tissue with bone marrow mesenchymal progenitor cells in a derivatized hyaluronan-gelatin composite sponge." *Tissue engineering* 5(6): 545-553.
- [3] Arora, A., P. Sharma and Katti, D. S. (2015). "Pullulan-based composite scaffolds for bone tissue engineering: Improved osteoconductivity by pore wall mineralization." *Carbohydrate Polymers* 123: 180-189.
- [4] Ataol, S., Tezcaner, A., Duygulu, O., Keskin, D. and Machin, N. E. (2015). "Synthesis and characterization of nanosized calcium phosphates by flame spray pyrolysis, and their effect on osteogenic differentiation of stem cells." *Journal of Nanoparticle Research* 17(2): 1-14.
- [5] Baek, H. S., Park, Y. H., Ki, C. S., Park, J.-C. and Rah, D. K. (2008). "Enhanced chondrogenic responses of articular chondrocytes onto porous silk fibroin scaffolds treated with microwave-induced argon plasma." *Surface and Coatings Technology* 202(22): 5794-5797.

- [6] Balakrishnan, B. and Jayakrishnan, A. (2005). "Self-cross-linking biopolymers as injectable in situ forming biodegradable scaffolds." *Biomaterials* 26(18): 3941-3951.
- [7] Balakrishnan, B., Joshi, N., Jayakrishnan, A. and Banerjee, R. (2014). "Self-crosslinked oxidized alginate/gelatin hydrogel as injectable, adhesive biomimetic scaffolds for cartilage regeneration." *Acta biomaterialia* 10(8): 3650-3663.
- [8] Balmayor, E. R., Baran, E. T., Azevedo, H. S. and Reis, R. L. (2012). "Injectable biodegradable starch/chitosan delivery system for the sustained release of gentamicin to treat bone infections." *Carbohydrate Polymers* 87(1): 32-39.
- [9] Bao, T.-Q., Franco, R. A. and Lee, B. T. (2012). "Preparation and characterization of a novel 3D scaffold from poly (ϵ -caprolactone)/biphasic calcium phosphate hybrid composite microspheres adhesion." *Biochemical Engineering Journal* 64: 76-83.
- [10] Barnes, M. J. and R. W. Farndale (1999). "Collagens and atherosclerosis." *Experimental gerontology* 34(4): 513-525.
- [11] Bharadwaj, S., G. Liu, Y. Shi, C. Markert, K.-E. Andersson, A. Atala and Y. Zhang (2011). "Characterization of urine-derived stem cells obtained from upper urinary tract for use in cell-based urological tissue engineering." *Tissue Engineering Part A* 17(15-16): 2123-2132.
- [12] Bhardwaj, N. and Kundu, S. C. (2010). "Electrospinning: a fascinating fiber fabrication technique." *Biotechnology advances* 28(3): 325-347.

- [13] Blau, H. M., Brazelton, T. and Weimann, J. (2001). "The evolving concept of a stem cell: entity or function?" *Cell* 105(7): 829-841.
- [14] Bohner, M. and Lemaitre, J. (2009). "Can bioactivity be tested in vitro with SBF solution?" *Biomaterials* 30(12): 2175-2179.
- [15] Bruneel, D. and Schacht, E. (1993). "Chemical modification of pullulan: 1. Periodate oxidation." *Polymer* 34(12): 2628-2632.
- [16] Butler, W. T. and Ritchie, H. (1995). "The nature and functional significance of dentin extracellular matrix proteins." *The International journal of developmental biology* 39(1): 169-179.
- [17] Cai, K., Yao, K., Cui, Y., Yang, Z., Li, X., Xie, H., Qing, T. and Gao, L. (2002). "Influence of different surface modification treatments on poly (D, L-lactic acid) with silk fibroin and their effects on the culture of osteoblast in vitro." *Biomaterials* 23(7): 1603-1611.
- [18] Causin, F., Pascarella, R., Pavesi, G., Marasco, R., G. Zambon, R. Battaglia and M. Munari (2011). "Acute endovascular treatment (< 48 hours) of uncoilable ruptured aneurysms at non-branching sites using silk flow-diverting devices." *Interventional Neuroradiology* 17(3): 357.
- [19] Chen, L., Hu, J., Ran, J., Shen, X. and Tong, H. (2014). "Preparation and evaluation of collagen-silk fibroin/hydroxyapatite nanocomposites for bone tissue engineering." *International journal of biological macromolecules* 65: 1-7.
- [20] Cheng, K. C., Demirci, A. and Catchmark, J. M. (2011). "Pullulan: biosynthesis, production, and applications." *Applied microbiology and biotechnology* 92(1): 29-44.

- [21] Cipitria, A., Skelton, A., Dargaville, T., P. Dalton and Hutmacher, D. (2011). "Design, fabrication and characterization of PCL electrospun scaffolds—a review." *Journal of Materials Chemistry* 21(26): 9419-9453.
- [22] Cutiongco, M. F. A., Tan, M. H., Ng, M. Y. K., Le Visage, C. and Yim, E. K. F. (2014). "Composite pullulan–dextran polysaccharide scaffold with interfacial polyelectrolyte complexation fibers: A platform with enhanced cell interaction and spatial distribution." *Acta biomaterialia* 10(10): 4410-4418.
- [23] Deng, M., Kumbar, S. G., Wan, Y., Toti, U. S., Allcock, H. R. and C. T. Laurencin (2010). "Polyphosphazene polymers for tissue engineering: an analysis of material synthesis, characterization and applications." *Soft Matter* 6(14): 3119-3132.
- [24] Ding, H., Pan, H., Xu, X. and Tang, R. (2014). "Toward a Detailed Understanding of Magnesium Ions on Hydroxyapatite Crystallization Inhibition." *Crystal Growth & Design* 14(2): 763-769.
- [25] Drury, J. L. and Mooney, D. J. (2003). "Hydrogels for tissue engineering: scaffold design variables and applications." *Biomaterials* 24(24): 4337-4351.
- [26] Du, K., X. Shi and Z. Gan (2013). "Rapid Biomimetic Mineralization of Hydroxyapatite-g-PDLLA Hybrid Microspheres." *Langmuir* 29(49): 15293-15301.
- [27] Du, K. F., Bai, S., Dong, X. Y. and Y. Sun (2010). "Fabrication of superporous agarose beads for protein adsorption: Effect of CaCO₃ granules content." *Journal of Chromatography A* 1217(37): 5808-5816.

- [28] Dulong, V., R. Forbice, E. Condamine, D. Le Cerf and L. Picton (2011). "Pullulan-STMP hydrogels: a way to correlate crosslinking mechanism, structure and physicochemical properties." *Polymer bulletin* 67(3): 455-466.
- [29] El-Ghannam, A., Ducheyne, P. and Shapiro, I. (1999). "Effect of serum proteins on osteoblast adhesion to surface-modified bioactive glass and hydroxyapatite." *Journal of Orthopaedic Research* 17(3): 340-345.
- [30] Emoto, M., Naganuma, Y., Choijamts, B., Ohno, T., Yoshihisa, H., N. Kanomata, T. Kawarabayashi and M. Aizawa (2010). "Novel chemoembolization using calcium-phosphate ceramic microsphere incorporating TNP-470, an anti-angiogenic agent." *Cancer science* 101(4): 984-990.
- [31] Enderle, J. D. and Bronzino, J. D. (2012). *Introduction to biomedical engineering*, Academic press.
- [32] Fang, J., Q. Yong, K. Zhang, W. Sun, S. Yan, L. Cui and J. Yin (2015). "Novel injectable porous poly (γ -benzyl-L-glutamate) microspheres for cartilage tissue engineering: preparation and evaluation." *Journal of Materials Chemistry B*.
- [33] Freyman, T., Yannas, I. and Gibson, L. (2001). "Cellular materials as porous scaffolds for tissue engineering." *Progress in Materials Science* 46(3): 273-282.
- [34] Fricain, J. C., Schlaubitz, S., Le Visage, C., Arnault, I., Derkaoui, S. M., R. Siadous, S. Catros, C. Lalande, R. Bareille and M. Renard (2013). "A nano-hydroxyapatite-Pullulan/dextran polysaccharide composite macroporous material for bone tissue engineering." *Biomaterials* 34(12): 2947-2959.

- [35] Fujioka-Kobayashi, M., Ota, M. S., Shimoda, A., Nakahama, K., K. Akiyoshi, Y. Miyamoto and S. Iseki (2012). "Cholesteryl group-and acryloyl group-bearing pullulan nanogel to deliver BMP2 and FGF18 for bone tissue engineering." *Biomaterials* 33(30): 7613-7620.
- [36] Fundueanu, G., Constantin, M. and Ascenzi, P. (2008). "Preparation and characterization of pH-and temperature-sensitive pullulan microspheres for controlled release of drugs." *Biomaterials* 29(18): 2767-2775.
- [37] Gishto, A., Farrell, K. and Kothapalli, C. R. (2015). "Tuning composition and architecture of biomimetic scaffolds for enhanced matrix synthesis by murine cardiomyocytes." *Journal of Biomedical Materials Research Part A* 103(2): 693-708.
- [38] Gómez-Guillén, M., Giménez, B., López-Caballero, M. and Montero, M. (2011). "Functional and bioactive properties of collagen and gelatin from alternative sources: A review." *Food Hydrocolloids* 25(8): 1813-1827.
- [39] Guan, X., X. Ma, Zhang, L., H. Feng and Ma, Z. (2014). "Evaluation of CD24 as a marker to rapidly define the mesenchymal stem cell phenotype and its differentiation in human nucleus pulposus." *Chinese medical journal* 127(8): 1474-1481.
- [40] Gupta, B., Tummalapalli, M., Deopura, B. L. and Alam, M. S. (2013). "Functionalization of pectin by periodate oxidation." *Carbohydrate polymers* 98(1): 1160-1165.
- [41] Gupta, M. and Gupta, A. K. (2004). "In vitro cytotoxicity studies of hydrogel pullulan nanoparticles prepared by AOT/N-hexane micellar system." *J Pharm Pharmaceut Sci* 7(1): 38-46.

- [42] Hanani, Z. N., Beatty, E., Roos, Y., Morris, M. and Kerry, J. (2012). "Manufacture and characterization of gelatin films derived from beef, pork and fish sources using twin screw extrusion." *Journal of Food Engineering* 113(4): 606-614.
- [43] Hart, A. P. (2005). "Bone Engineering of the Ulna of Rabbit."
- [44] Hermanson, G. T. (2013). *Bioconjugate techniques*, Academic press.
- [45] Hollister, S. J. (2005). "Porous scaffold design for tissue engineering." *Nature materials* 4(7): 518-524.
- [46] Hong, Y., Gao, C., Xie, Y., Gong, Y. and Shen J. (2005). "Collagen-coated polylactide microspheres as chondrocyte microcarriers." *Biomaterials* 26(32): 6305-6313.
- [47] Hoshikawa, A., Nakayama, Y., Matsuda, T., Oda, H., Nakamura, K. and Mabuchi, K. (2006). "Encapsulation of chondrocytes in photopolymerizable styrenated gelatin for cartilage tissue engineering." *Tissue engineering* 12(8): 2333-2341.
- [48] Hutmacher, D. W. (2000). "Scaffolds in tissue engineering bone and cartilage." *Biomaterials* 21(24): 2529-2543.
- [49] Hutmacher, D. W., Sittinger, M. and Risbud, M. V. (2004). "Scaffold-based tissue engineering: rationale for computer-aided design and solid free-form fabrication systems." *TRENDS in Biotechnology* 22(7): 354-362.
- [50] Ikawa, N., Kimura, T., Oumi, Y. and Sano, T. (2009). "Amino acid containing amorphous calcium phosphates and the rapid transformation into apatite." *Journal of Materials Chemistry* 19(28): 4906-4913.

- [51] Inouye, K., Kurokawa, M., Nishikawa, S. and Tsukada, M. (1998). "Use of Bombyx mori silk fibroin as a substratum for cultivation of animal cells." *Journal of biochemical and biophysical methods* 37(3): 159-164.
- [52] Jain, S. K., Awasthi, A., Jain, N. and Agrawal, G. (2005). "Calcium silicate based microspheres of repaglinide for gastroretentive floating drug delivery: Preparation and in vitro characterization." *Journal of Controlled Release* 107(2): 300-309.
- [53] Jamal, T., Rahman, A., Mirza, A., Panda, A. K, Talegaonkar, S. and Iqbal, Z. (2012). "Formulation, antimicrobial and toxicity evaluation of bioceramic based ofloxacin loaded biodegradable microspheres for periodontal infection." *Current drug delivery* 9(5): 515-526.
- [54] Jeon, O., Powell, C., Solorio, L. D., Krebs, M. D. and Alsberg, E. (2011). "Affinity-based growth factor delivery using biodegradable, photocrosslinked heparin-alginate hydrogels." *Journal of Controlled Release* 154(3): 258-266.
- [55] Jiang, S., Chen, Y., Pan, H., Zhang, Y. J. and Tang, R. (2013). "Faster nucleation at lower pH: amorphous phase mediated nucleation kinetics." *Phys. Chem. Chem. Phys.* 15(30): 12530-12533.
- [56] Jung, G. Y., Park, Y. J. and Han, J. S. (2010). "Effects of HA released calcium ion on osteoblast differentiation." *Journal of Materials Science: Materials in Medicine* 21(5): 1649-1654.

- [57] Kandemir, N., Yemenicioglu, A., Mecitoglu, C., Elmaci, Z. S., Arslanoglu, A., Goksungur, Y. and Baysal, T. (2005). "Production of antimicrobial films by incorporation of partially purified lysozyme into biodegradable films of crude exopolysaccharides obtained from *Aureobasidium pullulans* fermentation." *Food Technology and Biotechnology* 43(4): 343-350.
- [58] Kang, Q., Song, W. X., Luo, Q., Tang, N., Luo, J., Luo, X., Chen, J., Bi, Y., He, B. C. and Park, J. K. (2008). "A comprehensive analysis of the dual roles of BMPs in regulating adipogenic and osteogenic differentiation of mesenchymal progenitor cells." *Stem cells and development* 18(4): 545-558.
- [59] Kaplan, D. L., Mello, C. M., Arcidiacono, S., Fossey, S., Senecal, K. and Muller W. (1997). *Silk. Protein-based materials*, Springer: 103-131.
- [60] Kim, S. S., Park, M. S., Gwak, S. J., Choi, C. Y. and Kim, B. S. (2006). "Accelerated bonelike apatite growth on porous polymer/ceramic composite scaffolds in vitro." *Tissue engineering* 12(10): 2997-3006.
- [61] Kim, T. K., Yoon, J. J., Lee, D. S. and Park, T. G. (2006). "Gas foamed open porous biodegradable polymeric microspheres." *Biomaterials* 27(2): 152-159.
- [62] Kimoto, T., Shibuya, T. and Shiobara, S. (1997). "Safety studies of a novel starch, pullulan: chronic toxicity in rats and bacterial mutagenicity." *Food and chemical toxicology* 35(3): 323-329.
- [63] Kokkinos, P. A., Koutsoukos, P. G. and Deligianni, D. D. (2012). "Detachment strength of human osteoblasts cultured on hydroxyapatite with various surface roughness. Contribution of integrin subunits." *Journal of Materials Science: Materials in Medicine* 23(6): 1489-1498.

- [64] Kokubo, T. and Takadama, H. (2006). "How useful is SBF in predicting in vivo bone bioactivity?" *Biomaterials* 27(15): 2907-2915.
- [65] Kontoyannis, C. G. and Vagenas, N. V. (2000). "Calcium carbonate phase analysis using XRD and FT-Raman spectroscopy." *Analyst* 125(2): 251-255.
- [66] Kundu, B., Rajkhowa, R., Kundu, S. C. and Wang X. (2013). "Silk fibroin biomaterials for tissue regenerations." *Advanced drug delivery reviews* 65(4): 457-470.
- [67] Kundu, J., Poole-Warren, L. A., Martens, P. and Kundu, S. C. (2012). "Silk fibroin/poly (vinyl alcohol) photocrosslinked hydrogels for delivery of macromolecular drugs." *Acta biomaterialia* 8(5): 1720-1729.
- [68] Lack, S., Dulong, V., Le Cerf, D., Picton, L., Argillier, J. F. and Muller, G. (2004). "Hydrogels based on pullulan crosslinked with sodium trimetaphosphate (STMP): rheological study." *Polymer Bulletin* 52(6): 429-436.
- [69] Lalande, C., Miraux, S., Derkaoui, S., Mornet, S., Bareille, R., Fricain, J. C., Franconi, J. M., Le Visage, C., Letourneur, D. and Amédée, J. (2011). "Magnetic resonance imaging tracking of human adipose derived stromal cells within three-dimensional scaffolds for bone tissue engineering." *Eur Cell Mater* 21: 341-354.
- [70] Lamprecht, A., Schafer, U. F. and Lehr, C. M. (2000). "Characterization of microcapsules by confocal laser scanning microscopy: structure, capsule wall composition and encapsulation rate." *European Journal of Pharmaceutics and Biopharmaceutics* 49(1): 1-9.

- [71] Lamprecht, A., Schafer, U. F. and Lehr, C. M. (2000). "Visualization and quantification of polymer distribution in microcapsules by confocal laser scanning microscopy (CLSM)." *International journal of pharmaceutics* 196(2): 223-226.
- [72] Lanza, R., Langer, R. and Vacanti, J. P. (2011). *Principles of tissue engineering*, Academic press.
- [73] Leathers, T. D. (2003). "Biotechnological production and applications of pullulan." *Applied Microbiology and Biotechnology* 62(5-6): 468-473.
- [74] Li, H., J. Yang, X. Hu, J. Liang, Y. Fan and X. Zhang (2011). "Superabsorbent polysaccharide hydrogels based on pullulan derivate as antibacterial release wound dressing." *Journal of Biomedical Materials Research Part A* 98(1): 31-39.
- [75] Lin, A. C., Moralez, J. G., Webster, T. J. and Fenniri, H. (2005). "Helical rosette nanotubes: a biomimetic coating for orthopedics?" *Biomaterials* 26(35): 7304-7309.
- [76] Liu, G., Bharadwaj, S., Atala, A. and Zhang, Y. (2014). "Pd8-02 Enhance Myogenesis And Innervation After Implantation Of Urine-Derived Stem Cells Expressing Vegf In Collagen-I Hydrogel." *The Journal of Urology* 191(4): e217.
- [77] Liu, X., L., Smith, A., Hu, J. and Ma, P. X. (2009). "Biomimetic nanofibrous gelatin/apatite composite scaffolds for bone tissue engineering." *Biomaterials* 30(12): 2252-2258.
- [78] Liu, Z., Dreybrodt, W. and Liu, H. (2011). "Atmospheric CO₂ sink: Silicate weathering or carbonate weathering?" *Applied Geochemistry* 26: S292-S294.

- [79] Lu, Z., J. Zhang, Y. Ma, S. Song and W. Gu (2012). "Biomimetic mineralization of calcium carbonate/carboxymethylcellulose microspheres for lysozyme immobilization." *Materials Science and Engineering: C* 32(7): 1982-1987.
- [80] Malafaya, P. B., Silva, G. A. and Reis, R. L. (2007). "Natural-origin polymers as carriers and scaffolds for biomolecules and cell delivery in tissue engineering applications." *Advanced drug delivery reviews* 59(4): 207-233.
- [81] Martini, F. (1998). *Anatomy and Physiology*'2007 Ed, Rex Bookstore, Inc.
- [82] Meyer, Meyer, U., T. and Wiesmann, H. P. (2006). *Bone and cartilage engineering*, Springer Science & Business Media.
- [83] Mi, H. Y., Jing, X., Salick, M. R., Cordie, T. M., Peng, X. F. and Turng, L. S. (2014). "Morphology, mechanical properties, and mineralization of rigid thermoplastic polyurethane/hydroxyapatite scaffolds for bone tissue applications: effects of fabrication approaches and hydroxyapatite size." *Journal of Materials Science* 49(5): 2324-2337.
- [84] Mishra, B., Vuppu, S. and Rath, K. (2011). "The role of microbial pullulan, a biopolymer in pharmaceutical approaches: A review."
- [85] Miyazaki, T., Anan, S., Ishida, E. and Kawashita, M. (2013). "Carboxymethyl-dextran/magnetite hybrid microspheres designed for hyperthermia." *Journal of Materials Science: Materials in Medicine* 24(5): 1125-1129.

- [86] Mocanu, G., Nichifor, M., Picton, L., About-Jaudet, E. and Le Cerf, D. (2014). "Preparation and characterization of anionic pullulan thermoassociative nanoparticles for drug delivery." *Carbohydrate Polymers*.
- [87] Mouriño, V., Cattalini, J. P., Roether, J. A., Dubey, P., Roy, I. and Boccaccini, A. R. (2013). "Composite polymer-bioceramic scaffolds with drug delivery capability for bone tissue engineering." *Expert opinion on drug delivery* 10(10): 1353-1365.
- [88] Natesan, S., Baer, D. G., Walters, T. J., Babu, M. and Christy, R. J. (2010). "Adipose-derived stem cell delivery into collagen gels using chitosan microspheres." *Tissue Engineering Part A* 16(4): 1369-1384.
- [89] Nojehdehian, H., Moztarzadeh, F., Baharvand, H., Nazarian, H. and Tahriri, M. (2009). "Preparation and surface characterization of poly-L-lysine-coated PLGA microsphere scaffolds containing retinoic acid for nerve tissue engineering: in vitro study." *Colloids and Surfaces B: Biointerfaces* 73(1): 23-29.
- [90] Omenetto, F. G. and Kaplan, D. L. (2010). "New opportunities for an ancient material." *Science* 329(5991): 528-531.
- [91] Pachuau, L. and Mazumder, B. (2009). "A study on the effects of different surfactants on Ethylcellulose microspheres." *Int. J. Pharm. Tech. Res* 1(4): 966-971.
- [92] Pan, J.-f., L. Yuan, C.-a. Guo, X.-h. Geng, T. Fei, W.-s. Fan, S. Li, H.-f. Yuan, Z.-q. Yan and X.-m. Mo (2014). "Fabrication of modified dextran-gelatin in situ forming hydrogel and application in cartilage tissue engineering." *Journal of Materials Chemistry B* 2(47): 8346-8360.

- [93] Park, J. H., R. A. Pérez, G. Z. Jin, S. J. Choi, H. W. Kim and I. B. Wall (2013). "Microcarriers designed for cell culture and tissue engineering of bone." *Tissue Engineering Part B: Reviews* 19(2): 172-190.
- [94] Perez, R., Altankov, G., Jorge-Herrero, E. and Ginebra, M. (2013). "Micro- and nanostructured hydroxyapatite–collagen microcarriers for bone tissue-engineering applications." *Journal of tissue engineering and regenerative medicine* 7(5): 353-361.
- [95] Perez, R., El-Fiqi, A., Park, J. H., T. H. Kim, J. H. Kim and Kim, H. W. (2014). "Therapeutic bioactive microcarriers: Co-delivery of growth factors and stem cells for bone tissue engineering." *Acta biomaterialia* 10(1): 520-530.
- [96] Prajapati, V. D., Jani, G. K. and Khanda, S. M. (2013). "Pullulan: An exopolysaccharide and its various applications." *Carbohydrate Polymers* 95(1): 540-549.
- [97] Rajzer, I., Menaszek, E., Kwiatkowski, R., Planell, J. A. and Castano, O. (2014). "Electrospun gelatin/poly (ϵ -caprolactone) fibrous scaffold modified with calcium phosphate for bone tissue engineering." *Materials Science and Engineering: C* 44: 183-190.
- [98] Rao, J. J., Chen, Z. M. and Chen, B. C. (2009). "Modulation and stabilization of silk fibroin-coated oil-in-water emulsions." *Food Technology and Biotechnology* 31(4): 413.

- [99] Rath, S. N., Strobel, L. A., Arkudas, A., Beier, J. P., Maier, A. K., Greil, P., Horch, R. E. and Kneser, U. (2012). "Osteoinduction and survival of osteoblasts and bone-marrow stromal cells in 3D biphasic calcium phosphate scaffolds under static and dynamic culture conditions." *Journal of cellular and molecular medicine* 16(10): 2350-2361.
- [100] Rekha, M. and Sharma, C. P. (2011). "Hemocompatible pullulan–polyethyleneimine conjugates for liver cell gene delivery: In vitro evaluation of cellular uptake, intracellular trafficking and transfection efficiency." *Acta biomaterialia* 7(1): 370-379.
- [101] Renke-Gluszko, M. and El Fray, M. (2004). "The effect of simulated body fluid on the mechanical properties of multiblock poly (aliphatic/aromatic-ester) copolymers." *Biomaterials* 25(21): 5191-5198.
- [102] Reynolds, M. A., Aichelmann-Reidy, M. E. and Branch-Mays, G. L. (2010). "Regeneration of periodontal tissue: bone replacement grafts." *Dental Clinics of North America* 54(1): 55-71.
- [103] Rinaudo, M. (2011). "New amphiphilic grafted copolymers based on polysaccharides." *Carbohydrate Polymers* 83(3): 1338-1344.
- [104] Rockwood, D. N., Preda, R. C., Yucel, T., Wang, X., Lovett, M. L. and Kaplan, D. L. (2011). "Materials fabrication from Bombyx mori silk fibroin." *Nat. Protocols* 6(10): 1612-1631.
- [105] Rodan, S. B., Imai, Y., Thiede, M. A., Wesolowski, G., Thompson, D., Bar-Shavit, Z., Shull, S., Mann, K. and Rodan, G. A. (1987). "Characterization of a human osteosarcoma cell line (Saos-2) with osteoblastic properties." *Cancer Research* 47(18): 4961-4966.

- [106] Sabokbar, A., Millett, P., Myer, B. and Rushton, N. (1994). "A rapid, quantitative assay for measuring alkaline phosphatase activity in osteoblastic cells in vitro." *Bone and mineral* 27(1): 57-67.
- [107] Sahil, K., Akanksha, M., Premjeet, S., Bilandi, A. and Kapoor, B. (2011). "Microsphere: a review." *International journal of research in pharmacy and chemistry* 1(4): 1184-1197.
- [108] Sakai, D., Mochida, J., Iwashina, T., Watanabe, T., Nakai, T., Ando, K. and Hotta, T. (2005). "Differentiation of mesenchymal stem cells transplanted to a rabbit degenerative disc model: potential and limitations for stem cell therapy in disc regeneration." *Spine* 30(21): 2379-2387.
- [109] Salinas, A. J., Esbrit, P. and Vallet-Regí, M. (2013). "A tissue engineering approach based on the use of bioceramics for bone repair." *Biomaterials Science* 1(1): 40-51.
- [110] Schreiber, R. and Gareis, H. (2007). "The raw material 'Ossein'." *Gelatine handbook—theory and industrial practice*. Weinham: Wiley-VCH: 63-71.
- [111] Shi, X., Wang, Y., Ren, L., Gong, Y. and Wang, D. A. (2009). "Enhancing alendronate release from a novel PLGA/hydroxyapatite microspheric system for bone repairing applications." *Pharmaceutical research* 26(2): 422-430.
- [112] Shu, X. and Zhu, K. (2002). "Controlled drug release properties of ionically cross-linked chitosan beads: the influence of anion structure." *International Journal of pharmaceutics* 233(1): 217-225.

- [113] Siddhanta, A. K., Goswami, A. M., Shanmugam, M., Mody, K. H., Ramavat, B. K. and Mairh, O. P. (2002). "Sulphated galactans of marine red alga *Laurencia* spp.(Rhodomelaceae, Rhodophyta) from the west coast of India." *Indian journal of marine sciences* 31(4): 305-309.
- [114] Sudo, H., Kodama, H. A., Amagai, Y., Yamamoto, S. and Kasai, S. (1983). "In vitro differentiation and calcification in a new clonal osteogenic cell line derived from newborn mouse calvaria." *The Journal of cell biology* 96(1): 191-198.
- [115] Suganya, S., Venugopal, J., Ramakrishna, S., Lakshmi, B. and Dev, V. (2014). "Aloe vera/silk fibroin/hydroxyapatite incorporated electrospun nanofibrous scaffold for enhanced osteogenesis." *Journal of Biomaterials and Tissue Engineering* 4(1): 9-19.
- [116] Takaoka, S., Yamaguchi, T., Yano, S., Yamauchi, M. and Sugimoto, T. (2010). "The Calcium-sensing Receptor (CaR) is involved in strontium ranelate-induced osteoblast differentiation and mineralization." *Hormone and metabolic research* 42(09): 627-631.
- [117] Thakur, G., Mitra, A., Basak, A., Rousseau, D. and Pal, K. (2010). Characterization of oil-in-water gelatin emulsion gels: Effect of homogenization time. *Systems in medicine and biology (ICSMB), 2010 International Conference on, IEEE.*
- [118] Tran, N. Q., Y. K. Joung, E. Lih, K. M. Park and K. D. Park (2011). "RGD-conjugated in situ forming hydrogels as cell-adhesive injectable scaffolds." *Macromolecular Research* 19(3): 300-306.

- [119] Tuan, H. S. and Hutmacher, D. W. (2005). "Application of micro CT and computation modeling in bone tissue engineering." *Computer-Aided Design* 37(11): 1151-1161.
- [120] Umeki, N., Sato, T., Harada, M., Takeda, J., Saito, S., Iwao, Y. and Itai, S. (2010). "Preparation and evaluation of biodegradable microspheres containing a new potent osteogenic compound and new synthetic polymers for sustained release." *International journal of pharmaceutics* 392(1): 42-50.
- [121] Victor, S. P. and Kumar, T. S. (2008). "BCP ceramic microspheres as drug delivery carriers: synthesis, characterisation and doxycycline release." *Journal of Materials Science: Materials in Medicine* 19(1): 283-290.
- [122] Vold, I. M. N. (2004). "Periodate oxidised chitosans: structure and solution properties."
- [123] Wang, D., Ju, X., Zhou, D. and Wei, G. (2014). "Efficient production of pullulan using rice hull hydrolysate by adaptive laboratory evolution of *Aureobasidium pullulans*." *Bioresource technology* 164: 12-19.
- [124] Wang, X., Wenk, E., X. Hu, Castro, G. R., Meinel, L., Wang, X., C. Li, Merkle, H. and Kaplan, D. L. (2007). "Silk coatings on PLGA and alginate microspheres for protein delivery." *Biomaterials* 28(28): 4161-4169.
- [125] Wang, Y. H., Chang, C. M. and Liu, Y. L. (2012). "Benzoxazine-functionalized multi-walled carbon nanotubes for preparation of electrically-conductive polybenzoxazines." *Polymer* 53(1): 106-112.

- [126] Warner, S., J. Shea, S. Miller and J. Shaw (2006). "Adaptations in cortical and trabecular bone in response to mechanical loading with and without weight bearing." *Calcified tissue international* 79(6): 395-403.
- [127] Williams, J. M., A. Adewunmi, R. M. Schek, C. L. Flanagan, P. H. Krebsbach, S. E. Feinberg, S. J. Hollister and S. Das (2005). "Bone tissue engineering using polycaprolactone scaffolds fabricated via selective laser sintering." *Biomaterials* 26(23): 4817-4827.
- [128] Wong, V. W., K. C. Rustad, M. G. Galvez, E. Neofytou, J. P. Glotzbach, M. Januszyk, M. R. Major, M. Sorkin, M. T. Longaker and J. Rajadas (2010). "Engineered pullulan–collagen composite dermal hydrogels improve early cutaneous wound healing." *Tissue Engineering Part A* 17(5-6): 631-644.
- [129] Woodruff, M. A., C. Lange, J. Reichert, A. Berner, F. Chen, P. Fratzl, J.-T. Schantz and D. W. Hutmacher (2012). "Bone tissue engineering: from bench to bedside." *Materials Today* 15(10): 430-435.
- [130] Xian, C. J., F. H. Zhou, R. C. McCarty and B. K. Foster (2004). "Intramembranous ossification mechanism for bone bridge formation at the growth plate cartilage injury site." *Journal of orthopaedic research* 22(2): 417-426.
- [131] Xiao, S., Z. Wang, H. Ma, H. Yang and W. Xu (2014). "Effective removal of dyes from aqueous solution using ultrafine silk fibroin powder." *Advanced Powder Technology* 25(2): 574-581.
- [132] Xu, F., B. Weng, R. Gilkerson, L. A. Materon and K. Lozano (2015). "Development of tannic acid/chitosan/pullulan composite nanofibers from aqueous solution for potential applications as wound dressing." *Carbohydrate polymers* 115: 16-24.

- [133] Yamasaki, A., Itabashi, M., Sakai, Y., Ito, H., Ishiwari, Y., Nagatsuka, H. and Nagai, N. (2001). "Expression of type I, type II, and type X collagen genes during altered endochondral ossification in the femoral epiphysis of osteosclerotic (oc/oc) mice." *Calcified tissue international* 68(1): 53-60.
- [134] Yang, M. C., Wang, S. S., Chou, N. K., Chi, N. H., Huang, Y.Y., Chang Y. L., Shieh, M. J. and Chung T. W. (2009). "The cardiomyogenic differentiation of rat mesenchymal stem cells on silk fibroin-polysaccharide cardiac patches in vitro." *Biomaterials* 30(22): 3757-3765.
- [135] Yang, S., Leong, K. F., Du, Z. and Chua, C. K. (2001). "The design of scaffolds for use in tissue engineering. Part I. Traditional factors." *Tissue engineering* 7(6): 679-689.
- [136] Yannas, I. V. (2001). *Tissue and organ regeneration in adults*, Springer Science & Business Media.
- [137] Yasuda, T., Tada, Y., Tanabe, N., Tatsumi, K. and West, J. (2011). "Rho-kinase inhibition alleviates pulmonary hypertension in transgenic mice expressing a dominant-negative type II bone morphogenetic protein receptor gene." *American Journal of Physiology-Lung Cellular and Molecular Physiology* 301(5): L667-L674.
- [138] Yu, G. and Fan, Y. (2008). "Preparation of poly (D, L-lactic acid) scaffolds using alginate particles." *Journal of Biomaterials Science, Polymer Edition* 19(1): 87-98.

- [139] Zhang, H., Li, F., Yi, J., Gu, C., Fan, L., Qiao, Y., Tao, Y., Cheng, C. and Wu, H. (2011). "Folate-decorated maleilated pullulan–doxorubicin conjugate for active tumor-targeted drug delivery." *European Journal of Pharmaceutical Sciences* 42(5): 517-526.
- [140] Zhang, X., Schwarz, E. M., Young, D. A., Puzas, J. E., Rosier, R. N. and O’Keefe, R. J. (2002). "Cyclooxygenase-2 regulates mesenchymal cell differentiation into the osteoblast lineage and is critically involved in bone repair." *The Journal of clinical investigation* 109(109 (11)): 1405-1415.
- [141] Zhang, Y. Q., Shen, W. D., Xiang, R. L., Zhuge, L. J., Gao, W. J. and Wang, W. B. (2007). "Formation of silk fibroin nanoparticles in water-miscible organic solvent and their characterization." *Journal of Nanoparticle Research* 9(5): 885-900.
- [142] Zhu, P., Masuda, Y. and Koumoto, K. (2004). "The effect of surface charge on hydroxyapatite nucleation." *Biomaterials* 25(17): 3915-3921.

APPENDIX A

CALCIUM ASSAY CALIBRATION CURVE

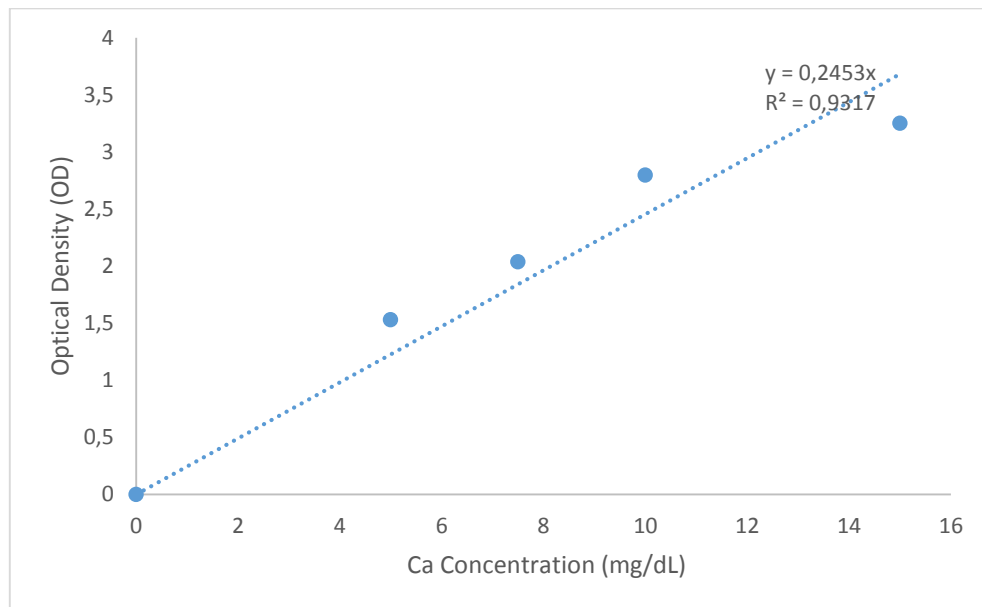


Figure A. Calibration curve for o-cresolphthalein complexone method for calcium content.

APPENDIX B

CELL NUMBER CALIBRATION CURVE FOR VIABILITY ASSAY (PART I)

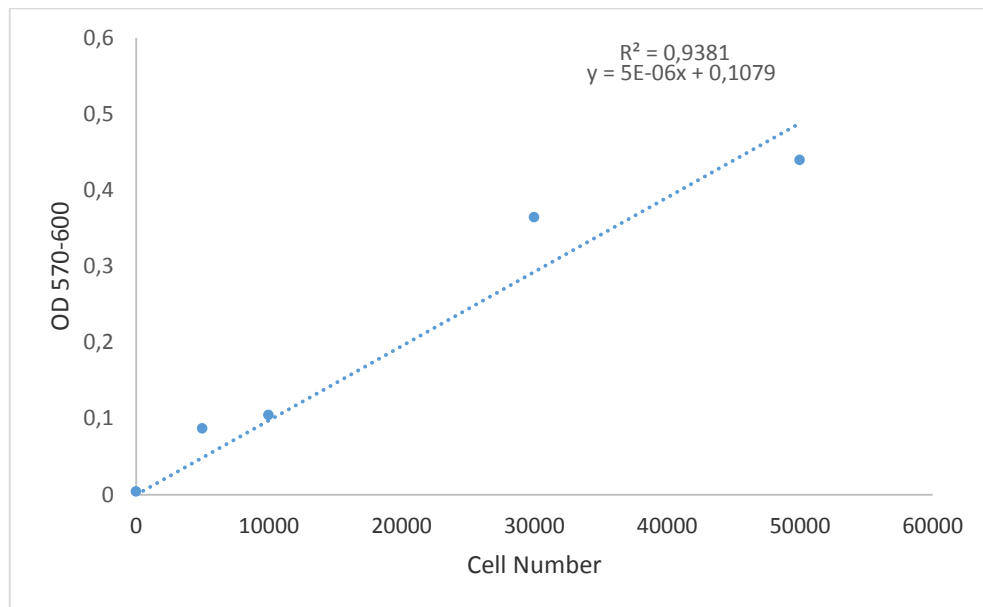


Figure B. Calibration curve for SaOs-2 cells for Alamar Blue viability assay.

APPENDIX C

CALIBRATION CURVE FOR ALP ACTIVITY ASSAY

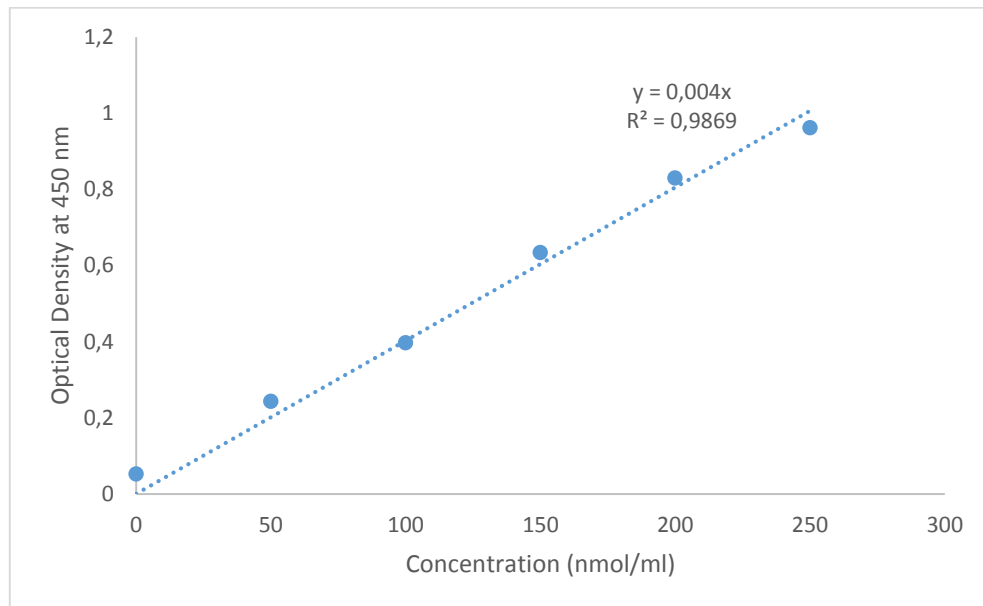


Figure C. The calibration curve constructed with p-nitrophenol for ALP activity assay

APPENDIX D

CALIBRATION CURVE FOR ALP ACTIVITY ASSAY

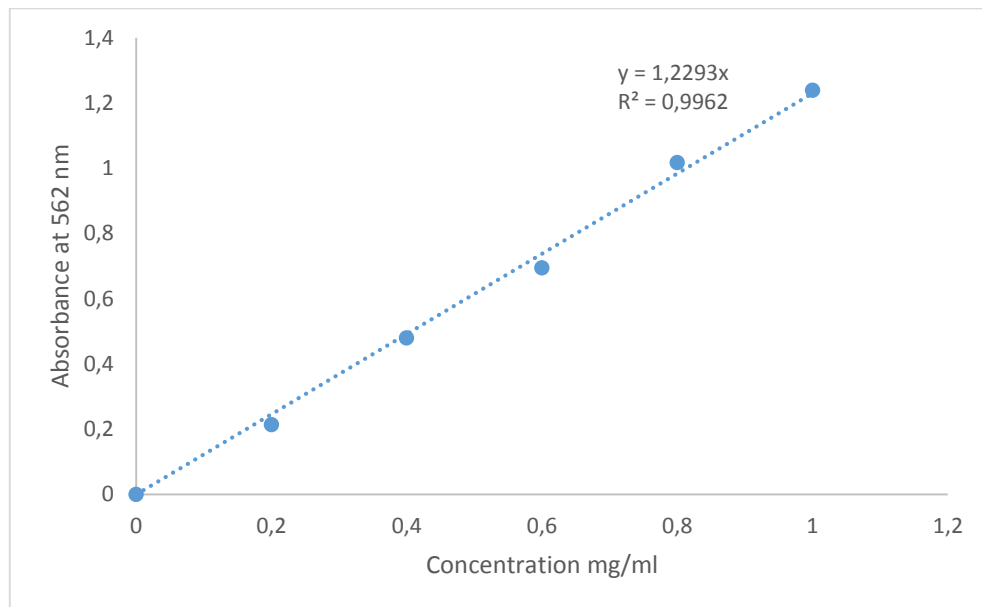


Figure D. The calibration curve of BCA assay constructed with bovine serum albumin as standard for protein amount determination.

APPENDIX E

ETHICS COMMITTEE APPROVAL REPORT

UYGULAMALI ETİK ARAŞTIRMA MERKEZİ
APPLIED ETHICS RESEARCH CENTER


ORTA DOĞU TEKNİK ÜNİVERSİTESİ
MIDDLE EAST TECHNICAL UNIVERSITY

DUMLUPINAR BULVARI 06800
ÇANKAYA ANKARA/TURKEY
T: +90 312 210 22 91
F: +90 312 210 79 59
ueam@metu.edu.tr
www.ueam.metu.edu.tr

Sayı: 28620816/ 77

19.02.2015

Gönderilen : Doç.Dr. Ayşen Tezcaner
Biyomedikal Mühendisliği Bölümü


Gönderen : Prof. Dr. Canan Sümer 
IAK Başkan Vekili

İlgi : Etik Onayı

Danışmanlığını yapmış olduğunuz Biyomedikal Mühendisliği Bölümü öğrencisi Hazal Aydoğdu'nun "Kemik Doku Mühendisliği için Mikrotasıyıcı Sistemlerin Geliştirilmesi" isimli araştırması "İnsan Araştırmaları Komitesi" tarafından uygun görülerek gerekli onay verilmiştir.

Bilgilerinize saygılarımla sunarım.

Etik Komite Onayı
Uygundur
19/02/2015


Prof.Dr. Canan Sümer
Uygulamalı Etik Araştırma Merkezi
(UEAM) Başkan Vekili
ODTÜ 06531 ANKARA

APPENDIX F

CELL NUMBER CALIBRATION CURVE FOR VIABILITY ASSAY (PART II)

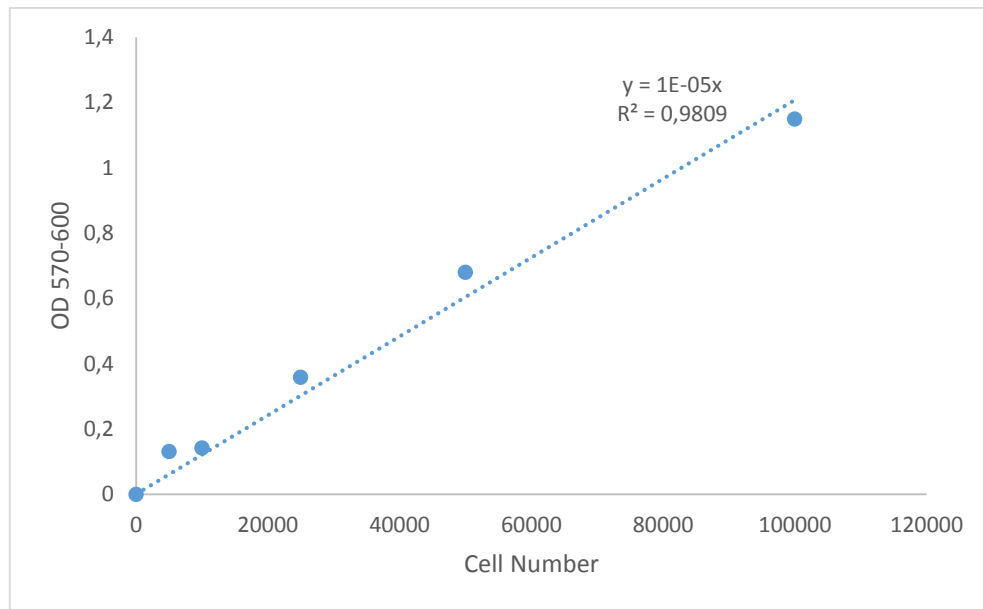


Figure F. Calibration curve for urine derived stem cells for Alamar Blue viability assay.